Viability of Supercapacitors for Energy Storage to Mitigate Renewable Energy Sources Intermittency

By

Renesh Rajan Thakoordeen
21028474

A thesis submitted in fulfilment of the requirements for the Master of Engineering Degree in the Department of Electrical Power Engineering, Faculty of Engineering and the Built Environment

Durban University of Technology

Supervisor: Dr Evans Eshiemogie Ojo
Co-Supervisor: Prof. Nelson M. Ijumba

October 2019

I undertake that all material presented in this thesis is my own work and has not been written for me, in whole or in part by any other person. I undertake that any quotation or paraphrase from the published or unpublished work of another person has been duly acknowledged in the work which I now present for examination.

Mr Renesh Rajan Thakoordeen
Student Number: 21028474
Approved for Final Submission

Supervisor: Dr Evans Eshiemogie Ojo

Co-Supervisor: Prof. Nelson M. Ijumba

Durban, 26 March 2019

Acknowledgements

I would like to thank and acknowledge the following people who have made this thesis possible.

First and foremost, to Dr Evans Eshiemogie Ojo for his continued support and wise words of inspiration. His professional input, second to none and for tirelessly working to ensure that this study be one that all mentioned in this acknowledgement can be proud of. This thesis could not be possible without his expert supervision.

To Prof Nelson Ijumba, for assisting me in my growth as a student, his support and input during the study.

A tremendous amount of gratitude is owed to the South African Weather Service (SAWS) for graciously providing the wind roses used in the study and to Elsa de Jager from SAWS for making the process as easy as possible.

I would like to say thank you to my parents, Rajan and Asha Thakoordeen for tirelessly working to give me the opportunities that have led me to study this far. Without their support and guidance, none of this would be possible.

To my brother and sister-in-law, Ashik and Preshnee Thakoordeen: for consistently tolerating challenging questions and challenging my own ideas and creativity and for their support throughout this venture.

To my colleagues, Ashley Dheena; Thembakazi Rubuluza; Craig Hills and Renard Senekal: for their professional input on the subject matter and patience when times have been trying.

To the Eskom on-site engineers, Richard Marr and John Behn for their professional input regarding higher levels of mechanical and electrical engineering.

Abstract

Energy storage is seen as a solution to assist in the integration of renewable energy by meeting intermittency. Such energy sources suffer from the widely known obstacle of intermittency. To overcome this issue, a formidable energy storage system is required. While large scale energy storage systems such as pumped-storage schemes and compressed air energy storage systems exist, renewable energy sources such as solar and wind power use batteries as a form of energy storage. Additionally, these large scale energy storage systems suffer from a number of drawbacks such as specific location and geophysical requirements. Photovoltaic arrays and wind turbines almost exclusively use batteries as the preferred method of energy storage.

Recent years has seen a surge in the advancement of supercapacitor technology. The two main characteristics of supercapacitors are: high power density and low charging time. This has drawn considerable attention to the technology and has thus been implemented in electric buses and hand tools. Other desirable characteristics, as compared to electrochemical batteries, include: smaller weight; lifespan and fewer toxic materials. The last characteristic mentioned is of notable concern since lead-acid batteries are known to emit dangerous gases such as hydrogen and also use sulphuric acid and lead in their production which can lead to laryngeal carcinoma.

Latest developments have seen an increase in the overall capacitance (and decrease in cost price) of supercapacitors which may allow supercapacitors to be used as energy storage system, either in a stand-alone or hybrid capacity or both. This study attempts to prove that supercapacitors can replace electrochemical batteries on a domestic scale through simulation where the number of supercapacitors required to supply a domestic load for 24 hours is determined. The time required to charge these supercapacitors is also ascertained. However, it was found that supercapacitor technology is limited to smaller applications or a hybrid design working in conjunction with batteries as protection surge currents.

Contents

List of Figures

List of Tables

Nomenclature

μ	Permeability (H/m)
A	Area(m^2)
B	Magnetic Flux density*(T)*
C	Capacitance*(F)*
EGO	Semi-Conductor band gap energy (eV)
ε	Permittivity (F/m)
f	Frequency (Hz)
I	Current (A)
J	Moment of Inertia ($kg.m^2$)
K	Boltzmann's Constant$1{,}38064852 \times 10^{-23} m^2 kg.s^{-2} k^{-1}$
ki	short circuit current of cell at 25°C at irradiance of 1000W/m^2
m	Mass (kg)
n	diode ideality factor
N	Speed (rpm)
P	True Power (W)
q	Charge (C)
Q	Reactive Power (Var)
R	Resistance (Ω)
S	Apparent Power (VA)
t	Time (s)
T	Period (s)
T_e	Electromagnetic torque ($N.m$)
T_m	Mechanical Torque ($N.m$)
T_n	Nominal Temperature (K)
T_{temp}	Temperature (K)
U_B	Energy Density in Magnetic Field (T)
U_w	Wind Speed (m/s)
V	Potential Difference (V)
v	Speed (m/s)
λ	tip speed ratio
ω	angular velocity (rad/s)
σ	Tensile strength (N/m^2)
ρ	Density (kg/m^3)

List of Abbreviations

AC	Alternating current
CAES	Compressed-air energy storage
C_p	Power Co-efficient
C_t	Torque Co-efficient
Cu	Copper
Cu_2SO_4	Copper (II) Sulphate
DC	Direct Current
DFIG	Doubly Fed Induction Generator
EDLC	Electric Double Layer Capacitor
EMS	Energy Management System
EPR	Equivalent Parallel Resistance
ESR	Equivalent Series Resistance
ESS	Energy Storage System
FES	Flywheel Energy Storage
HTF	Heat Transfer Fluid
HTS	High Temperature Superconducting
IGBT	Insulated gate bipolar transistor
KCL	Kirchhoff's Current Law
KVL	Kirchhoff's Voltage Law
LIC	Lithium-Ion Capacitor
MTBF	Mean Time between failures
MTR	Mean time to recovery
PSH	Peak Solar Hours
USA	United States of America
USD	United States Dollar
Zn	Zinc

Abbreviation of Units

A	Ampere
C	Coulomb
eV	electron Volts
F/m	Farad per meter
Hz	Hertz
K	Kelvin
Kg	Kilogram
N	Newton
m	meter
m/s	metre per second
rad/s	radians per second
rpm	revolutions per minute
s	seconds
T	Tesla
V	Volts
VA	Volt-Amp
Var	Volts-Amps-Reactive
W	Watt
Ω	Ohms

Chapter One

Introduction

1.1 Background

In recent years, the increasing demand for electrical energy has led to an energy crisis and dependence on imported fossil fuels[1]. This is evident in South Africa with the new coal fired power stations, Medupi Power Station with a capacity of 4764 MW and Kusile Power Station 4800 MW. This has forced power utilities to explore the possibility of changing from fossil fuel-based electricity to electricity from alternative renewable sources. The alternative renewable energy source can be in the form of wind, solar, tidal waves, geothermal. The increasingly dependence on imported fossil fuels has resulted in poor reliability with corresponding high electricity costs and environmental pollution.

Power plants powered by renewable energy sources have the capability to be a better alternative to the widely used fossil fuelled power station. This is because most renewable energy sources are largely environmentally friendly and are more functionally sustainable [2]. Although, the levelized cost of electricity (LCOE) for harnessing renewable energies has dipped below that of fossil fuels, intermittency is the principal preventing the penetration of renewable energy [3].

While weather prediction technologies have greatly improved, the problem of intermittency is still an ongoing impediment that requires investigation. Weather forecasting does provide the possibility of accurate planning and design of renewable energy plants. With the latest forecasting technology, smart grids are capable of taking full advantage of renewable energy sources [4]. Adequate planning enhances the reliable use of renewable energy since systems such as micro and/or smart grids may switch from one of renewable energy source to another. To further explain this, consider the example of a micro grid that has the option of wind and solar power. On a windy day, the system may select that the load be supplied using wind power while energy is captured using solar power. This might reduce the amount of fossil fuels used to remain operational.

Ultimately to address the issue of intermittency, appropriate energy storage systems (ESS)are required[5]. The Law of Conversation of Energy is applied when converting electrical or mechanical energy to other forms of energy that can be stored and used at a later stage. At present there are several different types of energy storage techniques and this will be discussed in detail in Chapter two. These include:

- Mechanical energy (pumped storage, flywheel energy storage, compressed-air energy storage)
- Chemical energy (hydrogen storage, biofuels)
- Biochemical (Starch)

- Electrochemical energy (batteries)
- Thermal energy (liquid nitrogen engine, solar pond, molten salt.)

The most widely used forms of energy storage are that of mechanical, electrochemical and thermal[6]. Electrochemical batteries, being the focal point of energy storage for solar and wind power plants.

This study intends to determine whether supercapacitors (also commonly referred to as ultracapacitors) can be used as an efficient energy storage device in the field of electrical power engineering.

1.2 Research Problem

The hypothesis of this study is that supercapacitors are a viable form of energy storage to meet the intermittency of renewable energy plants. The study focuses on determining whether or not supercapacitors are a viable option for energy storage. The total amount of energy stored and charging time in comparison to battery technology will form the basis of this research. Since energy storage is a prime inhibitor in the field of renewable energy, the compatibility of supercapacitors with photovoltaics (PV) and wind power shall be explored. However, an effective charging and discharging technique must be implemented to minimize losses while maximizing availability, reliability and sustainability, thereby improving viability. In addition, appropriate loads shall be selected in order to determine a range of viability for the technology.

1.3 Motivation

Electrochemical battery usage has increased as both the number of PV and wind power plants increased [7]. Batteries have been seen as the prime energy storage device for these renewable energy sources. Despite their drawbacks they remain as the only viable energy storage system.

The relatively new technology of supercapacitors, with advantages such as short charging duration, minimal or no leakage and high cyclability could potentially be a viable alternative to batteries.

Recent developments have seen supercapacitors being used in larger application such UPSs, electric vehicles and wind turbines [8]. With the range of applications increasing due to their fast charging nature, this technology could plausibly assist in the wider use of renewable energy by limiting the factor of intermittency. However, the low energy density of supercapacitors is one of the limiting issues around their application.

1.4 Aim of Research

This study focuses on the determination of whether or not the supercapacitors can be used as an energy storage system to supply power for domestic loads. Specifically, the duration that a

supercapacitor energy storage system can effectively supply domestic loads and how this compares with battery only designs. As previously stated, supercapacitors are already used in electric vehicles and UPSs therefore; testing domestic loads would be the next logical step in proving viability.

The aims of this study in relation to the concepts as explained in the previous paragraph are as follows:

- To carry out the analysis of the concepts of energy storage in renewable energy systems
- To investigates the problem and management of the renewable energy intermittency
- To explore the feasibility of supercapacitor technology as a viable means of storing power generated from renewable energy sources.
- To determine how constant supply of electricity can be achieved by the integration of supercapacitors onto renewable systems.
- To numerically evaluate how the use of energy storage technologies can improve the energy management of the electrical system.

To accomplish these, a load profile for a typical sized medium-income household was developed, incorporating AC loads. Effective and efficient circuit design incorporating modular switching is required to overcome the drawback of low specific energy of supercapacitor technology. The potential difference at the terminals of supercapacitors is relatively low therefore; an appropriate voltage booster is designed using the concepts of power electronics to produce the desired output voltage. Also, due to the fact that supercapacitors deliver direct current, a pulse width modulation (PWM) or sinusoidal pulse width modulation (SPWM) topology is required to invert the direct current to the alternating current.

1.5 Scope of Research and Methodology

This study is limited to determining suitable application for supercapacitors as a viable energy storage device in the power engineering environment. The main focus of the study is the viability of supercapacitors with regards to domestic systems/applications only. Besides in-depth study in areas such as chemistry, thermodynamics, infrastructure and environmental engineering will not be considered.

Capacitance forms an integral part of power transmission. This aspect, however, will be excluded as high voltage transmission is not part of the scope of this study. Other aspects that will be exempt include: signal processing/filtering, noise filtration and weapons application since these aspects are not related to energy stored in order to meet the intermittency of renewable energy sources.

Medium income homes in South Africa were selected for data collection.

Other forms of energy storage were studied to ascertain their benefits and drawbacks such that a comparison can be drawn with supercapacitor technology. Typical characteristics were identified by through this method. Since cost is a significant factor in engineering design, a brief cost analysis was conducted were the cost of a system with supercapacitors over the years was assessed.

Few designs exist where supercapacitors are used as an energy storage device for domestic loads. This study will centre on two overall designs.

Due to South Africa's availability of wind and solar energy, these two selected to provide the charging side of the supercapacitor. To effectively size the photovoltaic arrays, data for the peak sun hours was obtained from *ClimaTemps* who provide data on the world's climate. Wind speed data to size the appropriate wind turbine was obtained from the *South African Weather Service*. Subsequently, upon sizing, the relevant datasheets were obtained from suppliers of supercapacitors, solar panels and wind turbines to complete the necessary mathematical models and calculations.

This study employed the use of numerical analysis and computer simulation as the methodology to achieve the aims as stated in the previous section. The Matlab® and Simulink® programming environments were used, along with other software packages including CorelDraw®. This research can be sub-categorized as simulation based with analytical comparison. The study does attempt to find a solution to the issue of intermittency of renewable energy sources with regards to the application of energy storage for domestic loads.

1.6 Structure of the Thesis

The compilation of this document was done based on the following structure:

Chapter One- Introduction: This Chapter contains the background, problem statement, aims, research methodology and the outline of this thesis.

Chapter Two – Literature review. The current literature is evaluated to establish the present scholarly concepts, build up the application with a summation of the areas that have already been addressed. This will help to identify the area not yet addressed as regards to this research.

Chapter Three – Design and modelling. This chapter will focus on determining the electrical requirements of the domestic loads and how to meet these requirements using a mathematical model. The circuit design for the system will form the core of this chapter.

Chapter Four - Analytical analysis and numerical simulation. At this point, the mathematical model created in the previous chapter will be simulated using Matlab® and Simulink® including other software. The results obtained in this chapter and chapter 3 will be compared and discussed.

Chapter Five – Conclusion and recommendation. The question of whether or not supercapacitors are a viable option for energy storage on an electrical power engineering scale will be answered and further recommendations on the technology and its application will be made based on the results obtained.

Chapter Two

Literature Review

2.1 Energy Storage Technologies

Energy storage technologies are normally achieved by utilization of different physical and chemical properties. Figure 2.1 shows the commonly available energy storage technologies, which are suited for the use in renewable energy generation. The trend around the world these days seems to indicate the change in power generation from fossil fuels to renewable energies. Between 1992 and 2011, an increasing linear trend can be observed in the ratio of power produced from renewable sources to fossil fuels [9]. From this trend it is possible to predict that the future of electricity generation will be largely drawn from renewable energy sources, specifically wind and solar. However, renewable energy faces the problem of intermittency. Thus, any load that aims to rely on renewable energy power plants should possess a reliable energy storage system. At present, hydro pumped-storage schemes are capable of meeting the need for large scale energy storage systems[10].

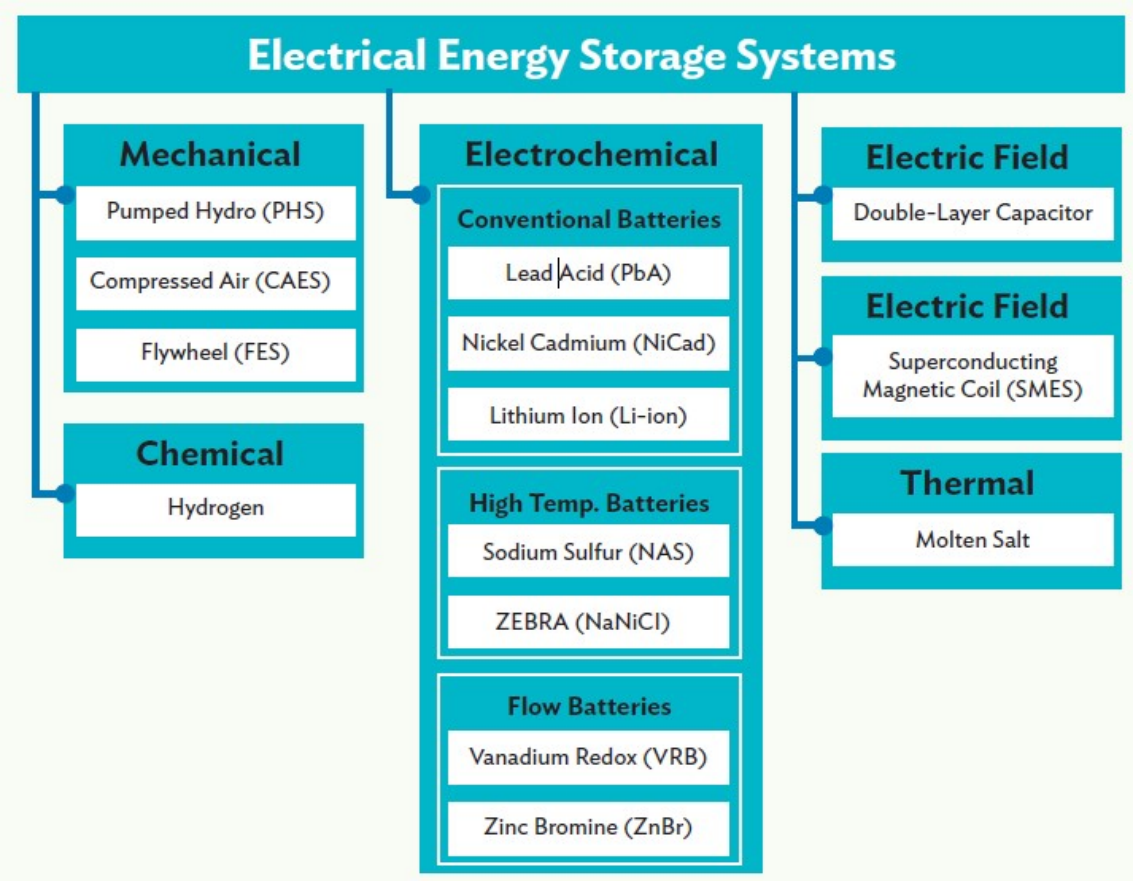

Figure 2.1. Types of Energy Storage Systems[11]

As already covered in the previous chapter, there exist multiple energy storage systems or techniques. However, it is not accurate to say that there is one prime technology to suit all applications. Several aspects must be analysed to determine the most suited for a particular purpose [12]. The criteria to determine its suitability is based on the following:

- *Efficiency*- several characteristics are relevant when assessing the efficiency of a storage system. These include the rate of charge, the rate of discharge; the rate of self-discharge and heat losses. Different devices and technologies have different storage techniques or mechanisms which play a role in efficiency. In electrochemical storage, electrodes decay over time, reducing the number of cycles. A loss of efficiency is also strongly related to self-discharge.
- *Durability*- this is another important factor in energy storage technologies since it directly deals with the number of cycles or cyclability. With the exception of material decay, ambient temperature tends to play a large role in durability. Certain devices such as batteries and supercapacitors tend to display greater durability when kept in rooms at standard temperature and pressure (STP) as opposed to rooms with higher or lower temperatures. This has led to HVAC systems being designed specifically for battery rooms and supercapacitor modules with self-cooling units much like that of personal home computers.
- *Energy and power density*- in this study, this factor may arguably be of highest importance. These factors to determine the weight and volume of an energy storage system. This is important in areas with limited space such as power plants and urban areas or households. The ragone plot in Figure 2.2, shows where supercapacitors rank in terms of specific power and specific energy (commonly referred to as power density and energy density). In an energy storage device a higher specific energy is desirable. Energy density refers to the amount of energy per unit mass and devices with larger energy densities are able to perform work for an extended period of time however, such devices have longer charging times. Devices with larger specific power are able to deliver large amounts of power in shorter times but are also quickly recharged. By studying the plot, it can be seen that supercapacitors still lag behind batteries in this respect. However, developments as will be discussed later in this study have proven that the supercapacitor area in the plot should soon extend beyond that of batteries[13].

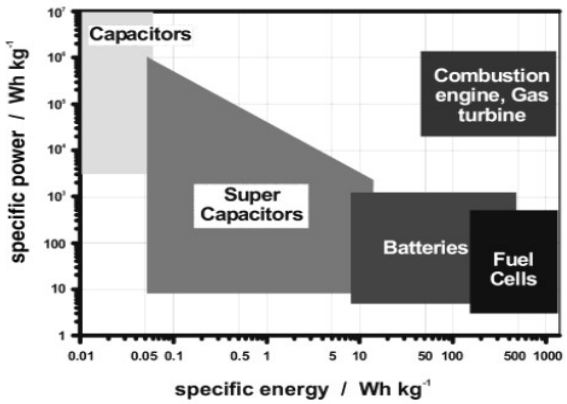

Figure 2.2.Ragone Plot of Specific Power vs Specific Energy [14]

- *Reliability*- the reliability of a device is the measure of the device carrying out its designed function over a specific length of time under specified design conditions. It is a measure of the probability that an item will perform its intended function for a specified interval under stated conditions. Commonly used factors in determining availability is the time that the device operates as designed which is determined as a function of the Mean Time Between Failures (MTBF) and the Mean Time to Recovery (MTR) [15]:

$$availability = \frac{MTBF}{MTBF+MTR} \tag{2.1}$$

Meantime Between Failure is defined as the ratio of total time in service to number of failures while failure rate is defined as the ratio between number of failures to total time in service. Availability is not only limited to the above equation but this equation forms part of a larger field of engineering referred to as reliability engineering. Another factor to be considered when determining reliability and availability is that of maintenance. On multiple commercial supercapacitor websites it is stated that the supercapacitor modules require no maintenance[16].This is in contrast to its counterpart, batteries, where electrolyte levels must be monitored and replaced from time to time[17].

Cyclability and the state of charge are also factored in when determining reliability. In the case of a battery, the depth of discharge will affect the cyclability with deeper discharges leading to lower cyclability and therefore lower reliability. Similarly supercapacitors have a specified cyclability where such factors as larger charging voltage may affect it.

- *Response Time*- the response time of a system or device is the measure of time to "turn-on" or to produce some effect to the system. As one would expect, larger systems possess a longer response time. Case in point, pumped-storage schemes have a response time generally less than 10 minutes. In comparison, batteries, supercapacitors and SMES have a near instantaneous response time (up to 5 seconds) [18]. Depending on the application that the

energy storage system is designed for, certain response times are acceptable. Even though for power grid application the response time for a pumped-storage scheme is minutes, this is acceptable in terms of the application.

2.2 Different Types of Energy Storage

Stored energy is often referred to as potential energy. Derivatives of potential energy include chemical potential energy; elastic potential energy; electric potential energy. Energy that is in the process of being released is kinetic energy and can be viewed as motion or heat. However, the line between potential and kinetic energy can be blurred in the sense that some forms of kinetic energy can be seen as potential energy, such as in the case of the flywheel where the rotation of a large mass is the potential from which energy can be drawn. To be accurate, in a flywheel kinetic energy is stored [19].

However, all forms of energy are either in the form of potential or kinetic energy with other forms being derivative. As indicated in Figure 2.1, energy storage systems can be in the following forms:

- Mechanical: Compressed air energy storage, flywheel energy storage, hydraulic accumulator
- Electrochemical: Batteries, flow batteries, fuel cells
- Electrical: Capacitor, supercapacitor, superconducting magnetic energy storage

2.2.1 Mechanical Energy Storage Systems

At present there exist a number of energy storage technologies considered as mechanical storage:
Pumped-storage schemes – these power plants store energy in the form of hydraulic potential energy or gravitational potential energy. Currently there are two types of pumped-storage schemes, namely, pure pumped hydro energy storage and pump-back pumped hydro energy storage. The difference being that pumped-back hydro energy storage uses an amalgamation of pumped water and natural water flow (much like that of common hydroelectric plants) [20].
The basic operation of pure pumped hydro energy storage plants is that they pump water up to a higher plane during off-peak periods and allow the water to flow down the same penstock during peak periods to rotate a turbine thereby generating electricity. The pumping activity requires 30% more energy to pump water up than it can generate. This difference results in pumped-storage schemes being used as peak power stations as opposed to base load power stations making them economically viable. They also possess quick response time (less than 10 minutes) which makes it applicable to black starts (restarting a national grid after a nationwide blackout).
These power plants often boast a mode of operation referred to as synchronized condensed operation where the unit provides grid frequency stabilization.

A large drawback of these plants is one of a geographical nature. To build such a plant requires a large difference in height over a relativity short distance (high head), and favourable geotechnical conditions.

Compressed-air energy storage (CAES) – this is the second largest form of energy storage. Both these technologies have the capability of large scale energy storage (over 300 MW per unit)[21].

CAES involves storing energy in the form of high pressure compressed air (elastic potential energy). During off peal periods, air is stored in underground caverns under high pressure. At peak demands periods, the compressed air is released from these caverns and heated in combustion chambers. It is then allowed to expand through a turbine, thereby driving a turbine coupled to a generator. As expected, due to the use of combustion chambers, there is a large quantity of waste heat. However, recuperators are installed to capture this heat before being released into the atmosphere[22].

This type of energy storage has positive attributes including longevity and low capital costs with an efficiency ranging between 25 and 45%[23]. The McIntosh Plant in USA has improved efficiency by reducing fuel consumption by 25%. This was accomplished by improving the compression cycle by installing intercoolers and aftercoolers, re-heaters and regenerators[24].

While this technology allows for large scale energy storage, it also faces a geological difficulty since the selected underground cavern must possess robust rock formations to contain extreme pressures, besides it requires large underground caverns. Recent years have seen the use of abandoned salt mines.

Flywheel energy storage (FES)-the concept of flywheels has been in existence for over a thousand years. Multiple sources date the use of flywheels back to the application of pottery. More recent wide spread application lies within the internal combustion engine [25]. The flywheel may be the least complicated form of energy storage discussed in this study. It involves the rotation of a large cylindrical mass about its axis (Figure 2.3).

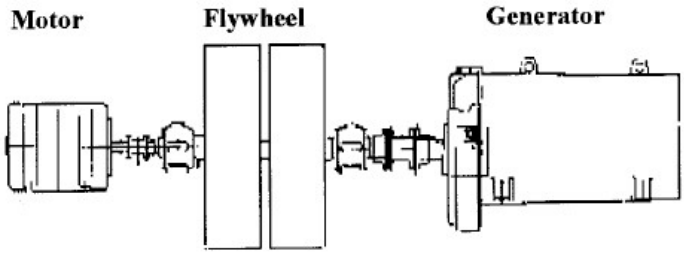

Figure 2.3. Motor-generator with Flywheel [25]

During the “charging” mode, a motor will rotate this mass to high speeds of the order of a thousand RPM for low speed applications and of the order of tens of thousands for high speed. At this point, a combination of Newton’s first and second laws of motion and the conservation of energy are relevant. In frictionless environment, once the “charging” phase is complete, this rotating mass would continue rotating indefinitely. As depicted in Figure 2.3, a motor will “charge” the flywheel by running it up to speed using available power from the grid or a renewable energy plant. The flywheel will then be “discharged” when the field winding within the rotor of the generator, to which it is coupled, is excited thereby generating electricity.

In a real environment containing various forms of friction, the mass will continue to rotate but will slow down. However, due to its large mass, a large amount of energy will be required to lower the speed of rotation. This rotation is where the energy storage actually occurs. It may be counter intuitive (since stored energy is often referred to as potential energy) but the energy is stored as kinetic energy. This is illustrated by the equation for kinetic energy:

$$E = \frac{1}{2}mv^2 \tag{2.2}$$

However, since the flywheel is a rotating mass, the energy stored is better represented by:

$$E = \frac{1}{2}J\omega^2 \tag{2.3}$$

Where J is the moment of inertia and ω is the angular velocity. It can therefore be easily deduced that the faster the flywheel rotates the more energy it can store. The limiting factor comes in the form of tensile strength of the material. At high speeds, the flywheel is exposed to a centrifugal force that could rip it apart should it exceed the maximum tensile strength of the material. The maximum energy that can be stored in a flywheel:

$$E_{max} = SF\frac{\sigma}{\rho} \tag{2.4}$$

Where SF is the shape factor, σ is the material’s maximum tensile strength and ρ is the material’s density. It may be assumed that the stronger and heavier material are selected for flywheels the better, but in reality, fibre composite materials are selected due to the way in which they fail, which is much less catastrophic as compared to metal alloys [26].

A large design consideration is that of friction losses. In addition to air resistance, the bearings which support rotation contribute to these losses. With regards to bearings, the lifespan is directly related to the lubricant which, in turn, is dependent on the operating temperature. By ensuring that the lubricant is kept within suggested design specification, it is theoretically possible for the bearings to experience an extended lifespan.

The losses imposed by bearings on the FES have been significantly reduced with the advent of high temperature superconducting (HTS) bearings. This technology has the potential to reduce friction losses by large order[27]. Other developments have seen the use of maglev technology and vacuum chambers to lower losses to near zero.
FES systems are proving to be a reliable form of energy storage and this is evident by its use around the world[28]. In addition to serving as an ESS, due to its quick response time, it can reduce harmonic distortions and meet transient fluctuations, therefore removing the requirement of frequency regulation.

American company, Active Power, is due to deliver 17 flywheels with an installed capacity of 4.75 MW [29]. The same company is reported to have already installed 900 MW in over 50 countries. The FES has received some recent attention do to its potential to meet intermittency in renewable energy sources [30]. Researchers at various universities, local and abroad, are developing flywheels to be used in conjunction with renewable energy sources such as wind and solar to meet the needs of the people without access to the electrical grid [31].

2.2.2 Electrical Energy Storage Systems

Similar to mechanical energy storage systems, there are a number of storage technologies and there are other different kinds of Electrical Energy:

Molten Salt **–**plants that use molten salt as a medium for energy storage are called concentrated solar plants (CSP). This type of plant involves the heating of water, using sunlight, to extreme temperatures in order to create superheated steam to rotate a turbine. The Rankine power cycle and direct steam generation are the most common methods of achieving the required steam.

Currently there are four types of CSPs. The difference between them comes in the form water is heated.

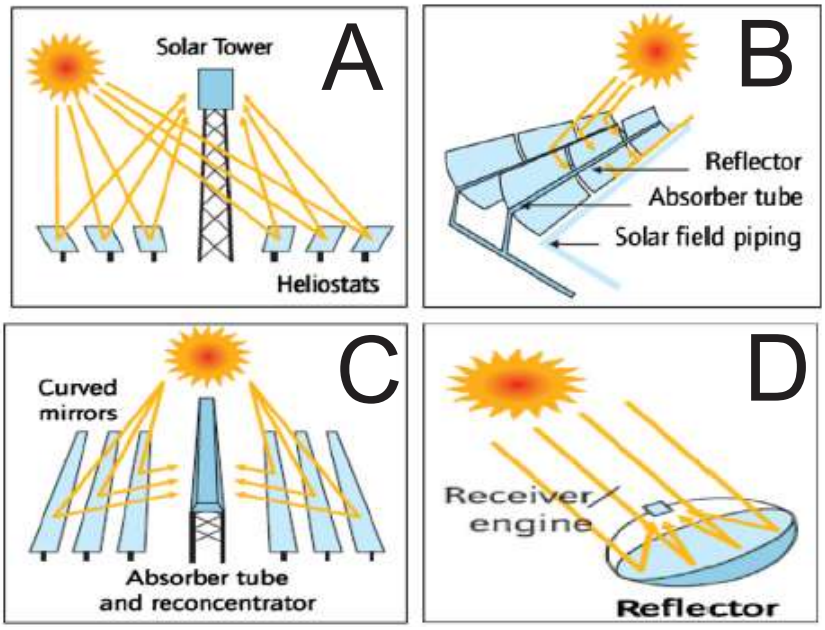

Figure 2.4. The four types of CSP[32]

The four CSP technologies are:

- Solar Power towers (Figure 2.4 A). These plants consist of a central tower where sunlight is reflected to achieve extremely high operating temperatures. To reflect sunlight to a central point, heliostat field collectors are used. At the top of the tower there is a receiver. Within the receiver is a heat transfer fluid (HTF) which absorbs heat from the sunlight. The fluid is then passed through heat exchangers which, in turn, produce steam. Some plants in commercial operation are known to use direct steam generation where no heat transfer fluid is required, thereby reducing costs. [33]
- Parabolic trough collector (Figure 2.4B). As the name suggests, the plant consists of reflectors that are parabolic in shape. The shape is such that instead of a focal point forming, a focal line is created. Within this focal line, an absorber tube is fixed. The absorber tube consists of glass and metal. The outer tube is made of glass while the inner tube is made of metal with the medium between the two tubes is either air or a vacuum depending on thermal expansion of the metal used. A design consideration for the tube is to minimize the heat losses since within the tube is a heat transfer fluid. Much like solar power towers, this technology is able to use heat transfer fluids or direct steam generation to produce electricity.
- Linear Fresnel reflectors (Figure 2.4C). The design philosophy behind linear Fresnel reflectors is similar to that of solar power towers and parabolic reflectors. Flat or slightly curved reflectors reflect sunlight to a focal line where the receiver is located. To maximize the sunlight captured, a secondary reflector is placed above the receiver.

This technology requires a lower capital investment due to the shape of the reflectors. The design also promotes the use of direct steam generation.

- Parabolic dish collectors (Figure 2.4 D). This system differs from the rest in that the receiver and the reflector (dish) tracks the movement of the sun throughout the day as opposed to only the reflectors in other systems. While this design does not require a heat transfer fluid, large quantities of independently operating modules are needed to produce electrical power of the order of tens of kilowatt. This is because each dish and receiver module independently generates electricity. The parabolic dish reflector promotes the highest heat transfer efficiency but is the least compatible with energy storage[34].

Concentrated solar plants have a novel method in which energy is stored. Since the process facilitates heat production, thermal energy storage is required. Excess heat is stored using a heat exchanger and a heat transfer fluid. The heat exchanger uses the heat surplus from the solar field to raise the temperature of the heat transfer fluid. During this process, the HTF is transferred from a cold tank to a hot tank which contains thermal insulation allowing the HTF to retain its thermal energy for extended periods. In plants without energy storage, the reflectors are defocused since the surplus would be wasted.

Currently there exist two types of thermal energy storage which are long and short term. Short term refers to storage to supply for days and nights whereas long term refers to storage in terms of seasons or months. Long term storage remains highly experimental and research is ongoing. However, latent heat storage and chemical heat storage are both being considered for long term storage [35].
A common HTF is the high cost molten nitrate salt which is a combination of potassium and sodium nitrate. Molten nitrate salt can be used in both direct and indirect thermal storage systems. Ideally, the selected molten salt should possess: low vapour pressure and chemical reactivity; reasonable specific heat; high density. Molten nitrate salt possesses all of these characteristics with the drawback of expense and that it solidifies at 221℃.

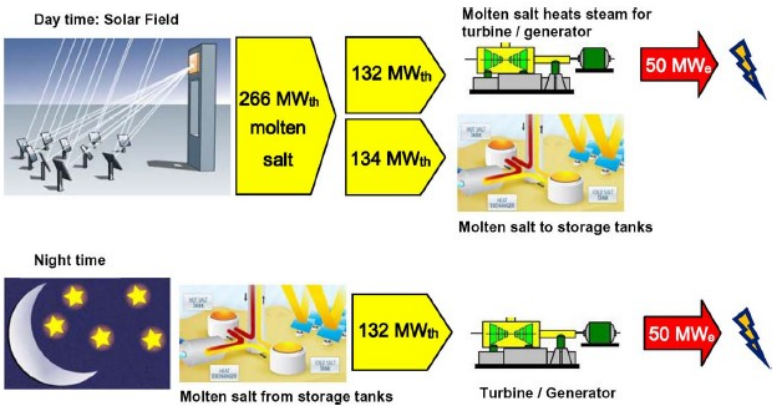

Figure 2.5.Day/Night Operation of CSP Plant [36]

Figure 2.5 illustrates how a CSP operates both in the presence and absence of sunlight. In the figure, it can be seen that the thermal input to the turbine/generator is 132 MW of thermal power, while the electrical output is 50 MW. This is due to the cycle efficiency of approximately 38% [36]. A drawback of the technology is that dust on the panels reduces efficiency by up to 12% [37].

The Gemasolar Thermosolar plant in Spain, with a nameplate capacity of 19.9 MW was able to generate electricity for 24 hours a day for a total period of 36 consecutive days [38]. The plant is of the solar tower type and uses molten salts as an HTF and energy storage medium.

Superconducting magnetic energy storage (SMES)–this device works in a similar fashion to an inductor. Energy is stored in a magnetic field which is generated by passing a direct current (DC) through superconducting coil. In non-superconducting coil, at the moment that the potential difference is removed, stored energy is released by means of ohmic losses as the magnetic field breaks down. The energy density or specific energy in a magnetic field is given by[39]:

$$U_B = \frac{B^2}{2\mu} \tag{2.5}$$

Where μ is the permeability of free space, and B is the magnetic flux density.

Due to the fact that superconducting materials have no ohmic losses, the magnetic field does not break down without reason. It can be seen from Figure 2.6 that the device is often fitted with a bi-directional DC/AC inverter to achieve charging and discharging since the charge mechanism requires DC [40].

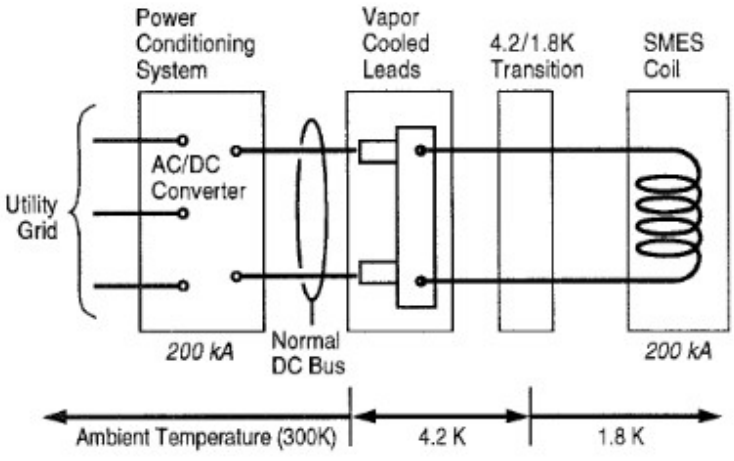

Figure 2.6.SMES Plant Generic Block Diagram [41]

The heart of the system is the superconducting coil. There have been multiple designs and redesigns however it seems to be generally accepted that the system becomes cost viable for large SMES above 5 MWh. This technology has very high charge/discharge efficiency. The literature attributes this to no energy conversion (electrical to mechanical) although it is stated that the energy is stored in the form

of a magnetic field. In 1995, it was predicted that SMES would be used on transmission lines since it boasts a response time of the order 100 ms with smaller units achieving even faster response times. Other uses include transmission line stability and power quality improvement[41].

It is due to these qualities that SMES has moved away from being regarded as an energy storage device. Now, it is viewed as an energy management system with the literature referring to it as Superconducting Energy Management Systems or SEMS.

Batteries – store electrochemical potential energy. This occurs between two electrodes in the presence of an electrolyte. Batteries are classified as either primary or secondary. The difference between the two is that secondary batteries possess the ability to be recharged. Several attributes of secondary batteries make them suitable for grid purposes. These include:

- Quick response time
- Ability to recharge
- Modular configuration
- Reasonable energy density
- Moderate cyclability

For the vast majority of the 20th century, lead-acid batteries have been a staple in industry. They have been known to have a cyclability ranging from 50 to2000 cycles. Cyclability in batteries depends on temperature, depth of discharge and structure of electrodes[42]. Since the advent of the lithium-ion battery, the electronics industry has seen a shift away from lead-acid. This is due to the larger longevity and lower self-discharge of the lithium-ion battery. The lithium-ion battery also possesses higher charge/discharge efficiency up to 98% while lead acid ranges between 75-80%. This is expanded upon in section 2.3.

Electrochemical cells have the ability to be connected in series and parallel, depending on the nature of the application. However, it must be noted that for power grid purposes, a large battery would require additional technology. This comes in the form of a heating, ventilation and air conditioning (HVAC) plant along with grid synchronizers.

The output voltage of batteries is in the form of direct current (DC). To be useful in the power grid sector, it must be inverted to alternating current and has reportedly done so beyond 100 kV with losses in the region of 2%[43]. Other technologies such as transformers must be included.

Photovoltaic arrays almost exclusively make use of batteries to meet their intermittency. Every household with the intention of being free from the electrical utility must incorporate some form of energy storage. Batteries are often the choice due to their relatively low maintenance and ease of installation.

With regards to large scale energy storage, it is generally preferred that such systems are: robust; possess longevity; are environmentally friendly; require minimal maintenance; high cyclability; large volumetric density; quick response time[10]. It is worth noting that often energy storage devices are

useful in more ways than simply storing energy. Some of the devices/methods already mentioned possess the ability to improve power quality or transmission line stability as is the case of pumped-storage schemes and the synchronized condensed operation mode.

Electrical energy storage systems have a wide range of applications aside from the already mentioned capability of supplying loads. In terms of load levelling, pumped-storage schemes already fulfil this application. As previously described, these power stations pump water up to a higher plane during off-peak periods and allow water to flow down the same penstock to generate electrical energy during peak periods. This can be seen as charging during off-peak and discharging during peak if one relates this type of power station to a battery that can be charged. Load levelling from these power stations ensures a uniform load for generation and transmission systems thereby improving the efficiency of the power system.

Load following is another important application that electrical energy storage systems meet. Specifically, SMES and pumped-storage schemes are capable of importing and exporting reactive power on a power grid. Supercapacitors also have this capability but are currently not pragmatic in the sense of high voltage applications due to breakdown voltages. However, capacitors (more accurately capacitances) are known to be used as power factor correction devices. Load following is also linked to spinning reserve or frequency control. The specific charge and discharge characteristics of electrical energy storage systems allows for them to seen as both a load and a source depending on the state of charge of the system/device. These characteristics allow for the power grid personnel to balance the scheduled load/production with the real load/production [44].

On large scale power grids, power quality forms one of the main areas of study in power engineering. Some of the challenges facing power grids in terms of power quality include: voltage dips; transient stability, voltage stability. ESS assists in this respect with their fast response time. In this application pumped-storage schemes would not be effective since their response is lower than what is required. Instead SMES have the capability of meeting this end.

ESS has the ability to make larger impacts closer to the end user through demand side management and contingency service. Admittedly, larger projects such as pump-storage schemes, CAES and SMES are far too large for consumers to construct on their premises but technologies such as batteries and supercapacitors do suit this application. It is not uncommon for users to buy off-peak energy and selling back during peak hours.

2.2.3 Electrochemical Energy Storage

Batteries store chemical energy which can be converted to electrical energy. A number of voltaic (or galvanic) cells connected in series with each other form a single battery. Reduction-oxidation reactions are the core of the energy conversion process.

Figure 2.7, below, demonstrates a simple cell. Two electrodes zinc (Zn) and copper (Cu), are placed inside a copper (II) sulphate (Cu_2SO_4) electrolyte in individual beakers separated by a potassium nitrate (KNO_3) salt bridge. A voltmeter is connected to each electrode to determine the potential difference.

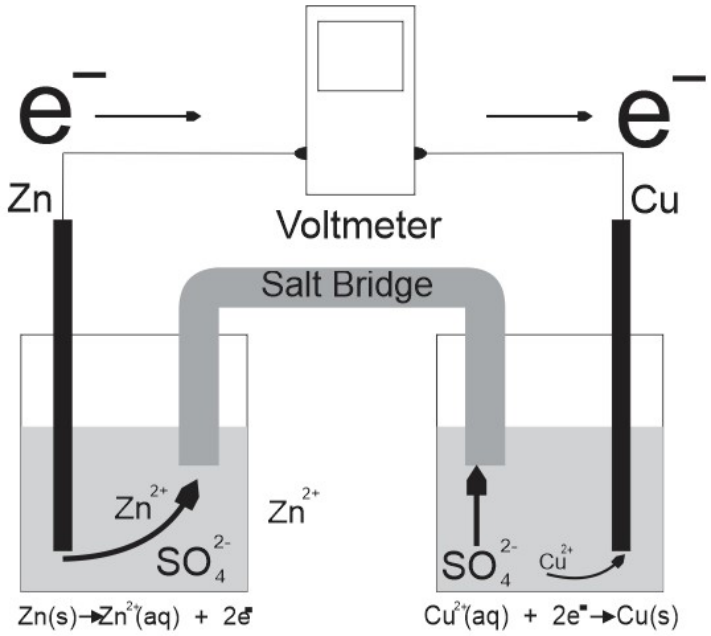

Figure 2.7. Redox Reaction: Zinc-Copper Cell[45]

In the grand scheme of electrochemical energy storage, secondary cells are exclusively used to store energy produced by solar PV arrays. The renewable energy sector makes abundant use of batteries. Industry uses secondary cells in a number of different applications such as:

- Uninterruptible Power Systems (UPS)
- Renewable energy (Photovoltaic systems, wind power)
- Emergency back-up systems
- Automotives

The most prevalent secondary cells are:

- Nickel Cadmium (NiCad)
- Lead acid
- Lithium-Ion

One of the most popular technologies in the battery sector is the Tesla Powerwall and Powerpack. Both products use Lithium-Ion technology. According to the Tesla Inc website[46], the Powerwall and Powerpack boast a total and usable energy of 14 kWh and 13.5 kWh, respectively.

While recent advancements in battery technology (such as that of Lithium-ion) have made renewable energy more attractive, there are few aspects that hinder this progress. These aspects include time to achieve full charge; overcharge; thermal runaway; formation of dendritic lithium (in lithium-ion batteries) and gas generation[47].Flammable gases such as oxygen, hydrogen and ethylene, together with known greenhouse gas, carbon dioxide, have led to battery rooms being constructed with critical gas extraction equipment[48]. Even though these obstacles prove to be problematic, secondary batteries are being used globally. One successful example is the Hornsdale Battery situated in South Australia. Hornsdale is supplied from a nearby wind farm which charges the battery with excess energy. Regarded as the world's largest lithium-ion battery, it has proven itself to possess an exceptional reaction time of 0.14 seconds[49].

2.3 Energy Storage and Renewable Energy

The problem of intermittency of renewable energy is well known and is well documented in literature. In fact it is often quoted as one of the leading inhibitors of the technology with issues such as output fluctuation, voltage dips and oscillation damping all due to intermittency. It is not difficult to establish that by addressing the issue of intermittency, the world could plausibly cease using fossil fuelled based power. Effective and efficient ESS can possibly solve intermittency.

With regards to wind power, fast output fluctuations are common. In fact, analysis of wind reports shows it can fluctuate in a matter of time of the order of a minute. In an isolated or micro power grid where wind power is used, voltage and frequency variation is not uncommon due to the fast output fluctuations. Several ESS technologies, such as dip proof inverters and rudimental uninterruptible power supplies, can potentially mitigate this problem. However, the selected ESS must meet a number of requirements. Due to the nature of wind power output large quantities of power, the ESS must be able to absorb large quantities of power quickly and possess high cyclability. Therefore, SMES and supercapacitors are most likely to be explored for this application[50].

Supercapacitors have already found applicationin wind power with supercapacitor modules being used for the specific purpose of reducing power fluctuations. Doubly-fed induction generators (DFIG) wind turbines are now designed to include supercapacitors in their DC-DC converters. Incorporating a control system, this allows for an optimized power output with minimal fluctuations[51].

In addition to supercapacitors, other storage systems such as flywheels and batteries and hybrids between supercapacitors, flywheels and batteries can be used to address power fluctuations in wind, solar and diesel power generation [52].

Other studies propose that the use of SMES in wind power plants or farms may reduce the capacity of bi-directional power converters by 60%. This is achieved by controlling the charging/discharge rates of the ESS[53].

In addition to power output fluctuations, the use of an ESS can mitigate low voltages or voltage dips. Should the design include grid connection, the system may be subject to the grid code laws for that country. Often, under these laws, voltage dips are not permitted since it could cause the failure of an entire network. Mitigation of voltage dips using an ESS is done in a similar fashion as that of power output fluctuations[53].

Supercapacitor and battery hybrid ESS are being used more and more in domestic renewable energy application. The positive properties of batteries and supercapacitors are both expressed in a hybrid system especially since commercial supercapacitors have yet to surpass batteries in terms of energy density. Lead-acid batteries, which are currently used in PV arrays, do not possess the ability of meeting fast power fluctuations in the same way that supercapacitors can. By combining the two technologies, supercapacitors are able to meet the instantaneous power demand thereby reducing the strain on the batteries and extending their life span while the lead-acid batteries are present to meet the energy demand [54].

A recurring theme in energy storage and renewable is that the same characteristics of an ESS tend to address the issues facing renewable energy plants. These characteristics are fast response time and high cyclability. This is expected due to the issues facing renewable energy plants being derivative of intermittency. In the same way that effective energy storage systems can resolve the issues already discussed. They can be applied to other difficulties such as load following, peak shaving, transmission curtailment, seasonal storage and time shifting.

2.4 Renewable Energy Power Generator

Photovoltaic arrays, as shown in Figure 2.8,output is direct current (DC). Since the vast majority of loads, both domestic and industrial, are that of an alternating current nature, the output of the PV array must be inverted. However, the energy storage system almost exclusively used with PV arrays is batteries. During the design of the battery bank, the designers ensure that the overall battery voltage is similar to that of the grid or system voltage. In terms of grid connection, it’s not always feasible to link enough battery cells to create a large enough voltage. In this case, transformers are used to bring the voltage level up to grid voltage.

Batteries are both charged and discharged with DC. This means, prior to DC/AC inversion, the batteries can be directly coupled to the PV array. While this is possible, the output voltage of the PV array is very seldom compatible with that of the required charge voltage of the battery. This is due to intermittency and the various ratings of components in the system. This gives rise to the need for a PV or a charge controller. These controllers consist of DC/DC converters (which raise or lower voltage as needed) and maximum power point tracking (MPPT).

This results in the system representation as shown in Figure 2.8. The PV generator or array feeds power to the PV controller. At this point the maximum possible power is extracted from the panels. The voltage is then adjusted to charge the battery bank. The DC output of the battery bank is then inverted to AC with the inverter which is directly coupled to the load. The figure shows a grid connected inverter instead of a simple inverter. This is due to the fact grid connected inverters contain a synchronizer within the design itself. The synchronizer ensures that the PV system is in phase with the grid before actually establishing a connection to the grid.

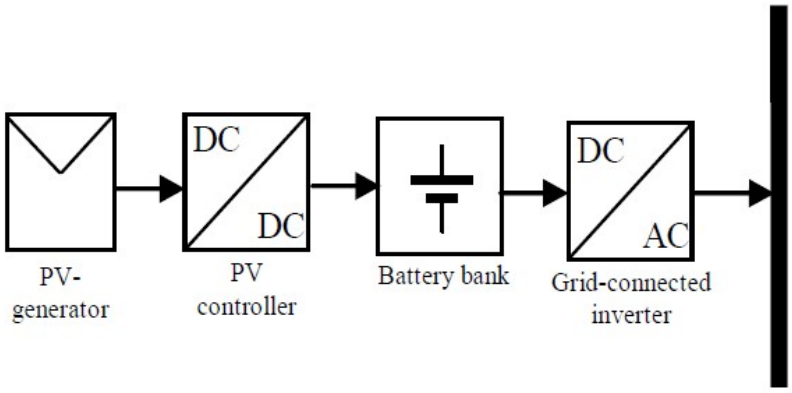

Figure 2.8. Grid Tied PV Generator System

The wind power system operates in a similar fashion with the exception that the output is AC. With grid tied systems, the AC is rectified to DC and back to AC. This is done so that batteries may be charged using DC. An energy storage system in renewable energy plants is vital for meeting intermittency but it also ensures a stable supply. Wind is more erratic than sunlight therefore an energy storage system with a quick response time is crucial to the quality of supply.

This study aims at determining whether or not supercapacitors would be a viable replacement for batteries in this respect. However, the circuit in which batteries are used must be altered to accommodate supercapacitors. Several concerns must be raised in determining an effective circuit. These being:

- Charge and discharge voltage. Supercapacitors can be connected together in series and parallel to adjust overall supercapacitor bank voltage. However, each connection topology has advantages and disadvantages such as increased resistance and decreased overall capacitance. Commercial suppliers have already pre-arranged these supercapacitors in modules to serve various purposes with a balance between voltage and capacitance in mind for the application. Nevertheless, circuitry is required to bring the charge voltage down to ensure that the supercapacitor charge voltage limit is not exceeded. On the discharge side, voltage must be stepped up without decreasing overall capacitance.

- Nature of charge and discharge. Supercapacitors must be charged using DC. Therefore, charging with a wind turbine will require rectification. With regards to discharge, as mentioned, majority of loads are AC in nature and hence an inverter will be required.
- Arrangement topology. These connection topologies may prove to be better for either charging or discharging. Specifically, a parallel connection may be better for charging while serial better discharge or vice versa.

With these areas as focal points, an appropriate circuit may be developed.

2.5 The Concepts of Supercapacitor (Ultracapacitor)

Capacitors can be found in many circuits. They can be found in many fields from small electronics to power transmission, serving a wide range of purposes (such as filtering and power factor correction).

A conventional capacitor stores electrical potential energy in the form of an electric field, between two conductors, across a dielectric or an electrolyte. Within a capacitor, the dielectric acts to increase the charge storage capacity.

Super or ultra-capacitors, henceforth referred to as supercapacitors, can be traced back to April 14th, 1954 when General Electric employee, Howard I. Becker applied for a patent termed "Low Voltage Electrolytic Capacitor"[55]. In this patent he describes that his invention utilizes porous activated carbon electrodes with a sal ammoniac (ammonium chloride NH_4Cl) electrolyte to achieve 6 Farad at 1.5 V_{DC}. Even at this early stage, it is known that the capacitor is limited to low voltages due to the low ionization voltage of the electrolyte (± 2.5 V) which remains as one of the primary limitations of the technology. Becker conceded that it is not fully understood what occurs when used as an energy storage device. He had originally constructed a model for the patent which was 5 cm in length with 1 cm diameter which had a capacitance of 0.8 F (at 1.5 V_{DC}).

Comparing Becker's invention with a conventional capacitor (assuming a separation distance of 1 mm with NH_4Cl as a dielectric):

$$C = \frac{\varepsilon A}{d} \tag{2.6}$$

$$0.8 = \frac{8.84\times10^{-12}\times7\times A}{0.001}$$

$$A = 12\ 928\ 248.22\ m^2$$

Permittivity of NH_4Cl is 7

Determining the energy in Becker's capacitor:

$$E = \frac{1}{2}CV^2 \tag{2.7}$$

$$E = \frac{1}{2} \times 0.8 \times 1.5^2$$

$$E = 0.9\,J$$

Therefore, the Becker's invention was able to store the same amount of energy as a conventional capacitor while occupying a fraction of the space.

Even though unable to fully explain the capacitor as an energy storage device, he does postulate that the exceptional capacitance is governed by the large surface area of the electrodes.

Supercapacitors are often referred to as electric double layer capacitors or EDLCs. They are classified into three categories according to the method of charge storage and subcategorized by the material of the electrodes:

- Electrostatic Double Layer Capacitors (non-Faradaic charge storage mechanism)
    - Activated carbon
    - Carbon aerogel
    - Carbon nanotubes

- Electrochemical Pseudocapacitors
    - Conducting polymers
    - Metal Oxides
- Hybrid capacitors
    - Composite hybrids
    - Asymmetric hybrids

Pseudocapacitors and EDLCs employ Faradaic and non-Faradaic charge storage mechanisms, respectively, while hybrid capacitors use an amalgamation of both. The prime difference between these processes is that Faradaic refers to a Redox or reduction-oxidation reaction while non-Faradaic is not an entirely chemical reaction. To further elaborate, a Faradaic process contains the transmission of electrons between the electrode and electrolyte as demonstrated in a Standard Reduction Potentials table (also referred to as the Standard Electrode Potentials Table).A non-Faradaic process does not constitute the breakdown of chemical bonds, nor the production, instead charge is stored electrostatically[56].

In EDLCs, the three main components found are the electrolyte, electrodes and a separator. As the name suggests, EDLCs store energy in the double layer formed at the interface between the electrode and electrolyte. It is this double layer and high surface area of electrode material that contribute to the

large capacitance and extremely high energy densities. By introducing a potential difference across the electrodes, positive charge accumulates on one electrode and negative on the other. Within the electrolyte, ions are attracted and repelled by the charged electrodes thereby creating a double layer at each electrode, as illustrated in Figure 2.9.

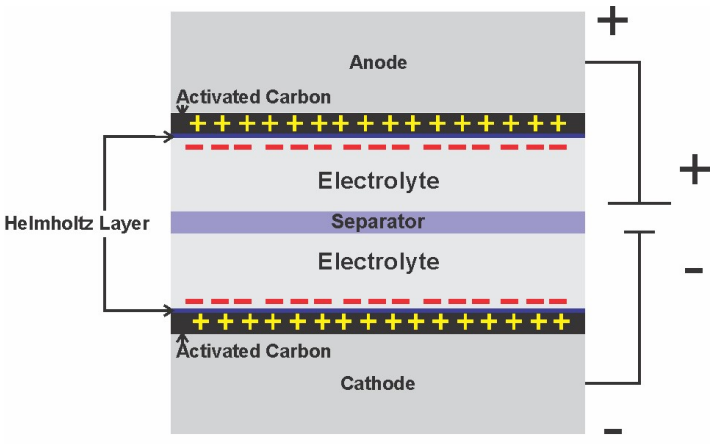

Figure 2.9.Structure of Supercapacitor[57]

This double layer is referred to as the Helmholtz Layer, named after Herman von Helmholtz who discovered this effect in the 19th century[58].

Cell voltages of EDLCs range between 1V and 3.5V depending on the type (aqueous or organic) of electrolyte used[59].

As previously mentioned, pseudocapacitors use a Faradaic process incorporating redox reactions, to store charge. Even though the Faradaic process allows for larger energy densities and capacitance, their cyclability is greatly reduced as compared to that of EDLCs. This is due to the mechanical stress placed on the electrodes during redox reactions[60].

The hybrid supercapacitor is an attempt to combine the positive attributes of both EDLCs and pseudocapacitors. These attributes are the high power and energy densities of pseudocapacitors with the large cyclability of EDLCs. To accomplish this electrodes from the aforementioned capacitors are combined in two ways resulting in two distinct types of hybrid supercapacitors. To construct an asymmetric hybrid, a single carbon based EDLC electrode is used in conjunction with a conducting polymer pseudocapacitor electrode. The composite hybrid electrodes are constructed by combining the materials from both supercapacitors[56].

Even though it is not incorrect to say that hybrid supercapacitors are a combination of pseudocapacitors and EDLCs, many authors refer to them as a combination of batteries and EDLCs. This may be due to the most prevalent hybrid in commercial production, the lithium-ion capacitor

(LIC). Lithium-ion batteries are well known throughout the world and are often considered the first choice in many design application such as mobile phones. The Hornsdale Battery in Australia, as previously mentioned, is also a lithium-ion battery.

LIC falls with the category of asymmetric hybrid since one electrode is fabricated of activated carbon (positive) and the other of one which allows intercalation of lithium ions (negative)[61]. Both Maxwell Technologies® and Nesscap® are just two examples of manufacturers that commercially produce LICs.

Supercapacitors, like conventional capacitors are capable of rapid charging, achieving full charge in seconds or minutes. The main limitation on this technology is the low specific energy. Lithium-ion batteries possess a specific energy of up to 250 Wh/kg[62], whereas the recently developed graphene based supercapacitors reaches up to 85.6 Wh/kg[60]. However, in a certain journal article[13], the authors describe a method in which a specific energy of 257 Wh/kg at a specific power of 867 W/kg was achieved by constructing a lithium-ion hybrid supercapacitor with a silicon carbon composite anode and a cathode comprising of biomass extract activated carbon, effectively surpassing lithium-ion batteries. Attributes of the supercapacitors that tends to draw attention is that of the large specific power and life cycle. They are capable of delivering large amounts of power within short periods while maintaining their energy storage capacity. In comparison, batteries tend to lose their ability to store energy due to the chemical reactions taking place within them[63].Research is ongoing with graphene showing promising results as researchers have identified that greater performance is based on the ion accessibility along with pore size and uniformity of electrodes[60].

2.6 Application of Supercapacitors

Supercapacitors are already pragmatic in a number of applications. Notably, in regenerative braking in vehicles and bicycles, where the supercapacitor stores the energy that would otherwise be lost during the braking process [64]. In this application, the supercapacitor is perfectly suited due to its ability to quickly store energy and high cyclability.

The supercapacitor has also been applied in hybrid capacity in electric vehicles (including hybrid and plug-in hybrid) to reduce the strain on the conventional car battery, thereby increasing the battery lifespan. To achieve this, the supercapacitor is used in regenerative braking, thereby preventing the battery from receiving short burst of energy. In a selected journal article[65], the system is designed to only use the battery when the supercapacitor (referred to as ultracapacitor in the article)voltage dips below that of the battery. The authors explore a few methods for an effective energy storage system (ESS) including designs incorporating a bi-directional buck-boost converter and an inverter (Figure 2.10). Since vehicles do not operate in constant speed or velocity, the authors outline four modes of operation for the ESS; constant low speed, constant high speed, acceleration and deceleration[65].

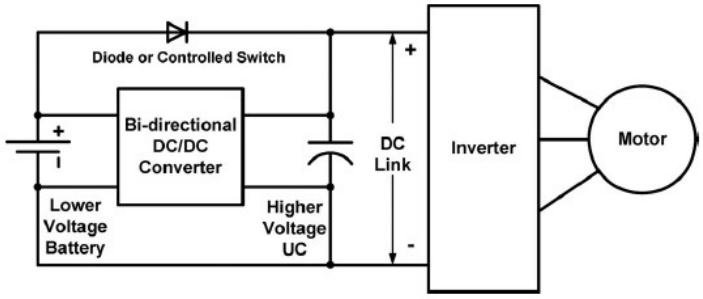

Figure 2.10.Hybrid Energy Storage System [65]

Implementing an effective energy management system (EMS) is often incorporated with designs regarding renewable energy (Figure 2.11). With the emergence of supercapacitors, EMSs have been designed using both batteries and supercapacitors, creating a hybrid ESS. Again, this type of ESS implements supercapacitors in a protective role by preventing exposure of large currents to the battery which may degrade it [66].

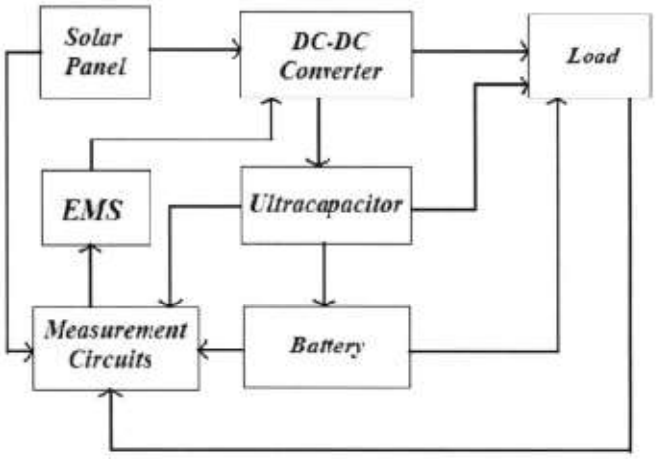

Figure 2.11. Block diagram of Solar Energy System [66]

In 2009 Shanghai, China had over 15 electric buses operating with supercapacitors. At the time, they have been running for three years without failure. The supercapacitor (referred to as ultracapacitors in the article) manufactured by Shanghai Aowei Technology Development Co. Ltd, possess a low energy density of 6 Wh/kg[67]. Sinautec Automobile Technologies together with the aforementioned company have implemented a technique which overcomes low energy density limitation of the supercapacitor used. Since the buses travel short distances, not much energy is required to reach each stop where it the supercapacitors can be re-charged using a solar powered charging station. Sinautec claims that due to the regenerative braking and the implementation of supercapacitors, the buses require 10% of the energy required by conventional diesel buses thereby achieving a fuel savings of

the order of hundreds of thousands of dollars within the lifespan of the vehicle[68]. This being due to the fact that larger engines are fuel inefficient with start-stop trips in urban areas.

Supercapacitors in the fields of energy storage and power engineering are rapidly gaining momentum with the rise in attributes such as specific energy and specific power. In recent years, supercapacitors have found pragmatic application in a number of environments, including aviation. In power generation, they have been found useful on providing an essential service in the form of peak power shaving, thereby reducing the size of generators [69].

2.7 Supercapacitor Transmission Line Model

Figure 2.12 depicts an equivalent model (the simplified model) for a supercapacitor where ESR and EPR stand for equivalent series resistance and equivalent parallel resistance, respectively. This type of model is often used for principle verification [70].

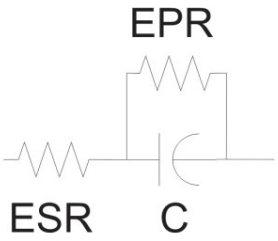

Figure 2.12. Supercapacitor Equivalent Model

As previously mentioned, in order to obtain the largest possible specific energy and capacitance for a supercapacitor it is necessary to increase the surface area between electrode and electrolyte. This may increase the total volume of the device although since it is desirable to obtain a large energy density, volume must be controlled. To achieve this, materials with high surface areas are used. These materials are often made of activated carbons or some derivative thereof.

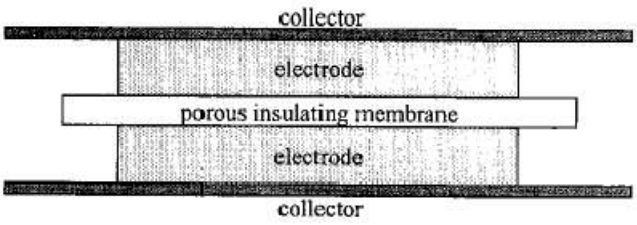

Figure 2.13. Supercapacitor Packaging Principle [71]

The Figure 2.13 above is a simplified version of Figure 2.9. However, it is from Figure 2.13 that the theoretical model of a supercapacitor can be obtained. Referring to this figure, it can be simply put

that supercapacitors are composed of activated carbon electrodes infused with an electrolyte. The electrodes are then separated by a porous membrane with the entire structure housed within metallic collectors [71].

Due to the number of materials used to construct a supercapacitor, its behaviour can only be described using a combination of resistors and non-linear capacitors as illustrated by Figure 2.14.

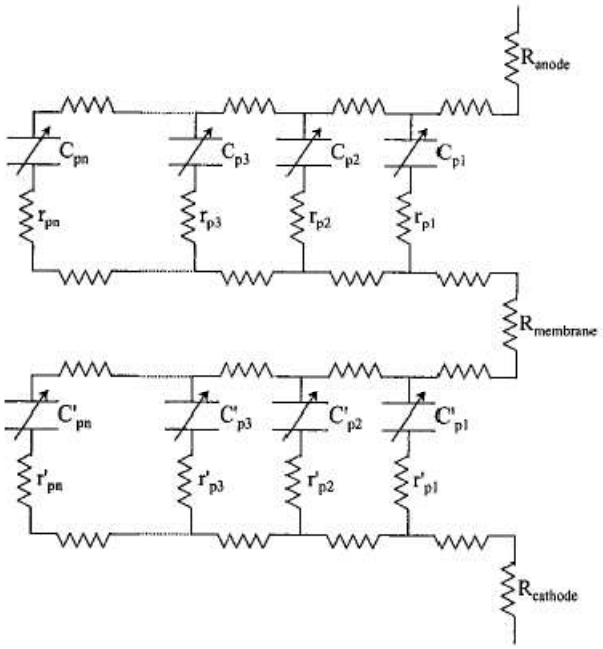

Figure 2.14. Theoretical Model of the Supercapacitor [72]

Each resistor in the figure depicts the resistance of a component of the supercapacitor. The parameters of these ultimately results in these resistances. These being:

- Electrode material
- Pore size
- Porosity of insulating membrane
- Housing material
- Electrolyte

By manipulating these key areas, the overall resistances are altered and so the specific energy and capacitance of the supercapacitor. Thus, the theoretical model of the supercapacitor can be regarded as similar to a transmission line with voltage dependant distributed capacitance [73].

For this study, the Maxwell 51V 189FDuraBlue^{TM} BMOD0189 P051 B2A was selected due to its relative large capacitance and voltage. According to the datasheet, the module is comprised of 18

individual supercapacitor cells. The derived equivalent circuit of this supercapacitor is shown in Figure 2.15[73]. This circuit can be used to determine the terminal behaviour of the module.

The total capacitance of the module can be expressed by a constant capacitor and a variable capacitor whose capacitance varies with cell voltage. The capacitance of singular cells that comprise a module is described in the following equation [73]:

$$C_{cell} = C + bV, \tag{2.8}$$

Where b is a constant to accommodate the varying capacitance.

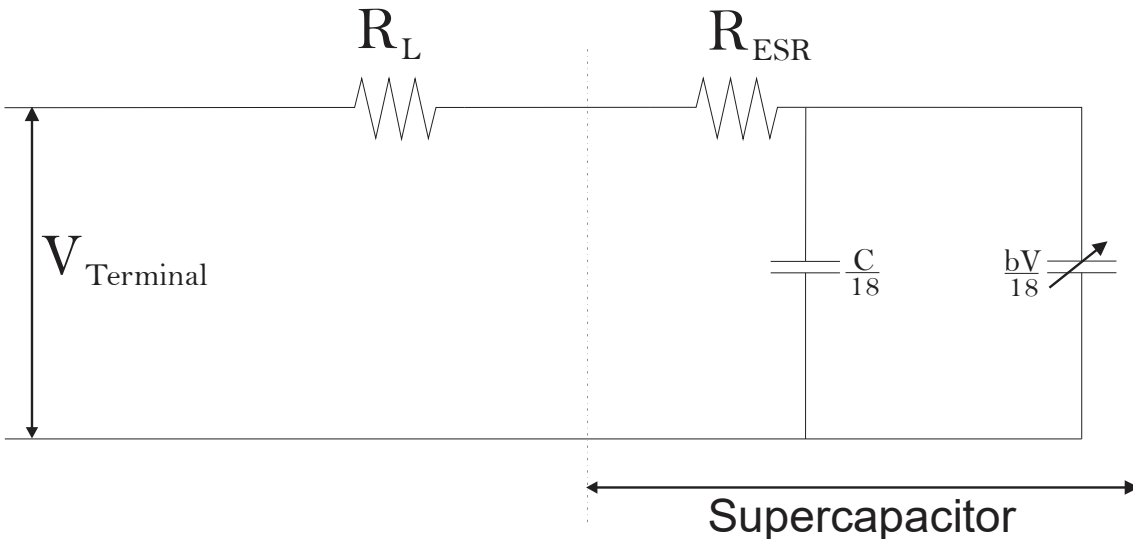

Figure 2.15.Derived Equivalent Circuit of Maxwell 51V DuraBlue™ BMOD0189 P051 B2A

In Figure 2.15, R_{ESR} represents the equivalent series resistance. It is this resistance that adds to the losses when the supercapacitor is being charged and discharged. Neglected from this circuit is the equivalent parallel resistance which is largely responsible for the self-discharge of the supercapacitor. The inductance which arises from the actual construction of the module is especially small and has not been represented in Figure 2.15.

The module contains 18 cells, the total capacitance is given by [73],

$$C_{tot} = \left[\frac{1}{C_1} + \frac{1}{C_2} + \cdots + \frac{1}{C_{18}}\right]^{-1} \tag{2.9}$$

$$C_{tot} = \frac{1}{18} C_{cell}$$

Substituting equation (2.9) in equation (2.8) results in:

$$C_{tot} = \frac{1}{18}[C + bV] \tag{2.10}$$

By linking the supercapacitor cells in series, a sequence of series connected resistances is formed. The total resistance is given by,

$$R_{ESR} = 18\, R_{esr} \tag{2.11}$$

By considering the two capacitances in Figure 2.15 as a single one C_{tot} and applying Kirchhoff's voltage law[73],

$$V_{Terminal} = \int \frac{i}{C_{tot}} dt + [R_L + R_{ESR}]i \tag{2.12}$$

However, $i = \frac{dq}{dt}$ therefore,

$$V_{Terminal} = \frac{q}{C_{tot}} + [R_L + R_{ESR}]\frac{dq}{dt} \tag{2.13}$$

Since $q = C_{tot}V$, where V is the capacitor voltage, equation (2.14) is formed which is subsequently simplified to equation (2.15) and derived to equation (2.16).

$$V_{Terminal} = \frac{C_{tot}V}{C_{tot}} + [R_L + R_{ESR}]\frac{d(C_{tot}V)}{dt} \tag{2.14}$$

$$V_{Terminal} = V + [R_L + R_{ESR}]\frac{dV}{dt}\frac{1}{18}[C + bV] \tag{2.15}$$

$$\frac{dV}{dt} = \frac{18\,(V_{Terminal} - V)}{(C+bV)(R_L+R_{ESR})} \tag{2.16}$$

Taking equation (2.12) and neglecting the infinitesimally small R_L, at the time of switching t = 0,

$$V_{Terminal} = R_{ESR}i + \int \frac{i}{C_{tot}} dt \tag{2.17}$$

The product of this equation and C_{tot} with the derivative,

$$0 = C_{tot}R_{ESR}\frac{di}{dt} - i \tag{2.18}$$

By multiplying the above equation with the total equivalent series resistance and noting Ohm's Law,

$$0 = \frac{dV}{dt}C_{tot}R_{ESR} - V \tag{2.19}$$

Solving this equation results in [73],

$$V = ke^{\frac{t}{R_{ESR}C_{tot}}} \tag{2.20}$$

2.8Economics of Supercapacitor Technology

As with all technology, cost has a vital role in supercapacitors. As this technology becomes more widely used its cost decreases making it more attractive to implement in design.

Table 2.1. Supercapacitor Cost Trend [73, 74]

Year	Cost/Farad in USD	Cost/kJ in USD
1996	0.75	281.55
1998	0.40	151.23
2000	0.01	32
2002	0.023	7.51
2006	0.010	2.85
2010	0.005	1.28

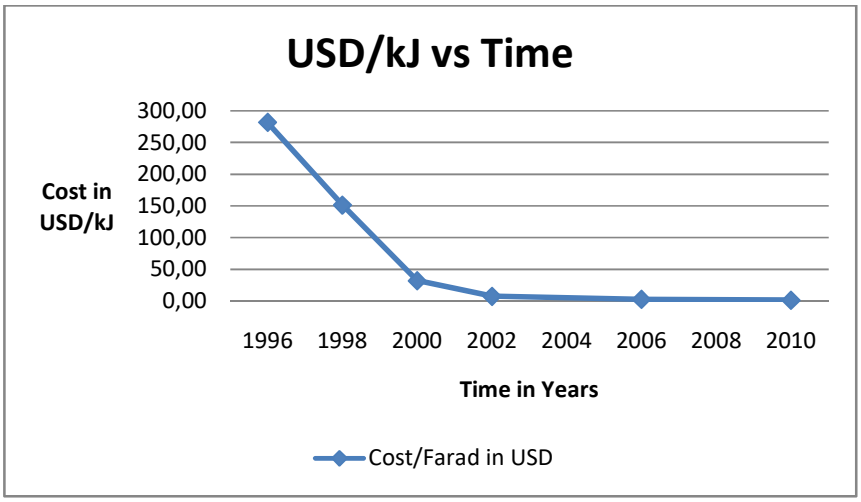

Figure 2.16.Graph of USD/kJ vs Time

It is evident from Table 2.1 and Figure 2.16, that the price of supercapacitors is dropping at a fast rate. This is further supported by news that the industry is expected to exceed $2 billion by 2022 from being below $700 million in 2016 [73, 74].

2.9 Potential Benefits of Supercapacitors

From the literature reviewed as presented in this chapter, it is apparent that supercapacitors do possess the potential to act as an energy storage device. Although this has only been tested with relatively smaller load applications, recent advancement in commercial and experimental supercapacitors [13, 64] may possibly allow for larger loads to be supplied with supercapacitors.

Research suggests that supercapacitors have already begun making an impact in the renewable energy sector. The charging mechanisms often discussed are fairly uncomplicated with supercapacitors connected in series with each other and parallel to the source, charging them via transformers and DC-DC converters depending on the source output. This lowers the effective voltage across the capacitor in order to prevent the applied voltage exceeding breakdown or ionization voltage. Often, these designs are of a hybrid nature due to their interconnection with batteries. This is commendable due to the fact that supercapacitors lag behind batteries in some respect therefore combining both technologies in a single design allows for the designer and user to take advantage of both attributes (Figure 2.17). The hybrid designs extend the lifespan of the battery by subjecting the supercapacitor to the larger in-rush (or surge) currents[65]. As mentioned in this chapter, the supercapacitor technology has the capability of being used in energy storage systems to curtail several issues facing renewable energy. With such issues many, if not all, stemming from intermittency.

Other charge topologies are not explored. While the present charge mechanism is reliable, capacitor interaction dictates that they can be charged in more than just one method. Connecting them in series reduces the overall capacitance while a parallel link retains the original voltage and increases capacitance.

With regards to discharge, there are no substantial loads applied while observing the decay over the supercapacitor. This is of paramount importance since supercapacitors, with the exception of the most recent experimental developments[13], tend to store less energy than their battery counterparts [62]. As mentioned in previous paragraphs, a serial connection lowers the overall capacitance. This reduces the effective useful duration of the supercapacitor making it impractical for larger loads. Nevertheless, the serial connection has proven itself in terms of using the supercapacitor in a protective capacity.

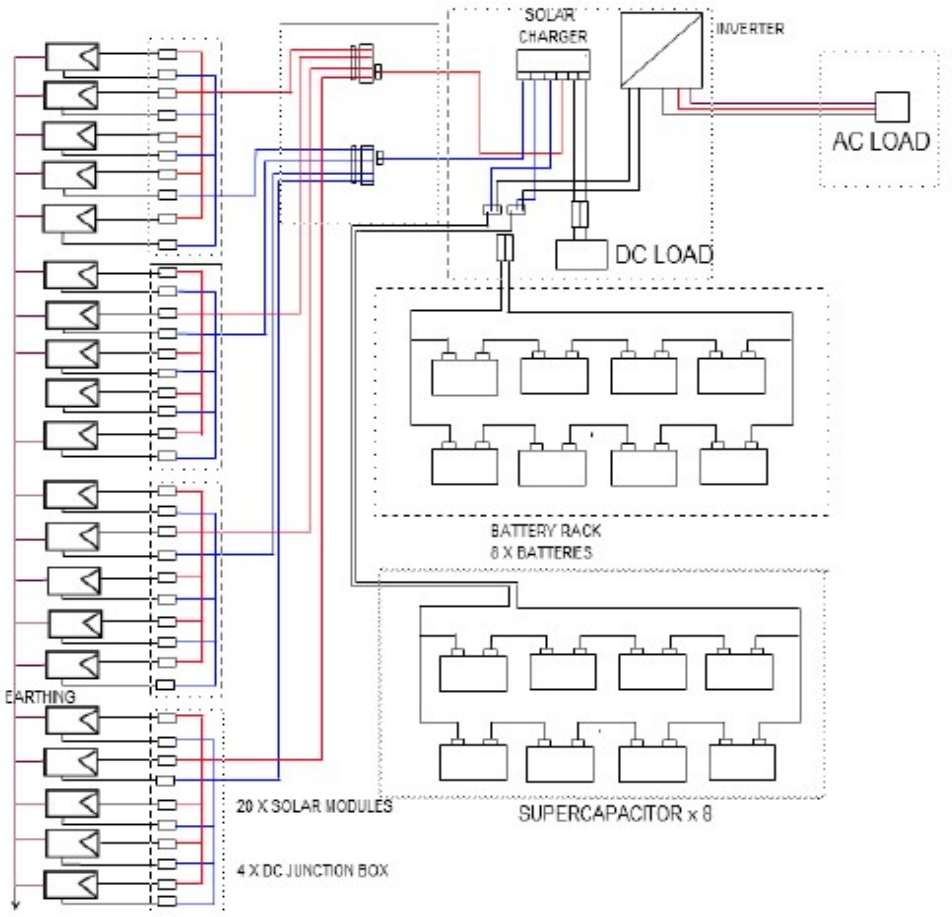

Figure 2.17. Solar PV System with Supercapacitors [75]

Other sectors have resigned to use supercapacitors for its quick release of energy for boost applications such as UPSs. Automotives requiring less energy and brief charging times have also found supercapacitors to be valuable. Should the Sinautec Automobile Technologies supercapacitor bus project[68] be implemented widely throughout China, carbon emissions in the country could be lowered by a large factor. These automotives also employ regenerative braking [64]which could, in theory, be applied to loads such as motors. In the example of a single or three phase motor, regenerative braking could be used to stop the rotor as an alternative to electrical plugging, brake pads or allowing the rotor to freely run down. Using this technique could charge up the supercapacitor to a usable degree.

The economic analysis provides data to prove that as supercapacitor technology disseminates throughout society, the overall cost decreases. More companies are applying supercapacitors as the technology continues to improve. Generally regarding cost, an asymptote is reached at some point, however this point is yet to be reached in this area. The cost may very well lower even further before they begin to rise.

Chapter Three

Specifications and Analytical Modelling

3.1 The Systems Specifications

The main aim of this study is to determine whether or not supercapacitors are a viable means of energy storage for power engineering applications on a domestic scale. The supercapacitor was used in conjunction with renewable sources such as wind and solar due to the problem of intermittency when supplying power. The industrial standard has thus far been used for electrochemical batteries for wind and solar plants. Therefore to incorporate supercapacitors, an innovative design is required.

The nature of current output from the wind turbines is AC. To charge the supercapacitor, this AC must be rectified to DC and the voltage stepped down to an acceptable level to prevent dielectric breakdown of the supercapacitor and the air in the vicinity of the terminals. The balance of the power generated can be converted back to AC to supply an AC load.

Depending on the number of panels connected in series, the voltage must either be stepped up or down. The general rule of thumb is to arrange a PV array to output at system voltage, therefore a DC/DC buck converter is required to step down the voltage to be suitable for supercapacitor charging.

Supercapacitors output is DC. The voltage output is low since commercial suppliers manufacture supercapacitors for specific applications. With capacitor fundamentals applied, the capacitance increases as voltage decreases. Consequently, the DC/DC booster and inverter is required or alternatively is an inverter and a transformer.

One of the prime advantages of supercapacitors over batteries is that supercapacitors cannot be overcharged. Once the supercapacitor is charged, it then operates as an open circuit. This eliminates need for additional circuitry as required by systems that include electrochemical batteries. However, other circuitry is required during the switching of supercapacitors.

Another advantage of supercapacitors is their high cyclability which can be applied here. Systems with batteries can have the battery bank in parallel with the source with a control system to determine from which source the load is supplied. A similar method can be used with supercapacitors. This is illustrated in Figure 3.1. The high cyclability and lifespan allows for a system without a control system. One in which the supercapacitor bank in consistently charging and discharging.

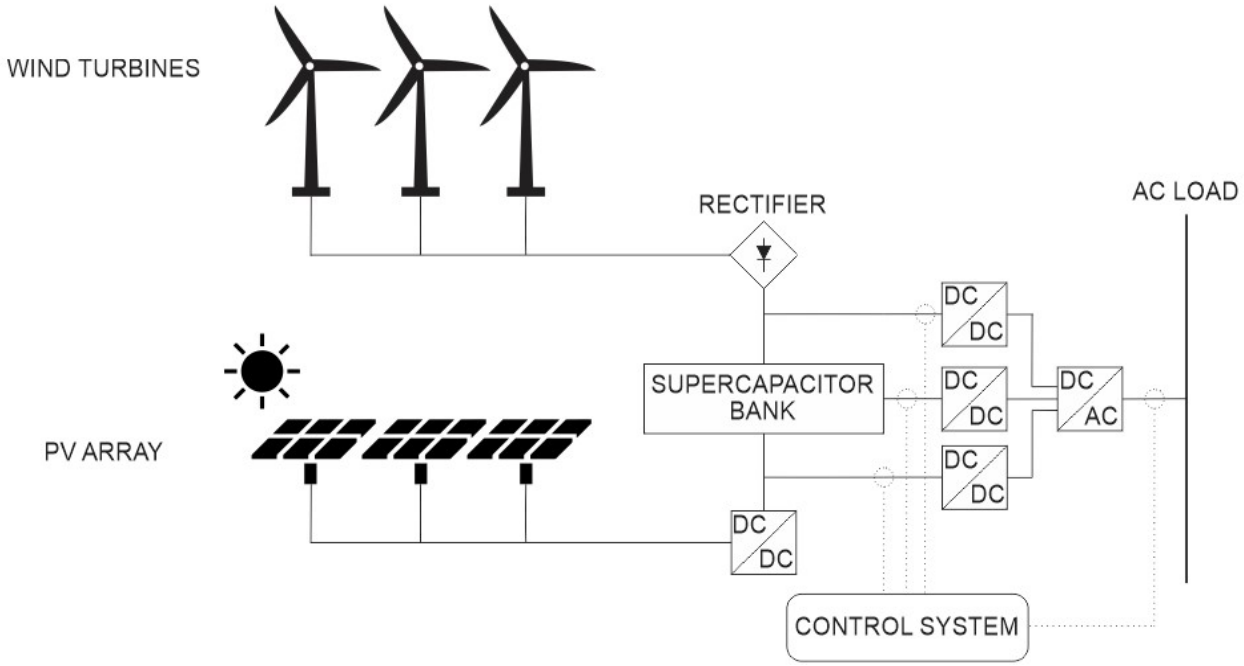

Figure 3.1. Supercapacitor System with a Control System

In this design, load is only supplied by the supercapacitor bank as shown in Figure 3.2. While this circuit may not require a control system in the conventional sense, a system to actively have one supercapacitor connected at all times is required. This is true for both circuits. The advantage of the circuit in Figure 3.2 includes a seamless response time since there is virtually no moment where supply is switched to the ESS. Also, another advantage is the lower cost due to less components, circuitry and no control system and simplicity. Its disadvantage is that the lifespan of the supercapacitor may be affected.

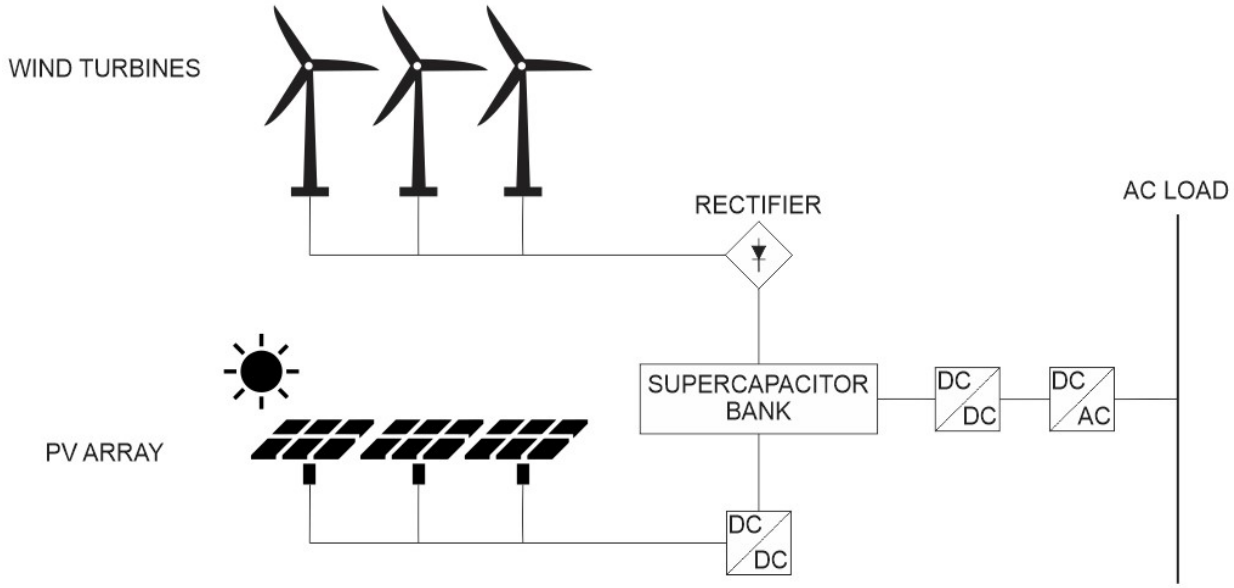

Figure 3.2. Supercapacitor System without a Control System

3.2 Load Schedule

Testing the viability of the supercapacitor requires a load. In this study, a single phase domestic load is tested using an assumed typical South African middle-income household. The loads documented in the Table 3.1, have been selected to operate at maximum capacity. By calculating the apparent, active and reactive power, a simulation was done, with the implementation on MATLAB/Simulink using the "Series RLC Load" block.

Table 3.1. Domestic Load Schedule

Appliance	Quantity	Power kW	Hours	kWh
Tumble Dryer	1	4	1	4
Stove	1	4	1	4
Oven	1	4	1	4
Geyser	1	3,5	12	42
Aircon	1	3	12	36
Water Tank	1	0,37	24	8,88
Hair Dryer	1	2	1	2
Radio	1	0.1	10	1
PC	1	0.2	8	1,6
Kettle	1	1,5	1	1,5
Dishwasher	1	1,5	1	1,5
Microwave	1	1	2	2
Washing Machine	1	1	2	2
Lights	20	0.06	12	14.4
Fridge combined	1	0,5	24	12
Television	2	0,3	12	7,2
Total	***36***	***27.03***	***124***	***144,08***

Note that the "water tank" is colloquially referred to as a "JojoTank pump", which supplements the household water supply.

All loads documented in the Table 3.1 are AC loads and possess a form of reactive and active power. Therefore, using the equations (3.1- 3.3), described below with the assumption of a 0.8 power factor, Table 3.2was constructed.

Thus, given that the system is 220V AC, the current can be calculated using the following equation:

$$S = V.I \tag{3.1}$$

The true power is already known hence the apparent power can be determined:

$$\cos\theta = \frac{P}{S} \tag{3.2}$$

Using the apparent power that from the previous equation, the reactive power can be calculated by rearranging the following:

$$S = \sqrt{P^2 + Q^2} \tag{3.3}$$

Table 3.2. Domestic Loads with Power Ratings and Current

Appliance	Quantity	Current (A)	Power Factor	Power		
				Apparent (kVA)	Active (kW)	Reactive (kVAr)
Tumble Dryer	1	22.728	0,8	5	4	3
Stove	1	22.728	0,8	5	4	3
Oven	1	22.728	0,8	5	4	3
Geyser	1	19.886	0,8	4,375	3,5	2,625
Aircon	1	17.05	0,8	3,75	3	2,25
Water Tank Pump	1	2.1	0,8	0,4625	0,37	0,2775
Hair Dryer	1	11.364	0,8	2,5	2	1,5
Radio	1	0.568	0,8	0,125	0,1	0,075
PC	1	1.136	0,8	0,25	0,2	0,15
Kettle	1	8.522	0,8	1,875	1,5	1,125
Dishwasher	1	8.522	0,8	1,875	1,5	1,125
Microwave	1	5.686	0,8	1,25	1	0,75
Washing Machine	1	5.686	0,8	1,25	1	0,75
Lights	20	6.814	0,8	1.5	1.2	0.9
Fridge combined	1	2.839	0,8	0,625	0,5	0,375
Television	2	3.411	0,8	0.75	0.6	0.45
Total	**36**	153,580	**0,8**	**35,59**	**28,47**	**21,35**

In reality, it is unlikely that these loads will operate simultaneously. In the event that they do run simultaneously, the main circuit breaker would trip on overcurrent. Therefore, the loads must be split. This would, in turn, reduce cable sizing, heating and hence, losses.

According to the Maxwell 51V Durablue™ datasheet each module can only deliver 100A (with absolute maximum being 1900A). This places a limitation on the load per module. By accounting for start-up inrush or surge current a reasonable assumption would be to limit a total of 70A applied to each module. Table 3.3 outlines how the loads were allocated. Circuit 1 carries the essential loads while the loads on circuits 2 and 3 were categorized by load size.

Table 3.3. Domestic Load Divided into Three Main Circuits

Circuit 1	Current (A)	Circuit 2	Current (A)	Circuit 3	Current (A)	Power Factor
Stove	22.728	Tumble Dryer	22.728	Oven	22.728	0.8
Geyser	19.886	Aircon	17.05	Hair Dryer	11.364	0.8
Lights	6.814	Computer	1.136	Radio	0.568	0.8
Fridge	2.839	Dishwasher	8.522	Kettle	8.522	0.8
Water Tank	2.1	Washing Mac.	5.686	Microwave	5.686	0.8
				TV	3.411	0.8
Total	**54.37**	**Total**	**55.122**	**Total**	**52.279**	

In this design, each circuit will carry a dedicated set of supercapacitor modules. From this set of supercapacitors, a single Maxwell 51V Durablue™ module will supply the circuit at any given time. Once this module depletes to a supply voltage outside a usable range (220-240V), it is switched off and the next available module is switched on to supply the circuit as illustrated in Figure 3.3.

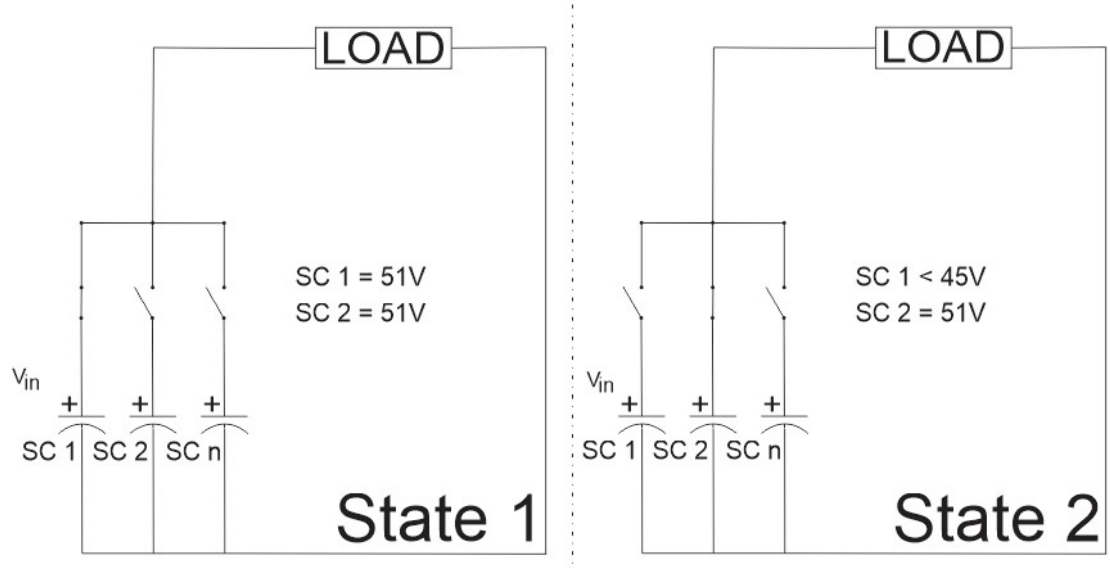

Figure 3.3. Supercapacitor Switching Strategy

3.3 Discharge Circuit

Capacitors and supercapacitors discharge using DC. This DC must be converted to AC using an inverter circuit. Supercapacitors are restricted to certain voltages. For this study, the Maxwell 51V 189F supercapacitor was selected due to its commercial availability and acceptable balance between potential difference and capacitance. In order to raise the voltage to the needed range of 220-240V, it is possible to design a serial arrangement by accepting that overall capacitance reduces accordingly. A

DC booster circuit is able to provide this increase in voltage without compromising on capacitance. Alternatively, incorporating a transformer in the design will achieve the same result, albeit with more losses. These topology overviews can be seen in Figure 3.4.

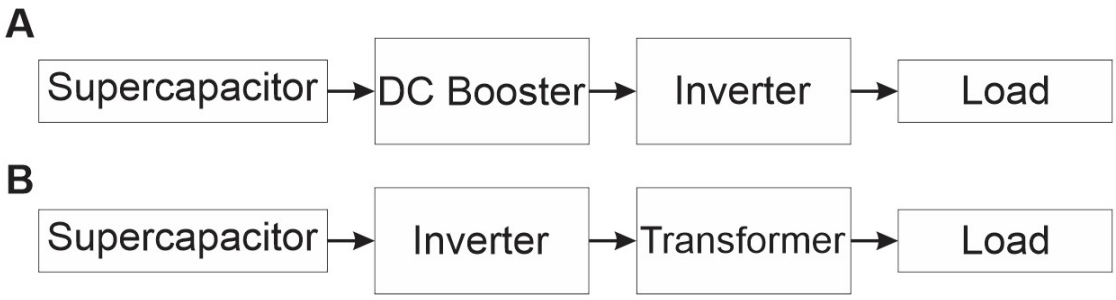

Figure 3.4.Simplified Overall Discharge Circuit with (A) DC Booster and (B) Transformer

3.3.1 The DC Booster Circuit

The circuit must output a voltage in the region of 250 V with an input voltage of 51V. It must also be able to deliver a current of up to 70A. Note that in this study, the load is of an AC nature and was calculated earlier to be $58.92\angle 36.88°$ A, $65.34\angle 36.86°$ A and $57.53\angle 31.43°$ A for circuits 1, 2 and 3 respectively. Due to the difference in nature between the load and source, the design of the DC booster will use the upper current limit per circuit of 70 A.

To design a DC Booster Circuit, as shown in Figure 3.5, there are a number of properties to be considered:

- Switching frequency (30 kHz)
- Duty cycle
- Size of inductor L
- Size of capacitor C

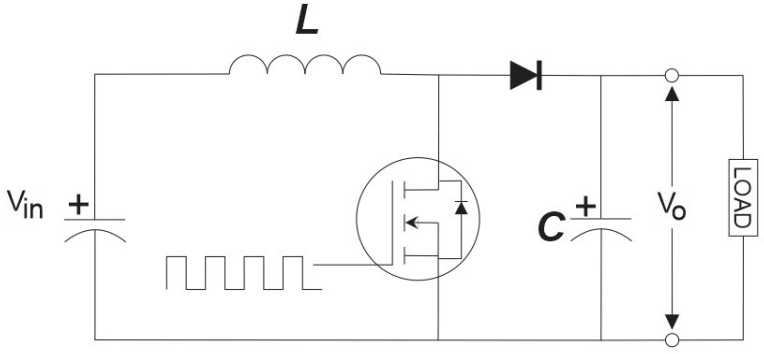

Figure 3.5. DC-DC Booster Circuit with a Supercapacitor providing V_{in}

Referring to Figure 3.5, to determine the duty cycle of the mosfet, the input and output voltages are required:

$$\frac{V_{out}}{V_{in}} = \frac{1}{1-D} \tag{3.4}$$

$$\frac{250}{51} = \frac{1}{1-D}$$

$$D = 0.796 \; or \; 79.6\%$$

The average current through the inductor:

$$I_{L(ave)} = \frac{I_{load}}{1-D} \tag{3.5}$$

$$I_{L(ave)} = \frac{70}{1-0.796}$$

$$I_{L(ave)} = 343.14 \; A$$

Assuming a 10% ripple in a current range given by:

$$\Delta I_L = 0.1 \; I_{L(ave)} \tag{3.6}$$

$$\Delta I_L = 0.1 \; \times 343.14$$

$$\Delta I_L = 34.314 \; A$$

Since the switching frequency is 30 kHz, the period is given by:

$$T = \frac{1}{f} \tag{3.7}$$

$$T = \frac{1}{30\,000}$$

$$T = 33.33 \; \mu s$$

The transistor turn on time:

$$t_{on} = D.T \tag{3.8}$$

$$t_{on} = 0.796 \times 33.33 \times 10^{-6}$$

$$t_{on} = 26.53 \; \mu s$$

Now, the inductance can be calculated:

$$L = \frac{V_{in} t_{on}}{\Delta I_L} \tag{3.9}$$

$$L = \frac{51 \times 26.53 \times 10^{-6}}{34.314}$$

$$L = 39.4\ \mu H$$

Ideally, the ripple voltage should be 0% however this is impossible so a 1% ripple voltage was selected:

$$\Delta V_c = 0.01.V \tag{3.10}$$

$$\Delta V_c = 0.01.(250)$$

$$\Delta V_c = 2.5\ V$$

Now, the size of the capacitor can be calculated:

$$C = \frac{I_{load} t_{on}}{\Delta V_c} \tag{3.11}$$

$$C = \frac{70 \times 26.53 \times 10^{-6}}{2.5}$$

$$C = 742.84\ \mu F$$

3.3.2 Single Phase Inverter

Single phase inverters can possess two different switching topologies namely, bipolar and unipolar. For this study, a full bridge bipolar switched inverter was opted for. Referring to Figure 3.6, this switching technique, allows transistor 1 and 2 to be on simultaneously while 3 and 4 remain off. Conversely, when 3 and 4 are switched on, transistors 1 and 2 will be off. Furthermore, the switching only takes place during certain conditions.

Referring to Figures 3.6 and 3.7, this switching occurs at:

- MS>V_{tri}, IGBT 1 and 2 are on, IGBT 3 and 4 are off
- MS <V_{tri}, IGBT 3 and 4 are on, IGBT 1 and 2 are off

Where MS is the modulating signal and V_{tri} is the triangle wave.

A modulating signal (MS) and a triangle wave are passed through a comparator using the conditions stated below. The output of the comparator (Figure 3.7) is fed to each gate of an IGBT to obtain the output waveform V_{io} in Figure 3.7. By sizing an appropriate RLC low pass filter, an approximate sine wave, V_o is achieved. Increasing the frequency of the triangle wave, outputs a closer approximation of a sine wave.

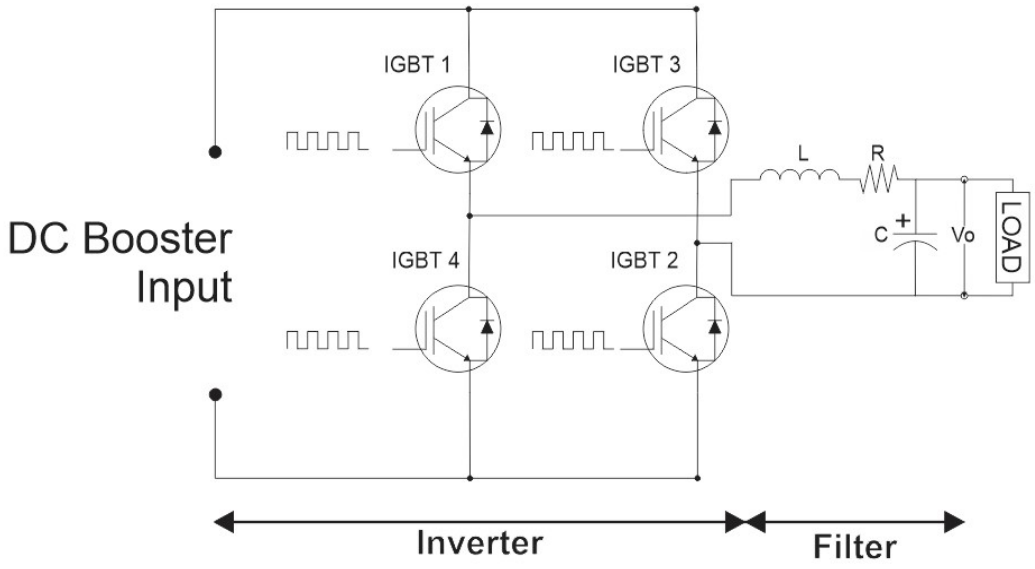

Figure 3.6. DC to AC Inverter and Filter Circuit

The output of the inverter circuit is depicted below the Figure 3.7, labelled as V_{io}. To obtain the close approximation of a sine wave previously mentioned, a low pass LC filter circuit is required.

The operating frequency of the circuit is 50 Hz. This must be overstated by 30% due to loading:

$$50\ Hz\ \times 130\% = 65\ Hz$$

$$f = \frac{1}{2\pi\sqrt{LC}} \tag{3.12}$$

$$65 = \frac{1}{2\pi\sqrt{LC}}$$

$$LC = \left(\frac{1}{2\pi 65}\right)^2$$

$$LC = 6\ \times 10^{-6}$$

From this point, an iterative process is followed to determine the values of L and C.

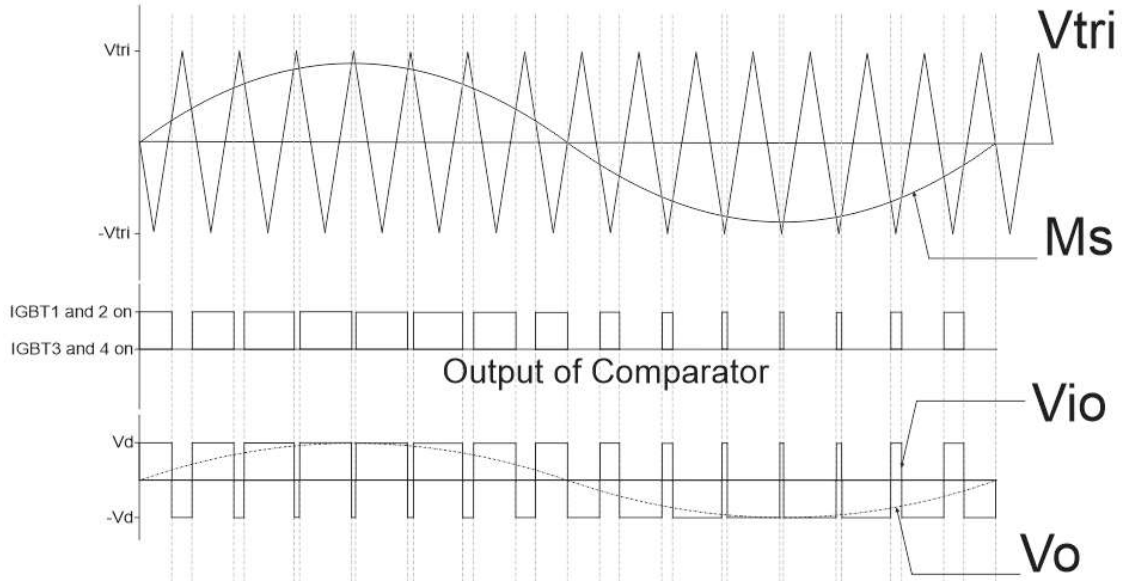

Figure 3.7. Inverter Waveforms

3.4 Supply/Charge Circuit

3.4.1 Solar Power

This system is designed for a Cape Town climate hence the peak solar hours is region specific. A normal PV system is first designed in order to determine the number of batteries required for the system. This number can then be compared with the number of supercapacitors required. The quantity of supercapacitors (Maxwell 51V 189F Durablue^{TM}) to meet the stated autonomy will be determined using an iterative process which will be dealt with in the following chapter.

Circuit 1 from the load profile as documented in Table 3.3 in the previous section contains the essential loads and will be used as a load here for the PV array. It's important to note that the number of panels and batteries in this design will be more than required in reality due to the assumption that these loads will be operating at full load simultaneously. Figure 3.8 depicts the overview of the PV array system.

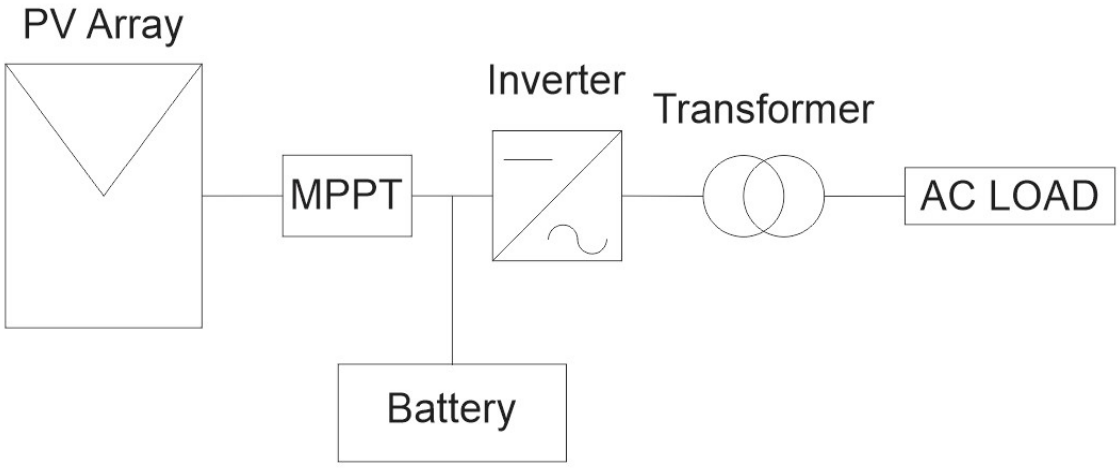

Figure 3.8. PV Array System

The inverter efficiency is assumed to be 90% which is depicted as adjustment factor in the Table 3.4.

$$Adjusted\ Power = \frac{Net\ rated\ Power}{Adjustment\ facto} \tag{3.13}$$

Table 3.4.Circuit 1 Load Schedule

Appliance	Power Rating (kW)	QTY	Net Rated Power (kW)	Adjustment factor	Adjusted Power (kW)	Used Hrs/day	Energy/day (kWh)
Stove	4	1	4	0.9	4.44	1	4.44
Geyser	3.5	1	3.5	0.9	3.89	12	46.67
Water Tank	0.37	1	0.37	0.9	0.41	24	9.87
Lights	0.06	20	1.2	0.9	1.33	12	16
Fridge/freezer	0.5	1	0.5	0.9	0.56	24	13.33
	8.43	**24**	**9.57**	**0.9**	**10.63**		**90.31111**

Table 3.5. PV System Component Data

Selected Solar Panel	RenewsysGalatic 380W Solar Panel
Solar panel module power output	380W
Voltage at maximum power point	39.4V
Selected Battery	SDDirectPro AGM+ 12V 200Ah
Battery Voltage	12V
Battery round trip efficiency	0.85
Depth of discharge	0.8
Capacity of selected battery	200 Ah
Inverter voltage	220V ac
Inverter efficiency	90%
Autonomy	1 day
Peak sun hours for Cape Town's winter month (June)	5.8

Using the data from Tables 3.4 and 3.5, the remaining calculations are completed below.

The singular battery is referred to as a cell which is connected in series and parallel to form a single larger battery. Using the 12V cell voltage, 20 are connected in serial to form a 240V battery.

To calculate the total amp-hours required by the system, the total energy demand in a single day is divided by the voltage of the battery:

$$Total\ Ah\ required\ per\ day = \frac{Total\ Energy\ Demand\ per\ day}{Battery\ Voltage} \tag{3.14}$$

$$Total\ Ah\ required\ per\ day = \frac{90311.11}{240}$$

$$Total\ Ah\ required\ per\ day = 376.3\ Ah$$

To accommodate for days without sunshine, a conservative value of one day of autonomy was selected. The required battery capacity to meet this autonomy is calculated:

$$Req\ Batt\ Cap = \frac{Autonomy}{Dept\ \ of\ Discharge\ limit} \times Total\ Ah\ req\ per\ day \tag{3.15}$$

$$Req\ Batt\ Cap = \frac{1}{0.8} \times 376.3$$

$$Req\ Batt\ Cap = 470.37\ Ah$$

The SDDirectPro AGM+ 12V 200Ah battery was selected for this study. Using the amp-hour rating together with the required battery capacity, the number of required cells (rounded up) in the battery:

$$No.of\ parallel\ batteries\ required = \frac{Required\ Battery\ Capacity}{Capacity\ of\ selected\ battery} \quad (3.16)$$

$$No.of\ parallel\ batteries\ required = \frac{470.37}{200}$$

$$No.of\ parallel\ batteries\ required = 2.352 \approx 3$$

This means that a total of 60 cells make up a single battery. 3 parallel rows of 20 cells each.

The overall battery capacity is higher than the required value calculated for the system:

$$Total\ Battery\ Ah\ capacity = no.of\ parallel\ batteries \times capacity\ of\ selected\ cell \quad (3.17)$$

$$Total\ Battery\ Ah\ capacity = 3 \times 200$$

$$Total\ Battery\ Ah\ capacity = 600\ Ah$$

To calculate the kilo-Watt-hour capacity of the battery:

$$Total\ Battery\ kWh\ capacity = Total\ Battery\ Ah\ capacity \times battery\ voltage \quad (3.18)$$

$$Total\ Battery\ kWh\ capacity = \frac{600 \times 240}{1000}$$

$$Total\ Battery\ kWh\ capacity = 144\ kWh$$

The PV array must be able to output enough energy per day:

$$Required\ array\ output\ per\ day = \frac{Total\ Energy\ demand\ per\ day}{Battery\ Round\ trip\ efficiency} \quad (3.19)$$

$$Required\ array\ output\ per\ day = \frac{90311.11}{0.85}$$

$$Required\ array\ output\ per\ day = 106\,248.4\ Wh$$

By multiplying the voltage at maximum power point with the round trip efficiency of the battery, the maximum power voltage of a PV module is calculated:

$$PV\ mod\ max\ power\ voltage = Voltage\ at\ max\ power\ point \times Batt\ Round\ trip\ eff \quad (3.20)$$

$$PV\ mod\ max\ power\ voltage = 39.4 \times 0.85$$

$$PV\ mod\ max\ power\ voltage = 33.49\ V$$

Using the lowest PSH for Cape Town's winter month of July as a worst case scenario, the minimum energy output per day from each module is:

$$Energy\ output\ per\ mod\ per\ day = Solar\ panel\ mod\ output\ \times peak\ sun\ hours \quad (3.21)$$

$$Energy\ output\ per\ mod\ per\ day = 380\ \times 5.8$$

$$Energy\ output\ per\ mod\ per\ day = 2204\ Wh$$

At this point the total number of solar modules or panels (rounded up) can be calculated by taking the ratio of the required array output to the energy output per panel:

$$No.of\ Modules\ required\ to\ meet\ energy\ req = \frac{Required\ array\ output\ per\ day}{Energy\ output\ per\ mod\ per\ day} \quad (3.22)$$

$$No.of\ Modules\ required\ to\ meet\ energy\ req = \frac{106248.4}{2\ 204}$$

$$No.of\ Modules\ required\ to\ meet\ energy\ req = 49$$

The nominal rated PV array output of the designed system:

$$Nominal\ Rated\ PV\ array\ ouput = Solar\ panel\ mod\ output\ \times No.of\ Modules\ req \quad (3.23)$$

$$Nominal\ Rated\ PV\ array\ ouput = 380\ \times 49$$

$$Nominal\ Rated\ PV\ array\ ouput = 18\ 620\ W$$

In order to simulate this on MATLAB/Simulink to determine the charging behaviour of supercapacitors, the circuit must be altered to incorporate them resulting in Figure 3.10. First the output from the maximum power point tracker must be decreased in order to fully charge the supercapacitor without causing dielectric breakdown. See Table 3.6 for Maxwell 51V 189F Durablue™data.

Table 3.6. Supercapacitor Data Extracted from Datasheet

Maxwell 51V 189F Durablue™	
Rated Capacitance	189 F
Maximum Capacitance	200 F
Maximum ESR	5.6 mΩ
Rated voltage	51 V
Absolute Maximum Voltage	54 V
Absolute Maximum Current	1 900 A

According to Table 3.5, the voltage at maximum point for the RenewsysGalatic 380W Solar Panel is 39.4 V. The PV array is designed such that the output of the PV array is 240V. Using a DC buck circuit as depicted in Figure 3.9, this voltage can be reduced to an appropriate charging voltage. Each supercapacitor module will be charged one at a time at which point it is disconnected from the circuit and another supercapacitor module is connected and the charging process continues.

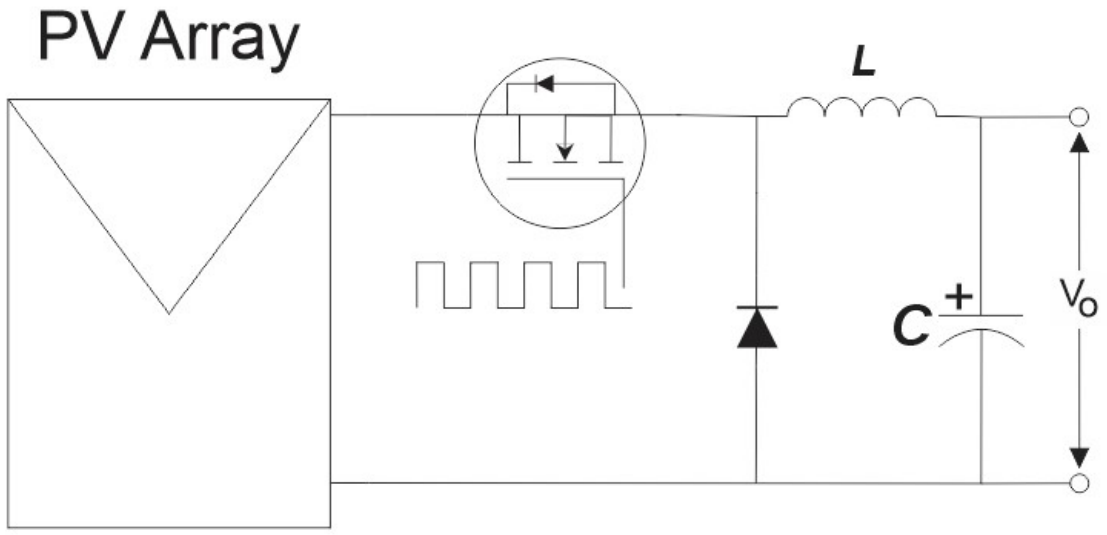

Figure 3.9. PV Array DC Buck Circuit

To calculate the duty cycle of the buck circuit V_{Out} is selected to be 60V, 9V higher than required as a safety factor:

$$D = \frac{V_{Out}}{V_{in}} \tag{3.24}$$

$$D = \frac{60}{240}$$

$$D = 25\ \%$$

By selecting a switching frequency of 30 kHz and assuming a 50A with a 30% inductor ripple, the buck circuit inductance is given by:

$$L = \frac{V_{out}(1-D)}{f\Delta I_L} \tag{3.25}$$

$$L = \frac{60(1-0.25)}{30000\times50\times0.3}$$

$$L = 0.1\ mH$$

To determine the capacitance of the Buck circuit while assuming a 1 mV ripple voltage:

$$C = \frac{(1-D)}{\frac{V_{ripple}}{V_{out}}8Lf^2} \tag{3.26}$$

$$C = \frac{(1-0.25)}{\frac{1\times10^{-3}}{60}\times8\times0.1\times10^{-3}\times30000^2}$$

$$C = 6.25\ F$$

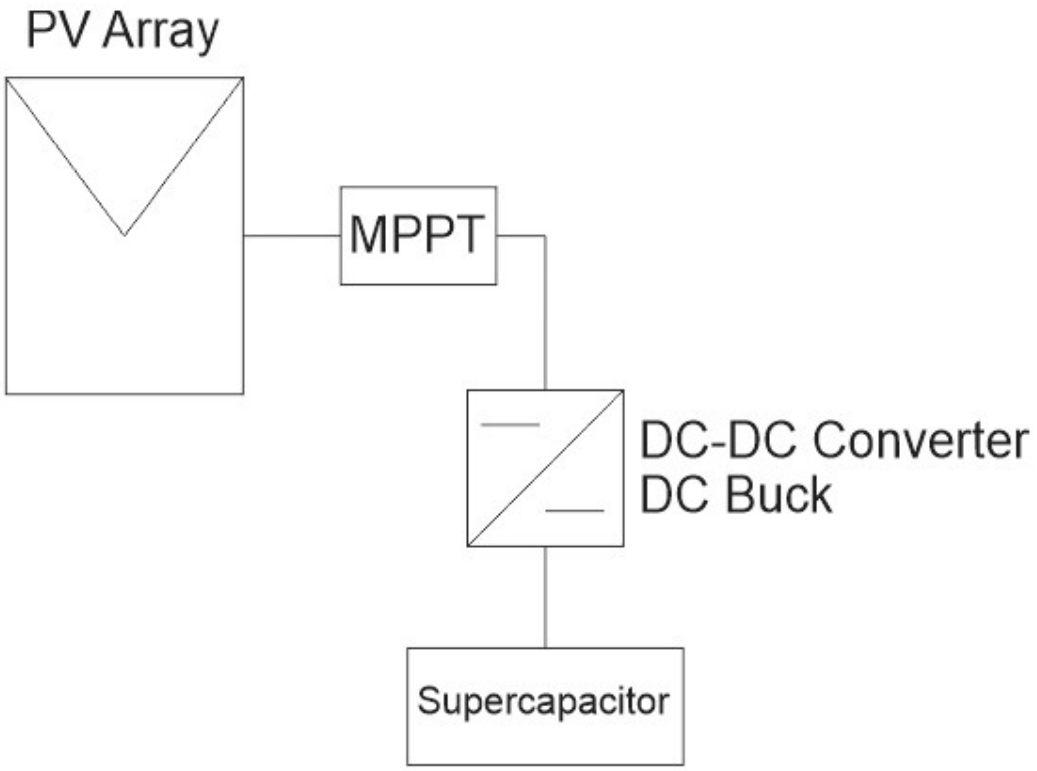

Figure 3.10.PV Array System to Charge Supercapacitors

3.4.2 Wind Power

Wind power has the potential to make a great difference across the globe in terms of renewable energy due to its capability of producing large amounts of power. However, by studying the wind rose, Figure 3.12, provided by the South African Weather Service, it can be determined that the city of Cape Town is not a prime location for wind power. Under the IEC Wind Class, the wind speeds fall far below the lowest wind class. Therefore, this section of the study will focus on charging supercapacitors using wind power as shown in Figure 3.11.

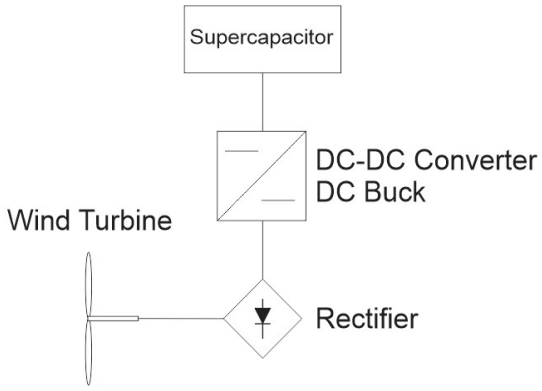

Figure 3.11.Wind Turbine System to Charge Supercapacitors

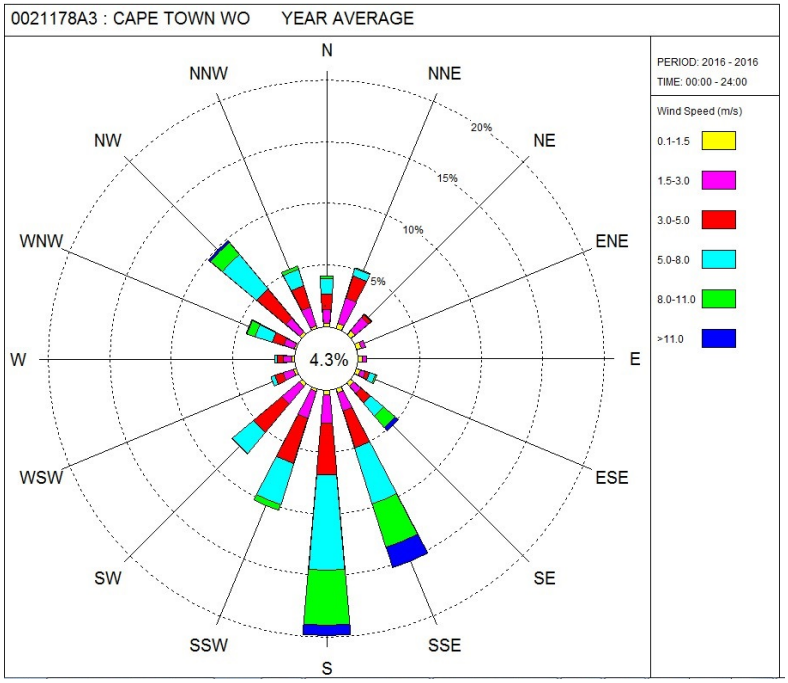

Figure 3.12. Cape Town Wind Rose for the Year 2016

Summarizing the data from the wind rose, Figure 3.12, with wind speeds greater than 1.5 m/s:

- 1.5-3 m/s - 15%
- 3-5m/s - 28%
- 5-8 m/s - 29%
- 8-11m/s - 13%
- >11 m/s - 3%

Using this data, a wind turbine can be selected for this study. The Etneo Small Vertical Axis Wind Turbine 700W Model DS700. Table 3.7 contains the relevant information regarding the turbine.

Table 3.7. Data of Selected Wind Turbine Extracted from the Datasheet

Selected Wind Turbine	**Etneo Small Vertical Axis Wind Turbine 700W Model DS700**
Rated Power	700W
Power output type	Three phase AC
Rated turbine speed	405rpm
Rated wind speed	12m/s
Cut-in wind speed	<3m/s
Cut-out wind speed	15m/s
Survivor wind speed	60m/s
Rotor diameter	1.930 m
Total height	3m

The low cut-in speed of this wind turbine makes it suitable for the Cape Town wind regime. The cut-out speed is 15m/s which is higher than speeds likely to be experienced in the region since wind speeds larger than 11 m/s occur only approximately 3% of the time. It is also important to note that there are no winds in any direction only 4.3% of the given time. The most relevant data that can be extracted from the wind rose and the given turbine data is that 88% of the time the turbine will produce usable power.

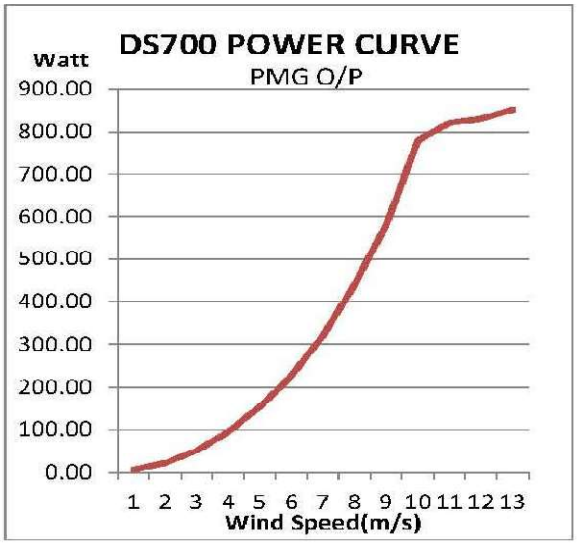

Figure 3.13. Power Curve for Etneo Small Vertical Axis Wind Turbine 700W Model DS700

Correlating the power curve, on Figure 3.13, and the data previously discussed, Figure 3.14 below illustrates the power that can be generated with the frequency of occurrence of the wind speed can be constructed.

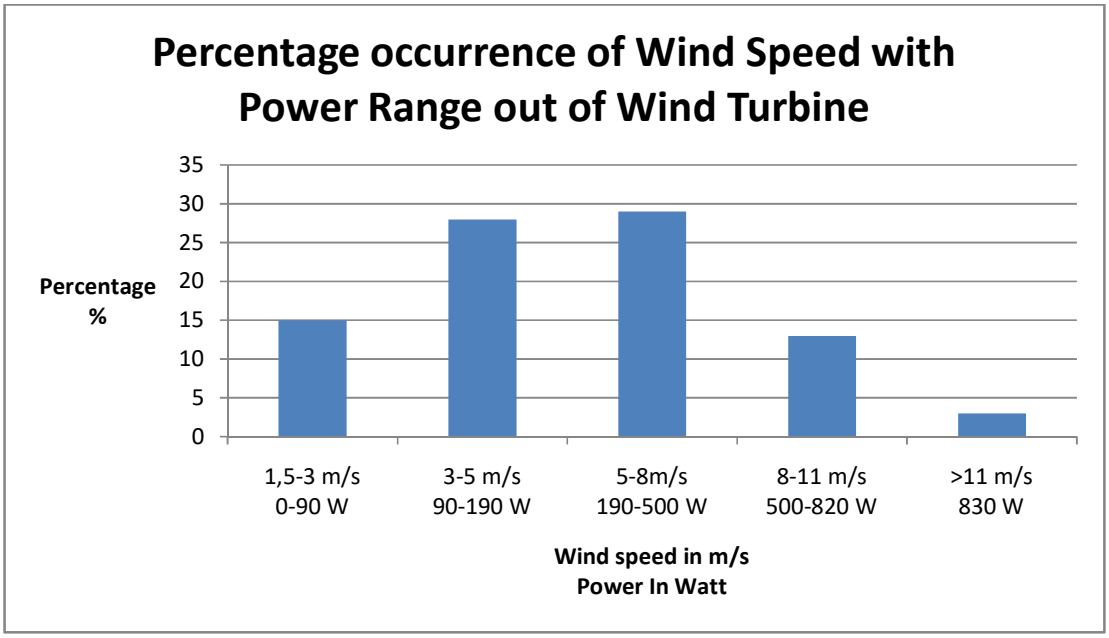

Figure 3.14.Percentage Occurrence of Wind Speed with Power Range out of Wind Turbine

Using the mean values of each power range with equation (3.27), the yearly energy output can be calculated and Table 3.8 populated.

$$Energy_{Wind\ out} = mean\ power \times yearly\ hours\ \times percentage\ occurrence \qquad (3.27)$$

Table 3.8. Yearly Energy Output of Wind Turbine

Wind Speed Range (m/s)	**Mean Power (Watt)**	**Yearly hours x percentage (hrs)**	**$Energy_{wind\ out}$**
1.5 – 3	45	1 314	59 130
3 – 5	140	2 452.8	343 392
5 – 8	345	2 540.4	846 438
8 – 11	660	1 138.8	751 608
>11	830	262.8	218 124
	Total	**7 708.8**	**2 248 692 Wh** **2 248.692 kWh**

Therefore, the total energy output of the wind turbine in a year is 2 248.692 kWh.

Wind turbines, like the selected one produces three phase AC power. In order to charge supercapacitors, this three phase AC must be rectified to DC and the DC voltage needs to be lowered using a buck converter as seen in Figure 3.12.

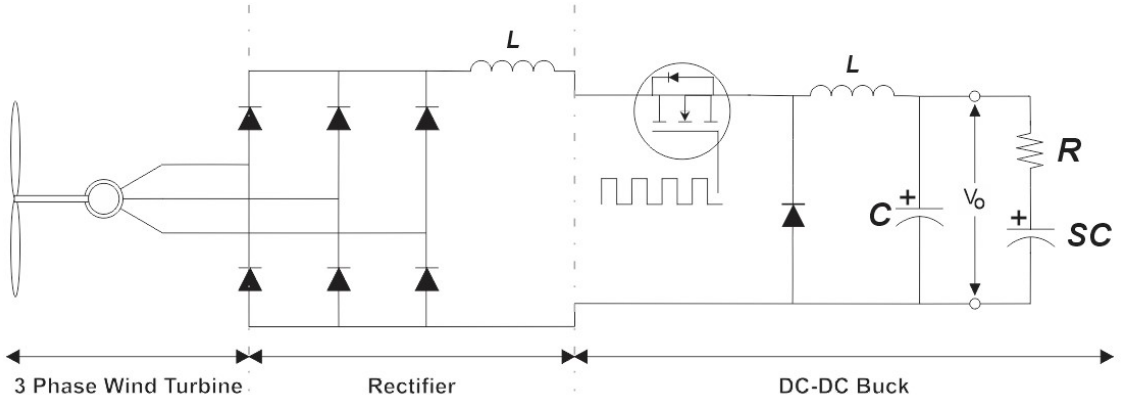

Figure 3.15. Wind Turbine Circuit to Charge Supercapacitors

The output of the wind turbine is 380 V ac. By rectifying this three phase AC to DC and using an 0.1 H inductance to filter the wave, the output voltage is 1.65 times the input.

$$380\ V_{AC} \times 1.65\ =\ 627\ V_{DC} \tag{3.28}$$

To calculate the duty cycle of the buck circuit using equation (3.24):

$$D = \frac{V_{Out}}{V_{in}}$$

$$D = \frac{60}{627}$$

$$D = 9.57\ \%$$

Using equation (3.25) and selecting a switching frequency of 30 kHz and assuming a 50A with a 30% inductor ripple, the buck circuit inductance is given by:

$$L = \frac{V_{out}(1-D)}{f\Delta I_L}$$

$$L = \frac{60(1-0.0957)}{30000\times50\times0.3}$$

$$L = 0.121\ mH$$

To determine the capacitance of the Buck circuit while assuming a 1 mV ripple voltage from equation (3.26):

$$C = \frac{(1-D)}{\frac{V_{ripple}}{V_{out}} 8Lf^2}$$

$$C = \frac{(1-0.0957)}{\frac{1\times10^{-3}}{60}\times8\times0.121\times10^{-3}\times30000^2}$$

$$C = 0.06228\,F$$

By consolidating the various designs in this chapter, the overall schematic diagram for system is shown by Figure 3.15.

Now, the circuits and values calculated and designed in this chapter, were simulated using MATLAB/Simulink and the results are considered in Chapter 4. As previously stated, the number of supercapacitors required for the system was determined using an iterative process as explained in the next chapter.

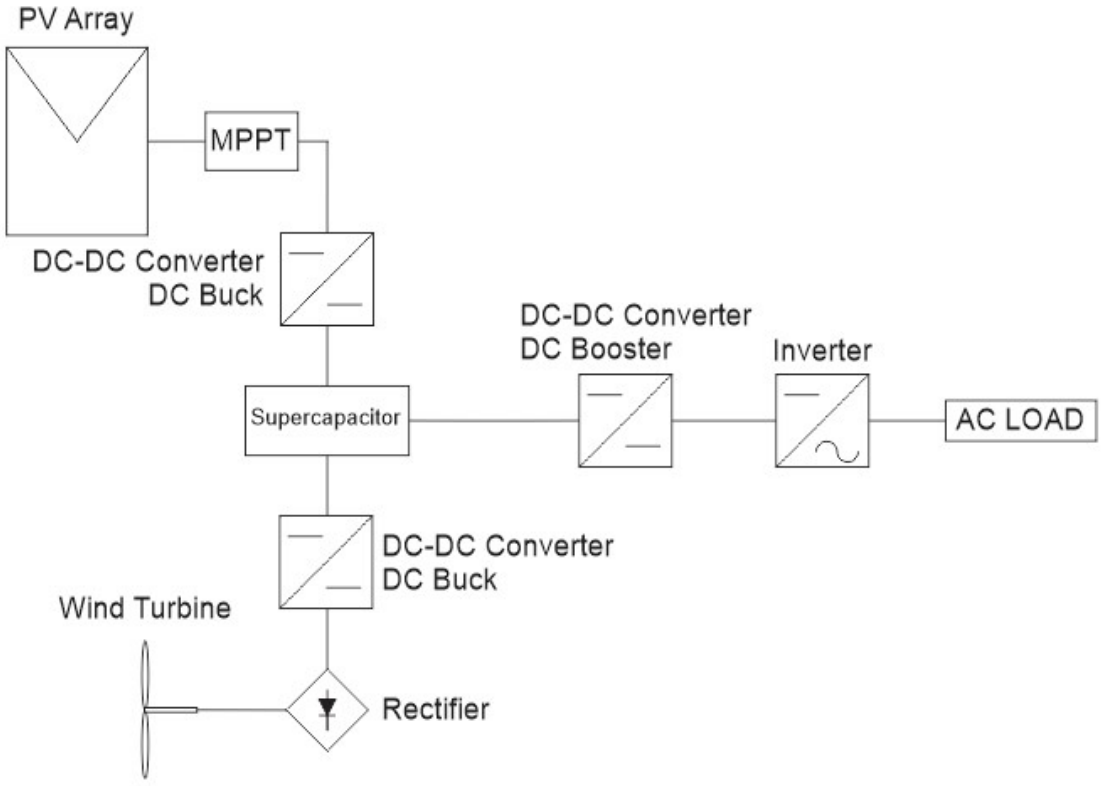

Figure 3.16. Consolidated System Incorporating Supercapacitor

3.5 Analytical Modelling

3.5.1 Modelling of PV Power Input Systems

A number of different types of PV modules exist. Each has its own advantages and disadvantages based on construction, efficiency, climate and application. For this study, the RenewSysGalatic 380W mono-crystalline silicon modules were selected.

To model such a panel, a basic circuit is first required. The Figure 3.17 represents an equivalent circuit of a PV system. In this figure, the light generated current is depicted as a current source. The parallel diode stands for the p-n junction's non-linear characteristic while the parallel or shunt resistance R_{SH} represents leakage and the series resistance R_S, losses.

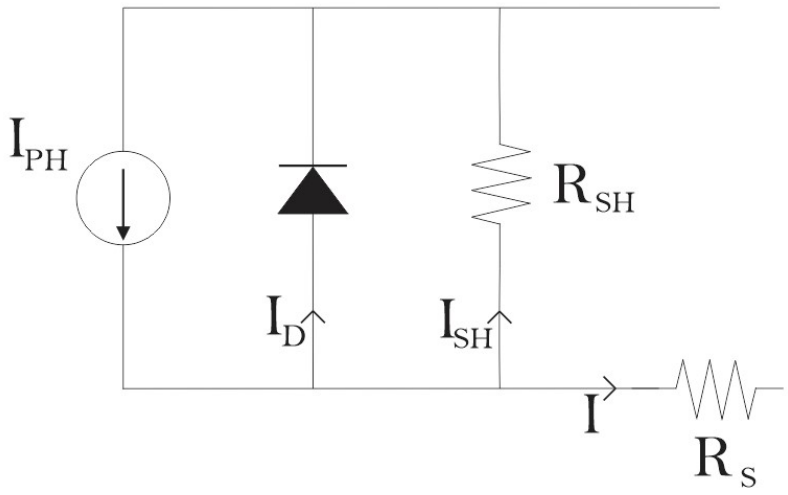

Figure 3.17. Simplified Photovoltaic Module Circuit

From Figure 3.17, illustrating the basic circuit of a PV module, the characteristic equation can be obtained using the Kirchhoff's Current Law (KCL),

$$I = I_{PH} - I_D - I_{SH} \tag{3.29}$$

Other equations used in the modelling process[76]:

Photo-current as a function of the area's irradiance (G),

$$I_{PH} = \frac{G}{1000}\left[I_{SC} + \left(T_{temp} - 298\right)k_i\right] \tag{3.30}$$

Where I_{SC} is the short circuit current, T_{temp} is the temperature and k_i is the short circuit current of the cell at 25°C, and irradiance of 1000 W.m^{-2}

The saturation (I_O) and reverse saturation (I_{RS}) currents are given by equations respectively,

$$I_O = I_{RS}\left[\frac{T_{temp}}{T_N}\right]^3 e^{\left[\frac{\left(\frac{1}{T_N}-\frac{1}{T_{temp}}\right)qE_{GO}}{nK}\right]} \tag{3.31}$$

$$I_{RS} = \frac{I_{SC}}{e^{\left[\frac{qV_{OC}}{nN_SKT_{temp}}\right]}-1} \tag{3.32}$$

Where q is the charge of an electron (1.6 x 10^{-19}C); T_N is nominal temperature; V_{OC} is the open circuit voltage; E_{GO} is the semiconductor band gap energy in eV; n is the diode ideality factor; K is Boltzmann's constant (1.38 x 10-^{23}J.K^{-1}); and N_S is the number of cells connected in series.

The current through the shunt resistor,

$$I_{SH} = \frac{IR_S+V}{R_{SH}} \tag{3.33}$$

The output current of the module is described by,

$$I = I_{PH} - \left[e^{\frac{(IR_S+V)q}{KnTN_S}} - 1\right]I_O - I_{SH} \tag{3.34}$$

Where R_S is the series resistance.

By implementing these equations in the Matlab/Simulink environment, the final model was obtained as shown in Figure 3.18 to Figure 3.24.

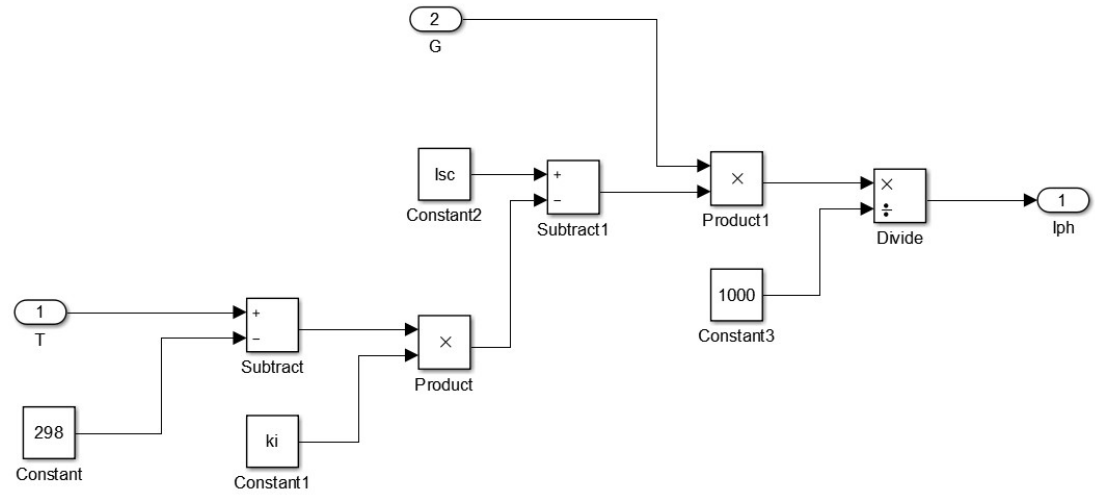

Figure 3.18. Equation (3.30) Modelled in Simulink to Obtain Photo Current

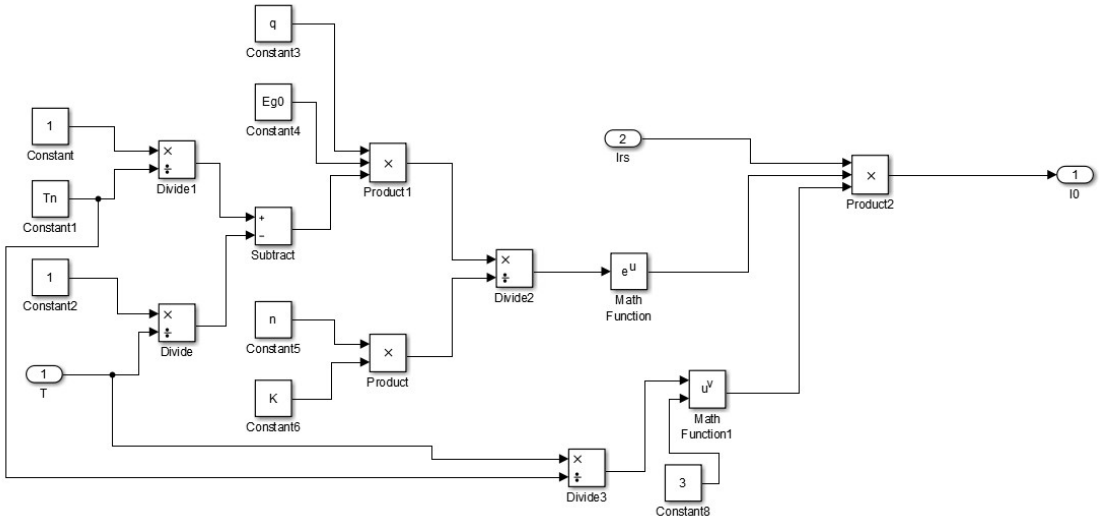

Figure 3.19. Equation (3.31) Modelled in Simulink to Obtain Saturation Current

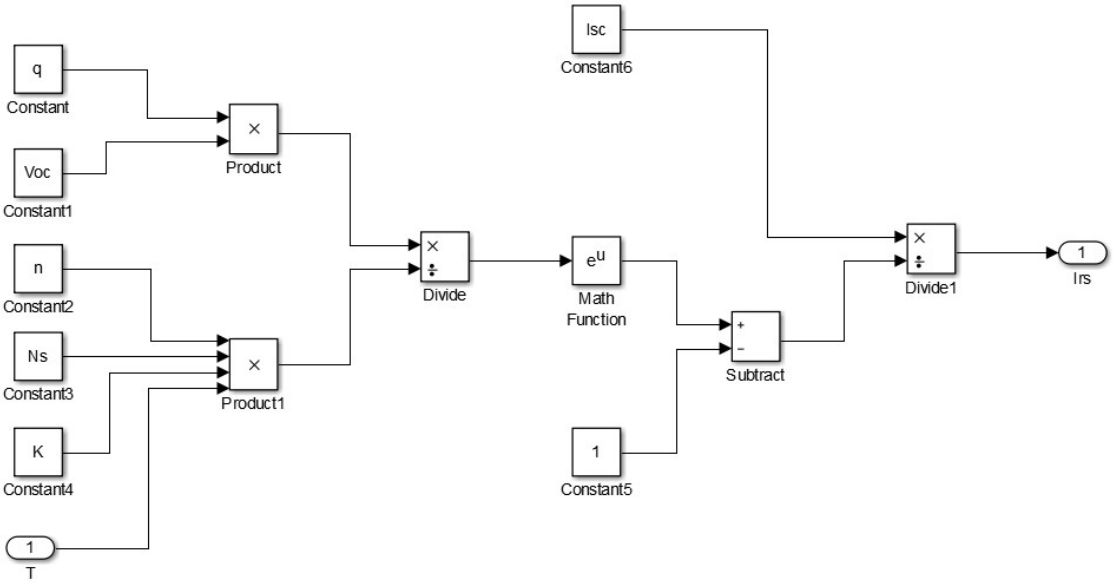

Figure 3.20.Equation (3.32) Modelled in Simulink to Obtain Reverse Saturation Current

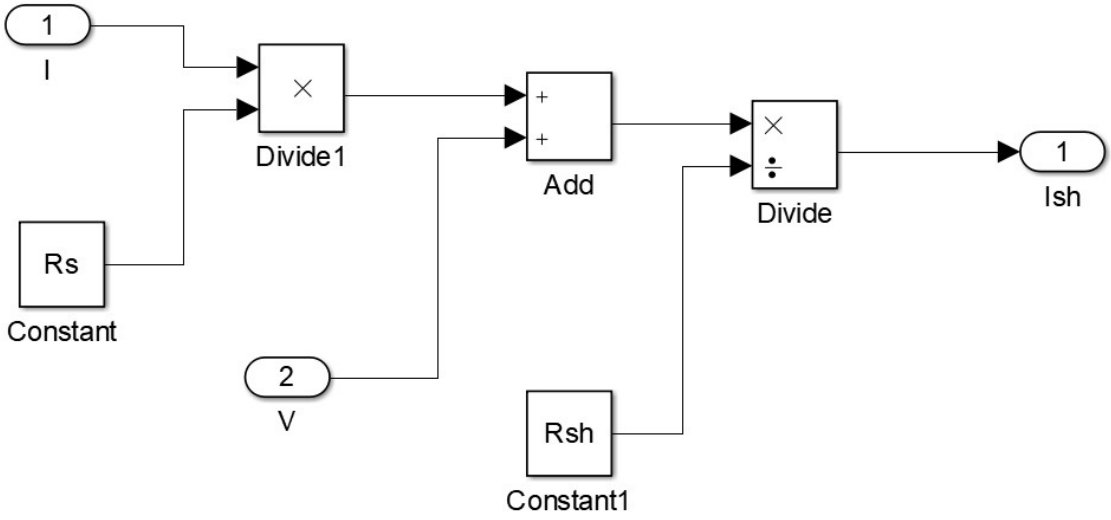

Figure 3.21. Equation (3.33) Modelled in Simulink to Obtain the Current Through the Parallel Resistor

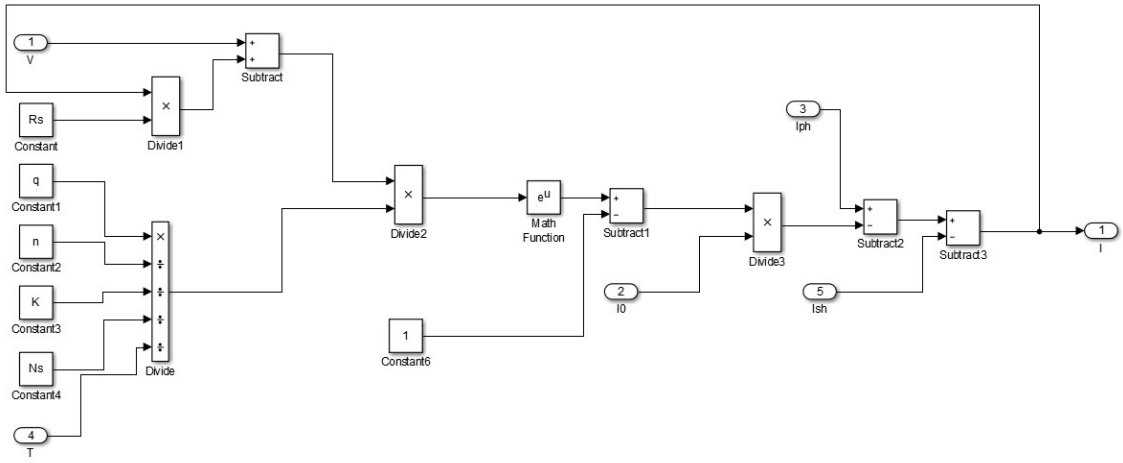

Figure 3.22. Equation (3.34) Modelled in Simulink to Obtain the Output Current

By compacting these figures into subsystems and appropriately interconnecting them, the PV model figure was obtained as shown in Figure 3.23.

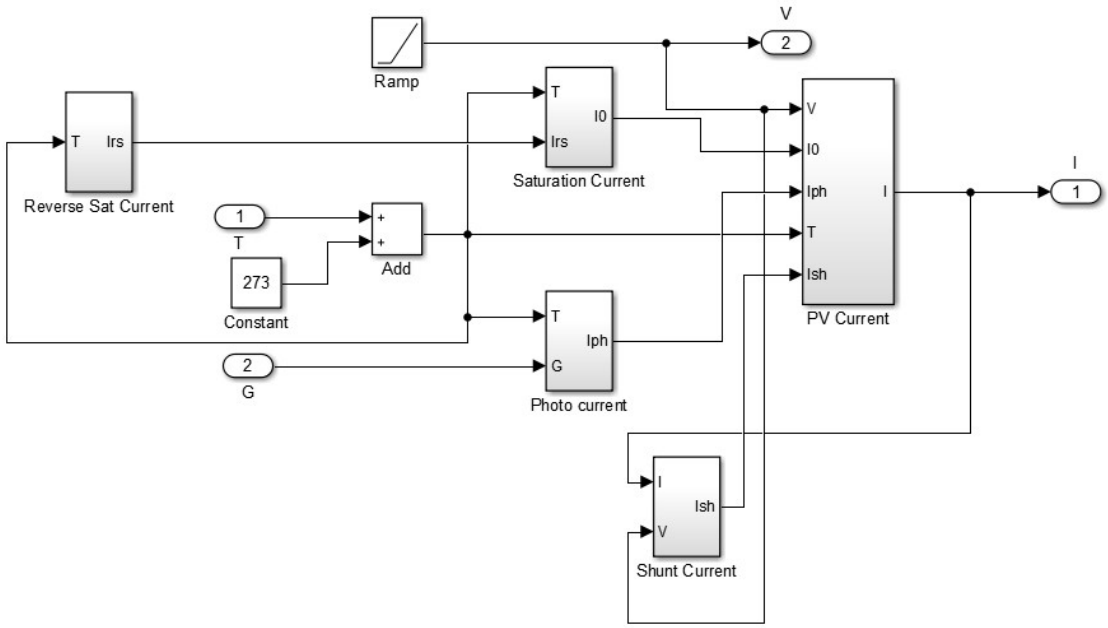

Figure 3.23.PV Model

Figure 3.23 is further compacted into another subsystem to create Figure 3.24. Using this figure the IV and PV characteristics of the module for different irradiances can be determined.

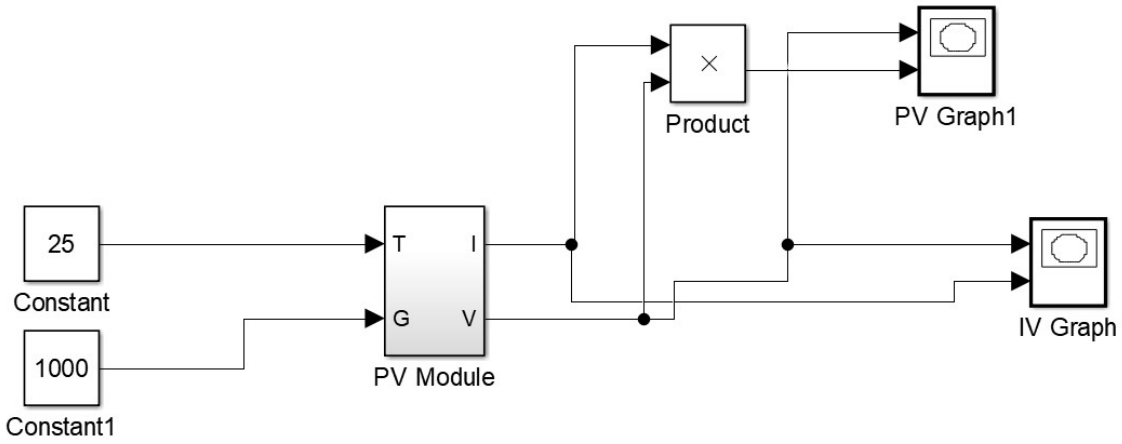

Figure 3.24. Compacted PV Module

The following constants were used in the implementation and analysis of the model:

Table 3.9. Constants Applied to Simulink Model

Constants		Value
ki	Cell short circuit current	0.0032 A
q	Charge of an electron	1.6×10^{-19} C
K	Boltzmann's constant	1.38×10^{-23} $m^2kgs^{-2}K^{-1}$
n	Diode ideality factor	1.3
EgO	Semiconductor band gap energy	1.1 J
Rs	Series resistor resistance	0.221 Ω
Rsh	Parallel resistor resistance	415.405 Ω
Tn	Nominal temperature	298 K
Voc	Open circuit voltage	46.70 V
Isc	Short circuit current	10.08 A
Ns	Number of series connected cells	144

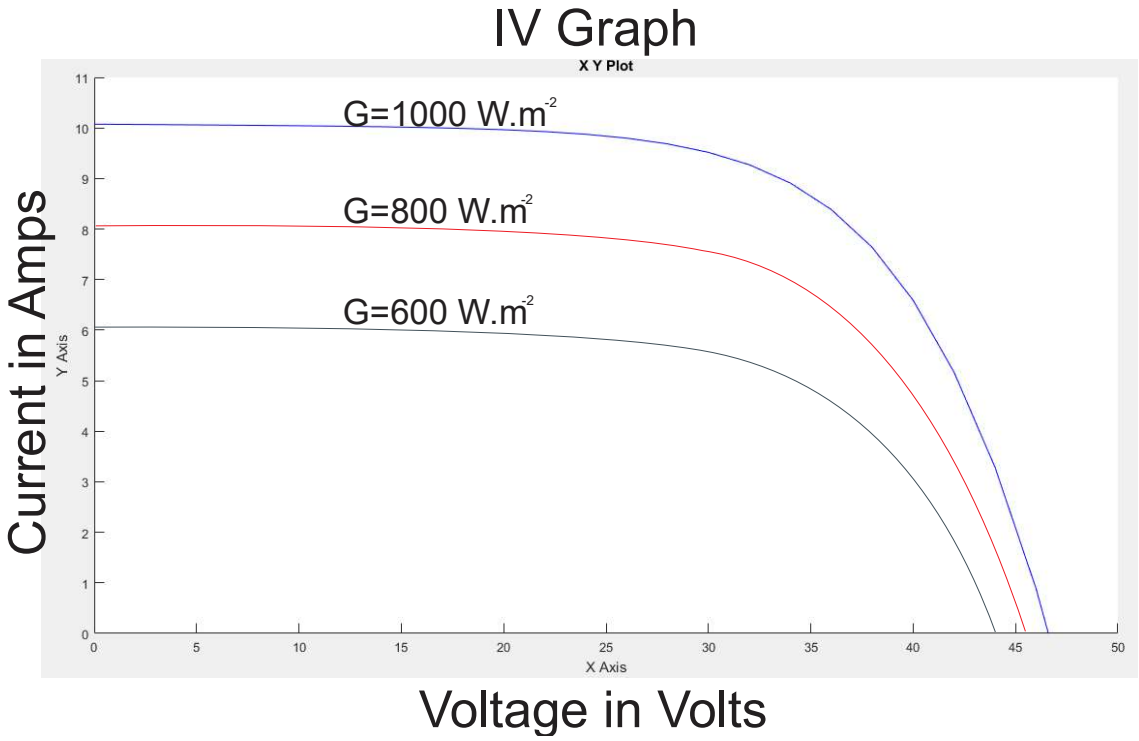

Figure 3.25. Characteristic IV Curve at Irradiation levels of 600, 800, 1000 W.m^{-2}

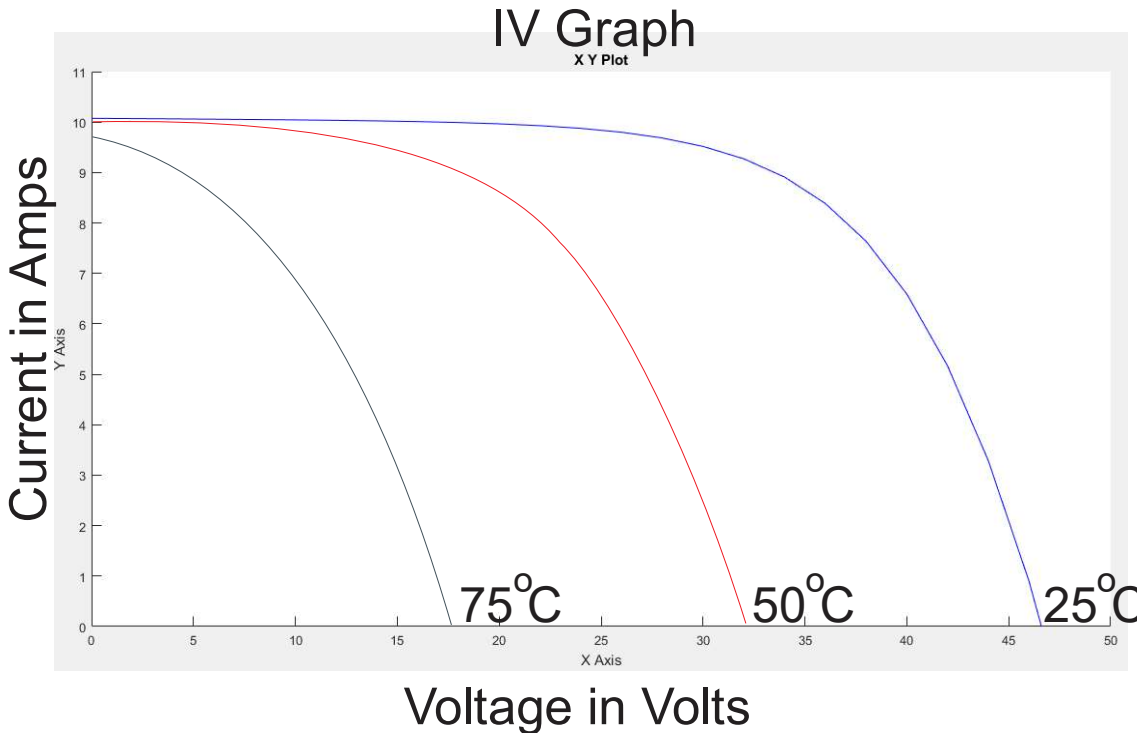

Figure 3.26. Characteristic IV Curve at Cell Temperatures 25°C; 50°C; 75°C

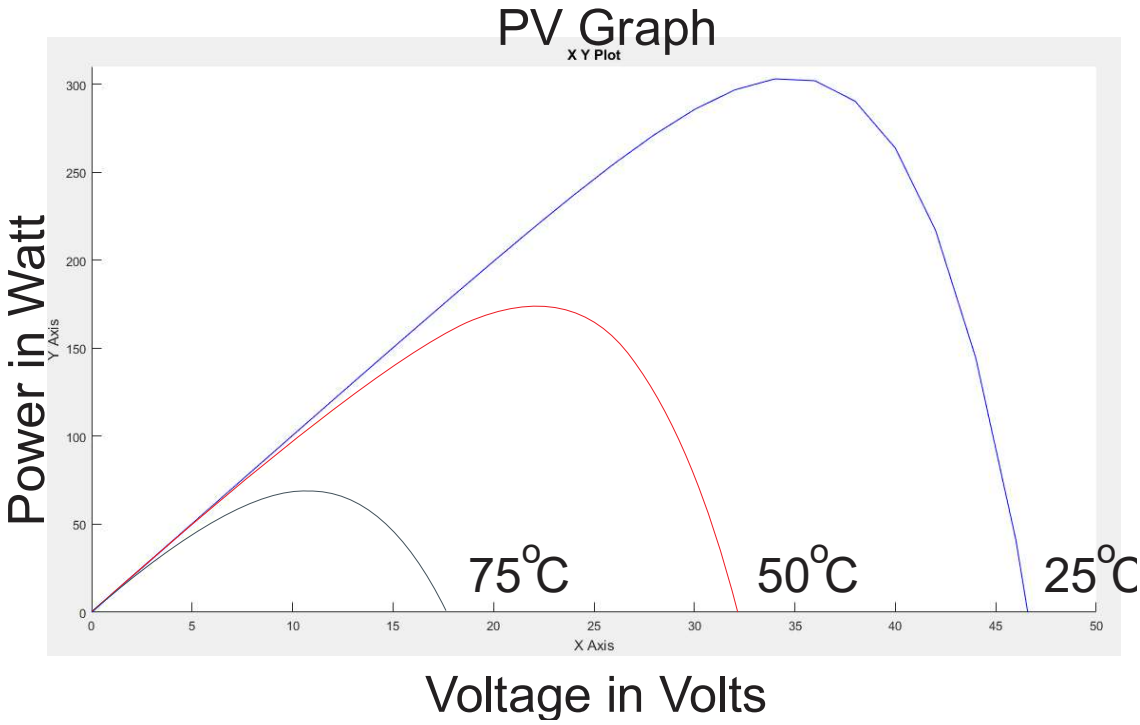

Figure 3.27. Characteristic PV Curve at Cell Temperatures 25°C; 50°C; 75°C

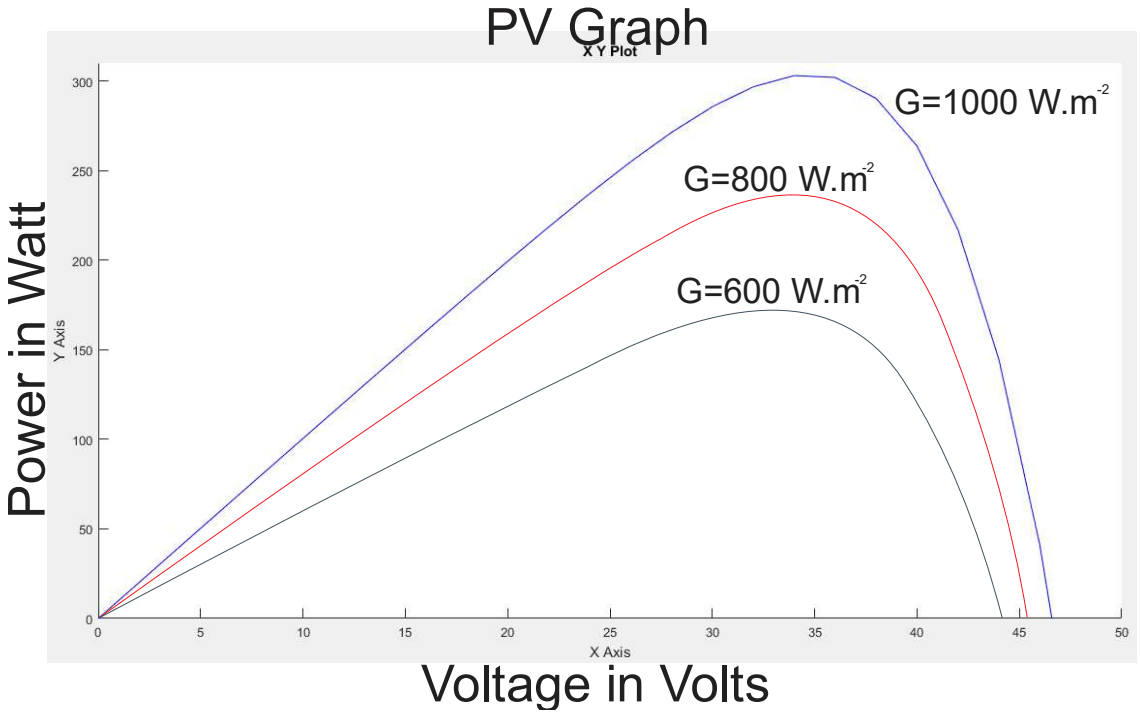

Figure 3.28. Characteristic PV Curve at Irradiation levels of 600, 800, 1000 W.m^{-2}

3.5.2 Modelling of Wind Power Input Systems

Wind power is derived from the extraction of kinetic energy via a wind turbine. The kinetic energy is converted to mechanical energy which is then, via a shaft, coupled to a generator which converts the mechanical energy to electrical energy. The model of a wind turbine is often referred to an aerodynamic model.

For this study, a vertical axis wind turbine (VAWT) coupled to a permanent magnet synchronous generator (PMSG) was selected due to its low cut-in speed and other advantages such as:

- Being omni-directional
- VAWT gearboxes are more accessible.
- VAWTs can be grouped closer together thereby more producing more power for a given space
- The option exists to install VAWTs in conjunction with HAWTs

The aerodynamic power is described by [77],

$$P_m = \frac{1}{2} C_p \rho A U_w^3 \tag{3.35}$$

Where: A is the wind turbine sweep area; C_p is the power coefficient of the wind turbine; ρ is the air density at standard temperature and pressure; U_w is the wind speed.

Cp, the power coefficient is the wind turbine aerodynamic efficiency. It is described as a function of the tip speed ratio, λ, and the pitch angle Θ,

$$C_p(\lambda,\ \theta) = 0.22\left(\frac{116}{\beta} - 0.4\theta - 5\right)e^{-\frac{12.5}{\beta}} + 0.0068\beta \tag{3.36}$$

Where

$$\beta = \left[\frac{1}{\lambda + 0.08\theta} - \frac{0.035}{1+\theta^3}\right]^{-1} \tag{3.37}$$

The tip ratio is given by the following equation where ω_m is the angular speed of the rotor and R is the rotor radius.

$$\lambda = \frac{\omega_m R}{U_w} \tag{3.38}$$

The relationship between the Power coefficient Cp and the tip speed ratio λ is illustrated in Figure 3.29. From Figure 3.29 it can be determined that the maximum power coefficient of 0.47978 occurs at a tip speed ratio of 8, where the pitch angle is 0°

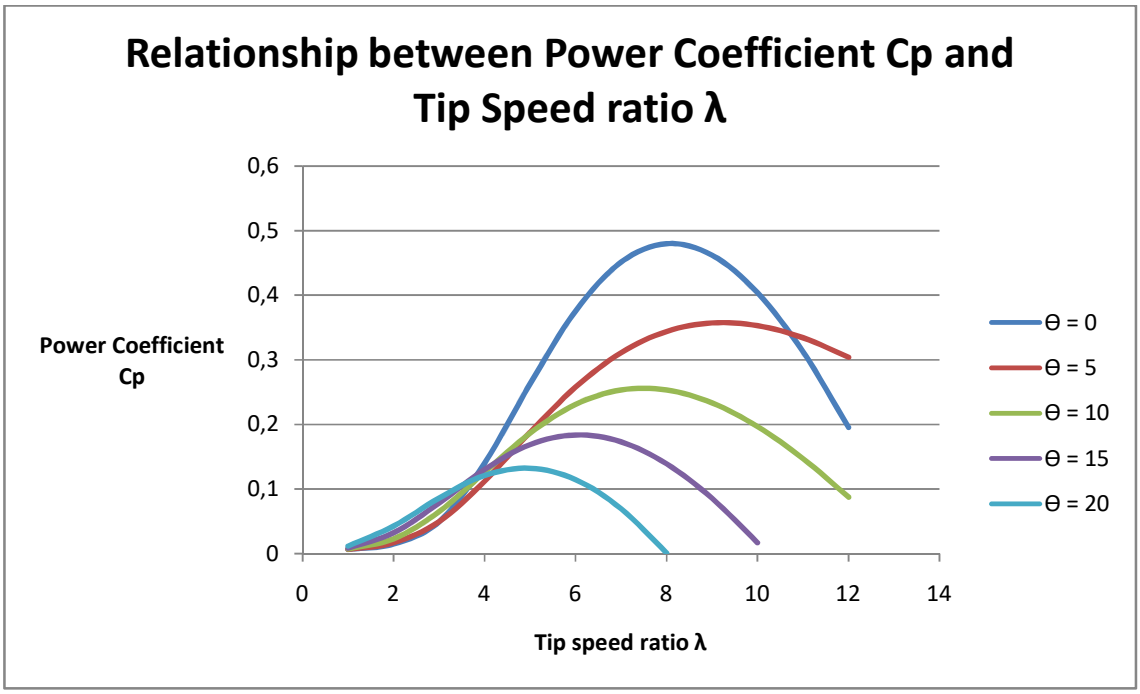

Figure 3.29. Relationship Between Power Coefficient and Tip Speed Ratio

The mechanical torque about the turbine is:

$$T_m = \frac{P_m}{\omega_m} \tag{3.39}$$

The torque coefficient for the wind turbine can be expressed by the ratio of the power coefficient to the tip speed ratio:

$$C_t = \frac{C_p}{\lambda} \tag{3.40}$$

By substituting these equations, an expression for mechanical torque is obtained:

$$T_m = \frac{1}{2} C_t U_w^2 \rho R A \tag{3.41}$$

Since the selected wind turbine is coupled to a PMSG, it is possible that, during operation, a disturbance or transient variation may lead to the rotor accelerating or decelerating. During such a disturbance, an imbalance occurs in the power output and input. This imbalance produces a net torque. The swing equation mathematically describes this motion[78]:

$$J \frac{d^2 \theta_m}{dt^2} = J \frac{d\omega_m}{dt} = T_{net} = T_m - T_e \tag{3.42}$$

In the above equation: J is the moment of inertia; T_m represents the mechanical torque while T_e represents the electromagnetic torque; ω_m is the angular speed of the rotor; and Θ_m is the rotor's angular position.

In order to model the PMSG, the following equations were used:

The Park transform and its inverse simplifies the synchronous generator for modelling and describes the relationship between dq0, the rotating reference, and abc, the three phase rotation [79],

$$\begin{bmatrix} u_d \\ u_q \\ u_o \end{bmatrix} = \sqrt{\frac{2}{3}} \begin{bmatrix} Cos\ \theta_e & Cos\left(\theta_e - \frac{2\pi}{3}\right) & Cos\left(\theta_e + \frac{2\pi}{3}\right) \\ -Sin\ \theta_e & -Sin\left(\theta_e - \frac{2\pi}{3}\right) & -Sin\left(\theta_e + \frac{2\pi}{3}\right) \\ \frac{\sqrt{2}}{2} & \frac{\sqrt{2}}{2} & \frac{\sqrt{2}}{2} \end{bmatrix} \begin{bmatrix} u_a \\ u_b \\ u_c \end{bmatrix} \tag{3.43}$$

$$\begin{bmatrix} u_a \\ u_b \\ u_c \end{bmatrix} = \sqrt{\frac{2}{3}} \begin{bmatrix} Cos\ \theta_e & -Sin\ (\theta_e) & \frac{\sqrt{2}}{2} \\ Cos\left(\theta_e - \frac{2\pi}{3}\right) & -Sin\left(\theta_e - \frac{2\pi}{3}\right) & \frac{\sqrt{2}}{2} \\ Cos\left(\theta_e + \frac{2\pi}{3}\right) & -Sin\left(\theta_e + \frac{2\pi}{3}\right) & \frac{\sqrt{2}}{2} \end{bmatrix} \begin{bmatrix} u_d \\ u_q \\ u_o \end{bmatrix} \tag{3.44}$$

Assuming that the conditions are balanced, ie $u_o = 0$, in the dq axes, the instantaneous stator voltages,

$$u_d = Ri_d + \frac{di_d}{dt} L_d - \omega_e L_q i_q \tag{3.45}$$

$$u_q = Ri_q + \frac{di_q}{dt} L_q + \omega_e (L_d i_d + \lambda_o) \tag{3.46}$$

For a PMSG, by assuming inductances across the different axes (q and d) are equal, the dynamic electrical model can be described by [80],

$$\frac{di_d}{dt} = -\frac{R_s}{L} i_d + \omega_e i_q + \frac{1}{L} u_d \tag{3.47}$$

$$\frac{di_q}{dt} = -\frac{R_a}{L_q} i_q - \left(i_d + \frac{1}{L}\lambda_o\right)\omega_e + \frac{1}{L} u_q \tag{3.48}$$

Where λ_o is the permanent magnetic flux; ω_e is the rotational electrical speed; Ra is the armature resistance. The following are around the different axes (q and d) as denoted by the subscripts:

- i_d and i_q are currents flowing through
- u_d and u_q are voltages across the load

The electromagnetic torque, where p represents pole pairs, is described by [81]:

$$T_e = \frac{3 i_q \lambda_o p}{2} \tag{3.49}$$

The angular rotor speed can be converted from rpm (N) to rad/s:

$$\omega_m = \frac{2N\pi}{60} \tag{3.50}$$

To obtain the frequency from angular speed:

$$f = \frac{p\omega_m}{2\pi} \tag{3.51}$$

The voltage generated by the PMSG [82]:

$$V_s = \frac{6\lambda_o \omega_m p}{\sqrt{2}} \tag{3.52}$$

Using these equations the model for the permanent magnet synchronous generator was constructed in Matlab/Simulink environment[83], shown in Figure 3.30:

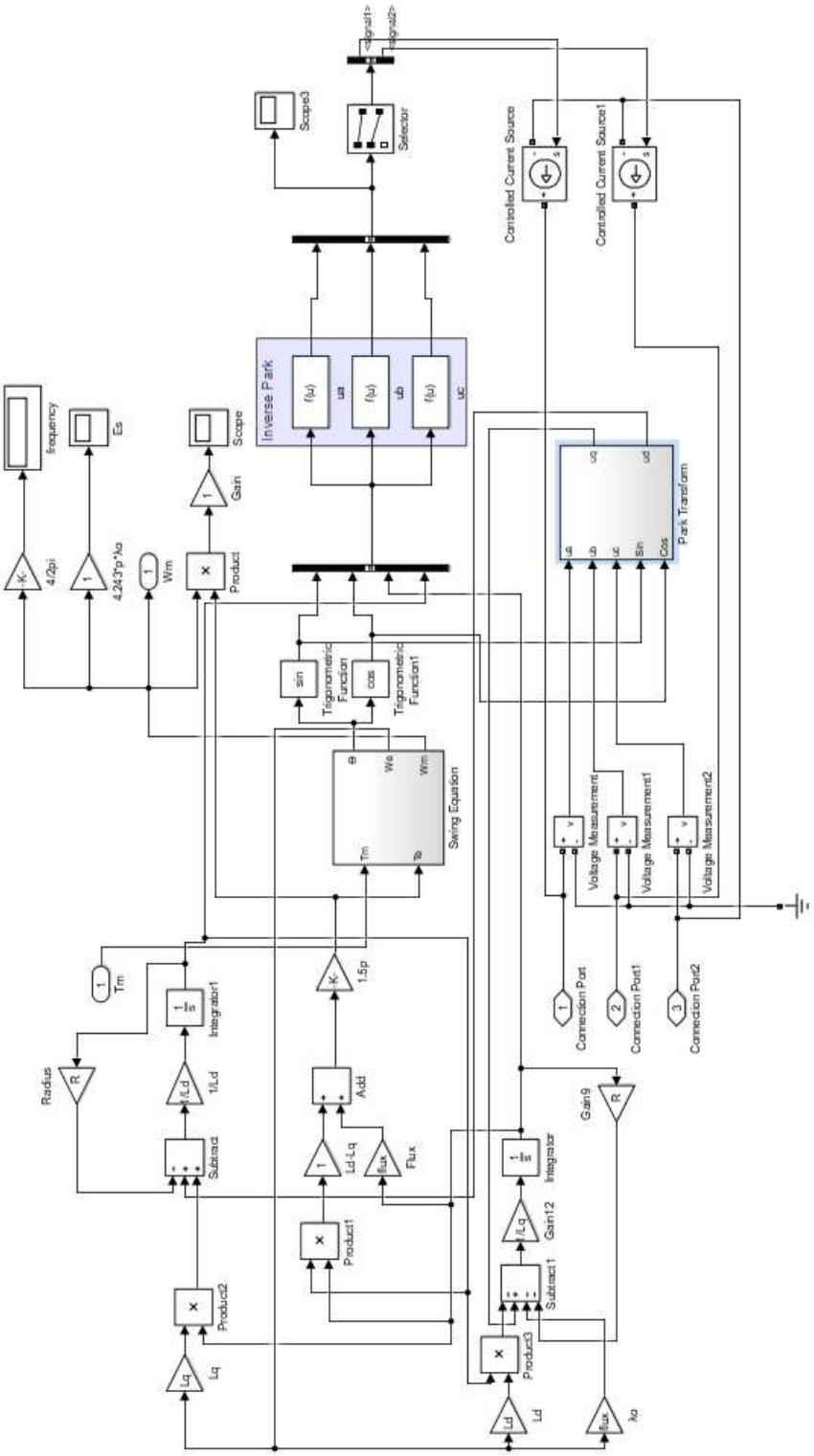

Figure 3.30.Matlab/Simulink Model of Permanent Magnet Synchronous Generator

In Figure 3.30, the Park Transformation subsystem is obtained using the matrices equation (3.43). This subsystem is shown in Figure 3.31.

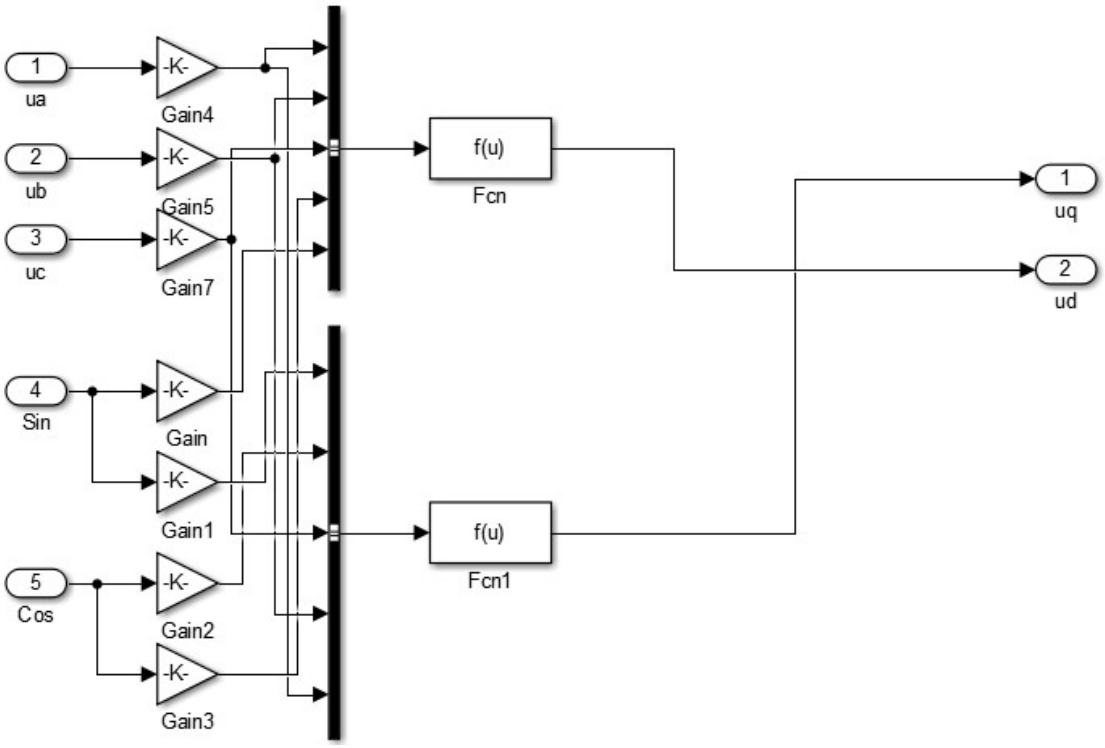

Figure 3.31. Park Transformation Subsystem

The Figure 3.31 illustrates the Swing Equation subsystem which was modelled using equation (3.42).

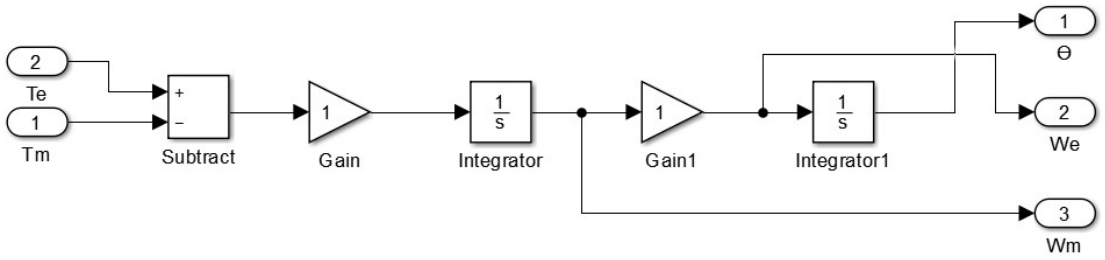

Figure 3.32. Swing Equation Subsystem

Chapter Four:

Simulation, Results and Discussion

4.1 Discharge Circuit Verification

Prior to operating the main circuit with the supercapacitors, verification of the discharge circuit is required. The first circuit, as constructed in Matlab/Simulinkis the DC Booster circuit is depicted in Figure 4.1. A fixed dummy resistance was calculated and included in the circuit to set the circuit current to 70A which can be seen in the Figure 4.1.

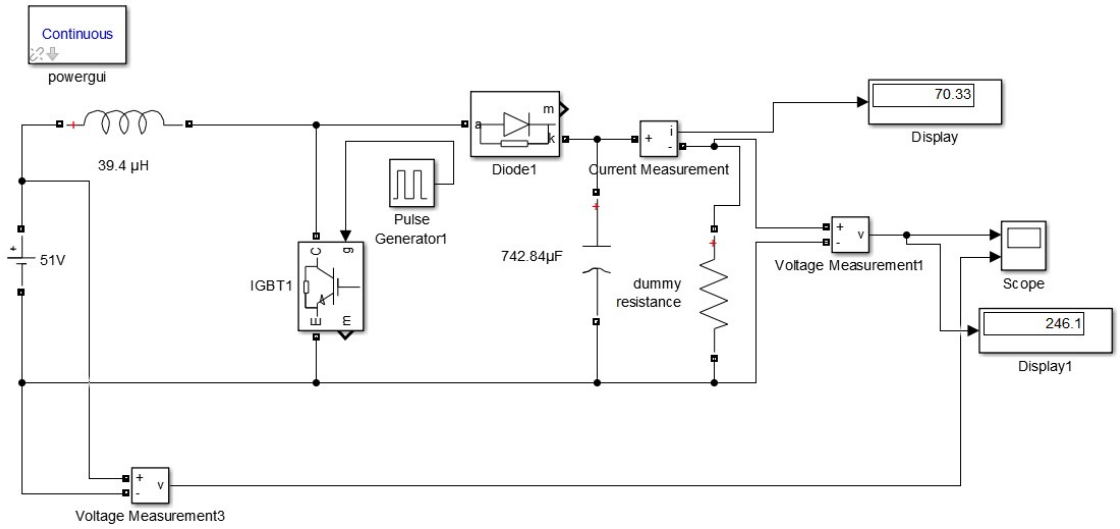

Figure 4.1. DC Booster Circuit Verification

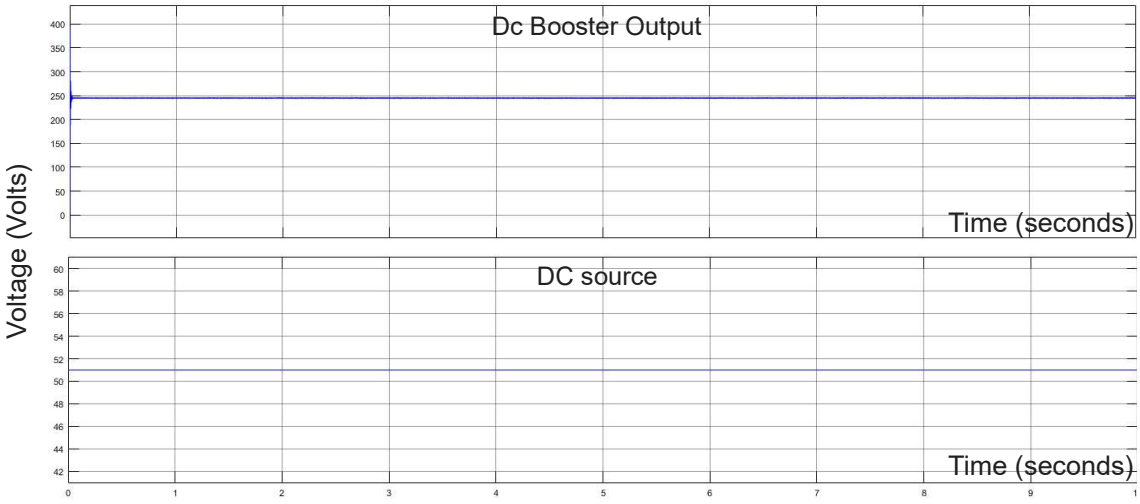

Figure 4.2. DC Booster Outputs

As shown in Figure 4.2, the circuit does operate as expected. The constant input DC source is set to 51V and the output of the DC booster circuit is in the region of 240V.

Consequently, the output of the DC Booster must be inverted to produce a sine wave or an AC voltage. To verify this, the SPWM circuit, a constant voltage source was introduced for the DC booster circuit output. This is depicted in Figure 4.3 and the produced sine wave or an AC voltage is shown in Figures 4.4 and 4.5.

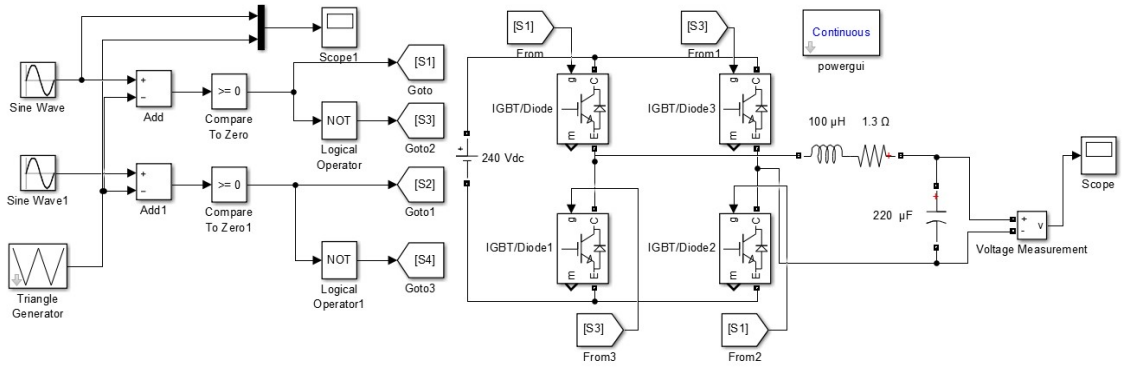

Figure 4.3. SPWM Circuit Verification

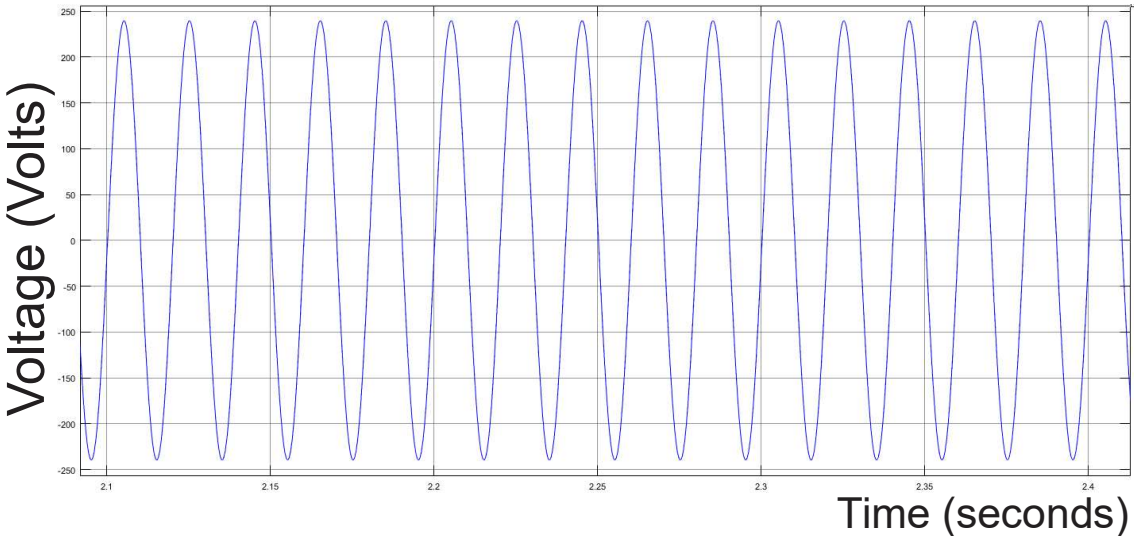

Figure 4.4. SPWM Inverter Circuit Output

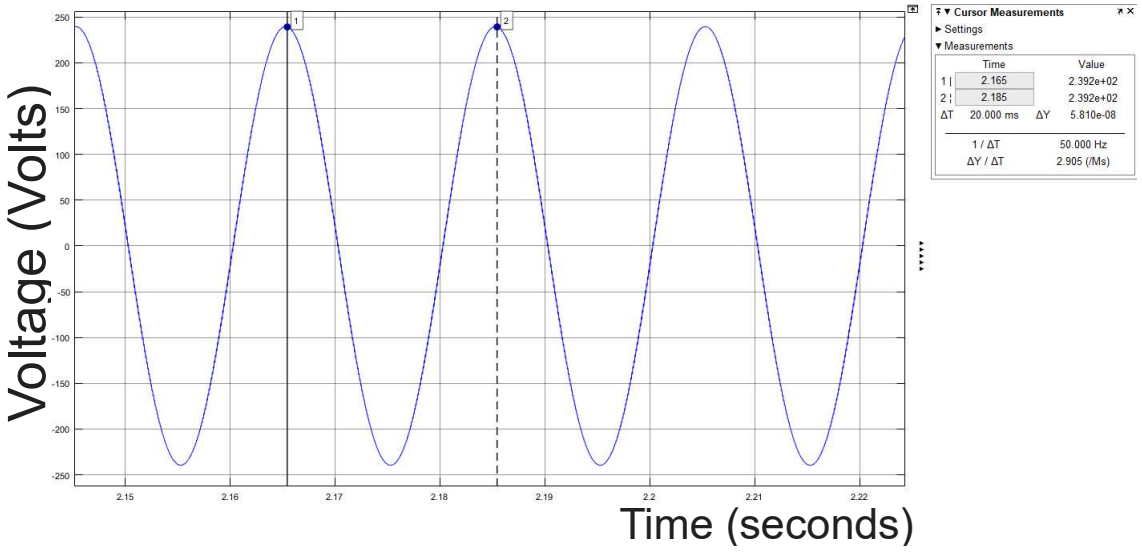

Figure 4.5. Frequency Verification of SPWM Inverter Output

As shown in Figures 4.3 and 4.4, it can be seen that the output of the SPWM circuit operates precisely as required. Both the shape and frequency of the output are of that of a sine wave with a frequency of 50 Hz.

Combining the DC Booster circuit, from Figure 4.1, and the SPWM inverter circuit, from Figure 4.3, results in the combination DC booster/SPWM inverter circuit depicted in Figure 4.6.

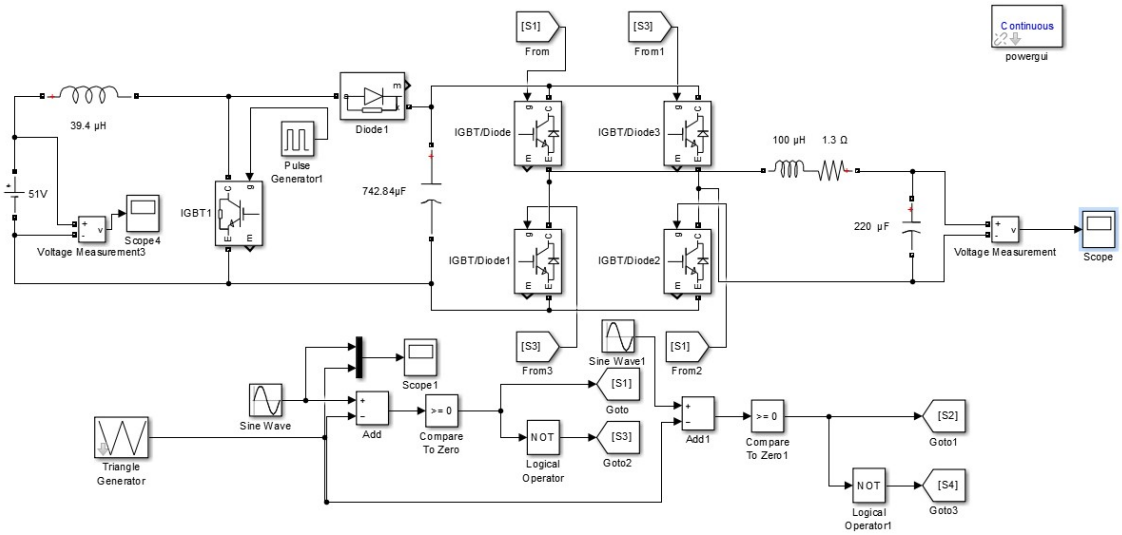

Figure 4.6. Combined DC Booster and SPWM Inverter Circuit

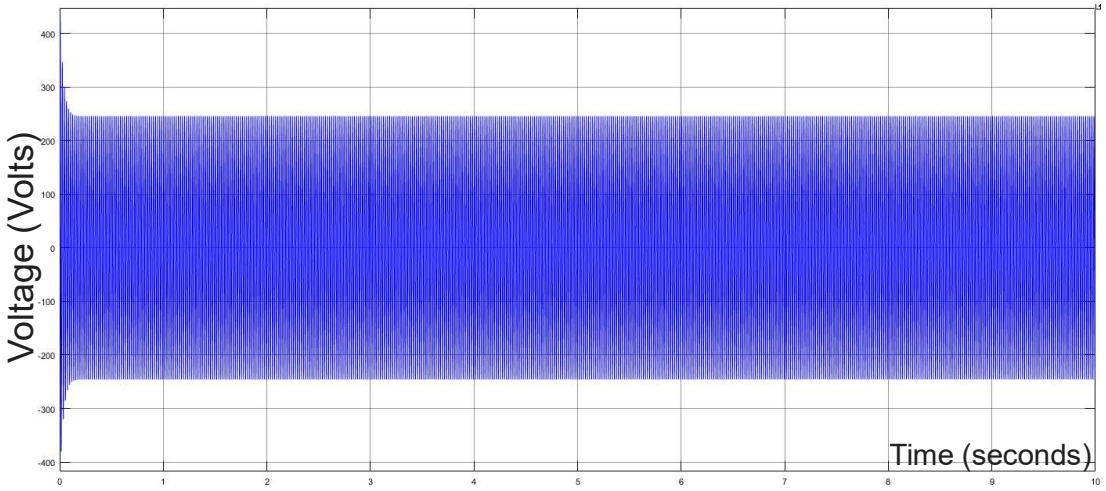

Figure 4.7.Output of Combined DC Booster and SPWM Inverter Circuit

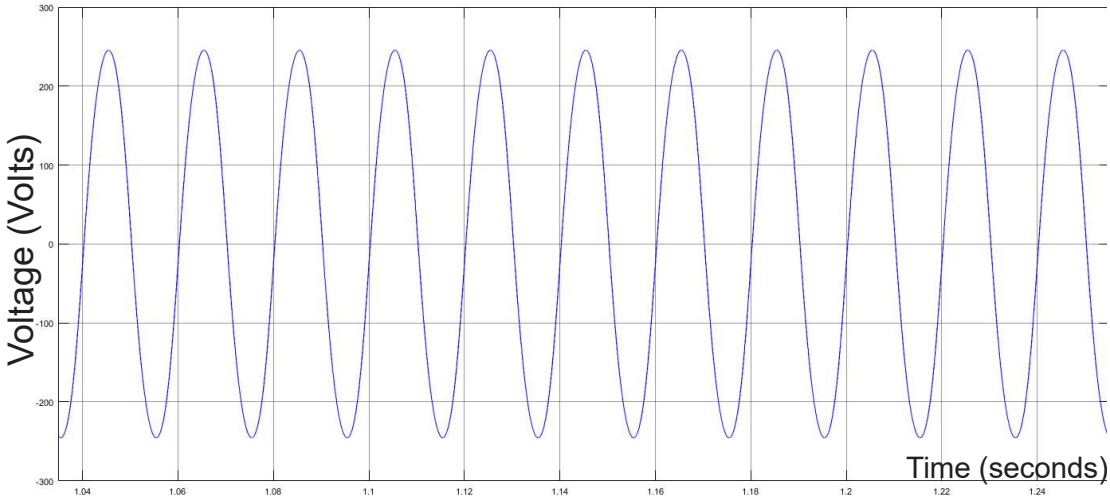

Figure 4.8. Zoomed-in Output of Combined DC Booster and SPWM Inverter Circuit

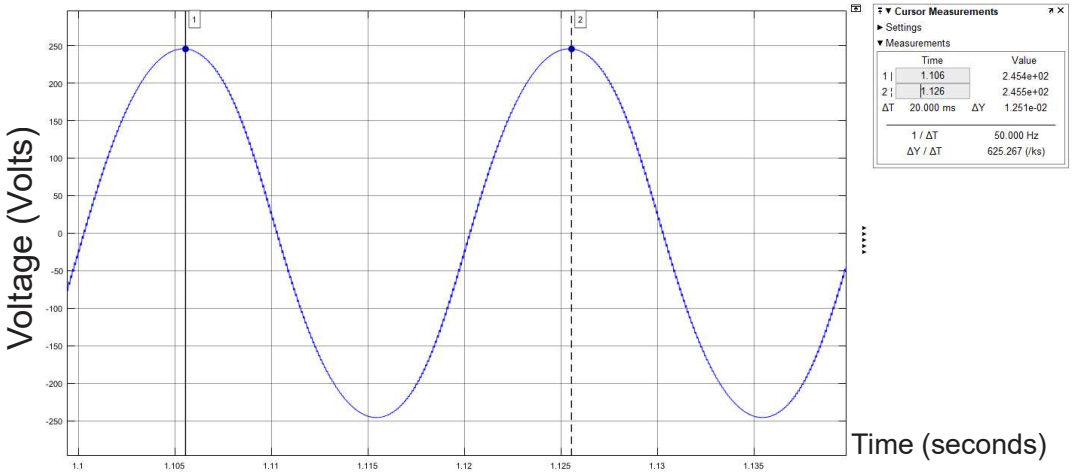

Figure 4.9. Frequency Verification of Combined DC Booster and SPWM Inverter Circuit

Figure 4.7 shows the output of the combination DC Booster/SPWM inverter circuit while Figure 4.8 is a zoomed version of Figure 4.7. From these figures it can thus be seen that the shape of the wave is that of a sine wave with Figure 4.9 illustrating the magnitude and frequency of 250V and 50 Hz respectively.

4.2 Rectifier Circuit Design

For the wind turbine charging circuit, the source is depicted as $380V_{AC}$. This is due to limited processing power. The AC is first rectified using the designed circuit in Figure 4.10.

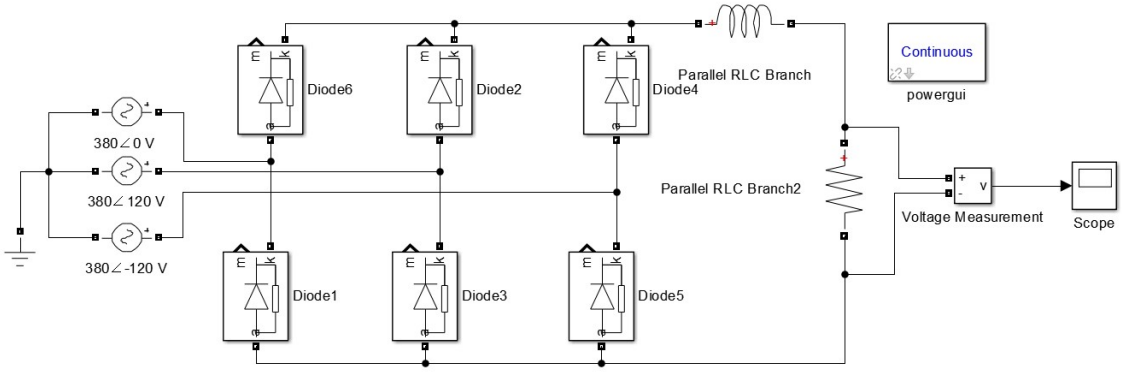

Figure 4.10. Wind Turbine Rectifier Circuit Verification

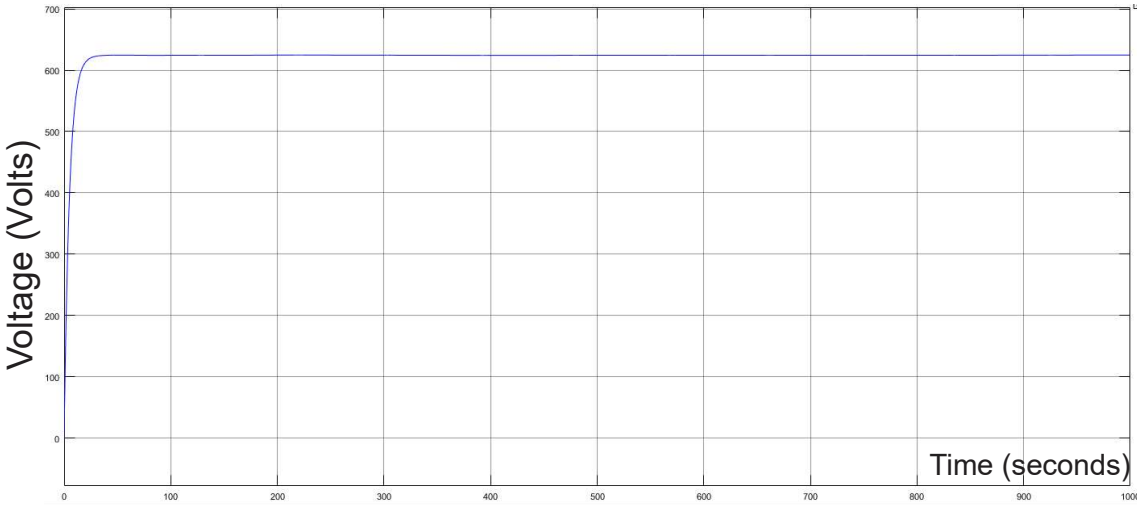

Figure 4.11. Wind Turbine Rectifier Circuit Output Verification

As predicted, the output of the rectifier is approximately $627V_{DC}$. This was established as illustrated from the value obtained in Figure 4.11.

This DC voltage is represented as a constant DC source in Figure 4.12 where it is reduced from 627V to 59V using the DC Buck circuit with output voltage shown in Figure 4.13.

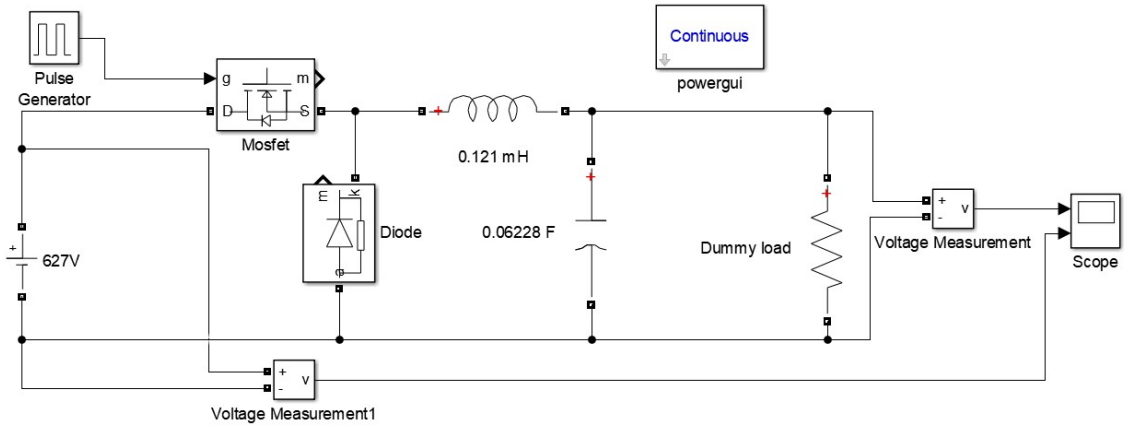

Figure 4.12. Wind Turbine Buck Circuit Verification

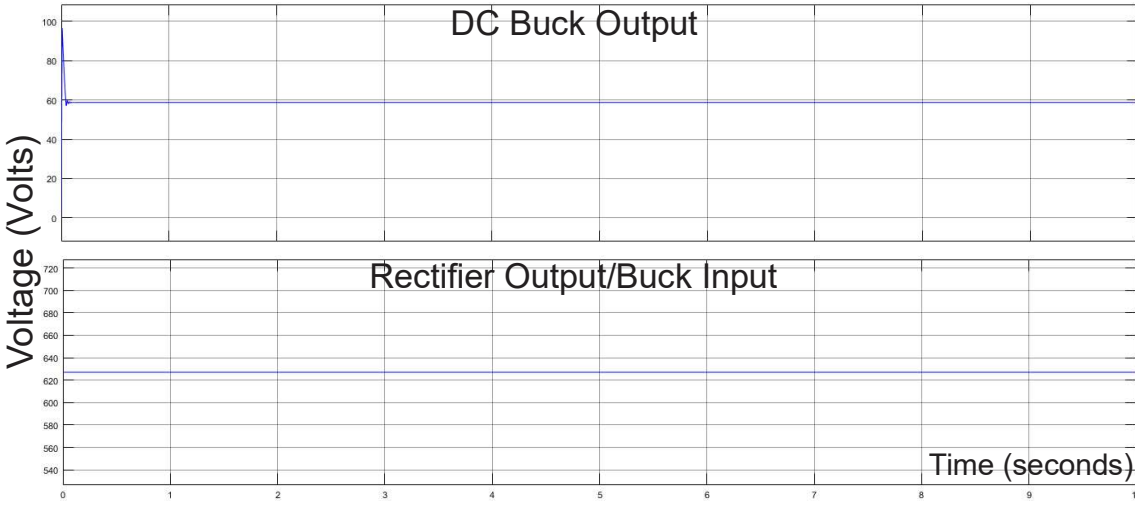

Figure 4.13. Wind Turbine Buck Circuit Output Verification

It can be seen from Figure 4.13 that the charging circuit does reduce the voltage to an acceptable charging voltage for the supercapacitor.

Figure 4.14 is the charging circuit using the PV array. In this figure, the PV Array is represented by a constant $240V_{DC}$ source. This voltage is reduced to $59V_{DC}$ using a DC buck circuit.

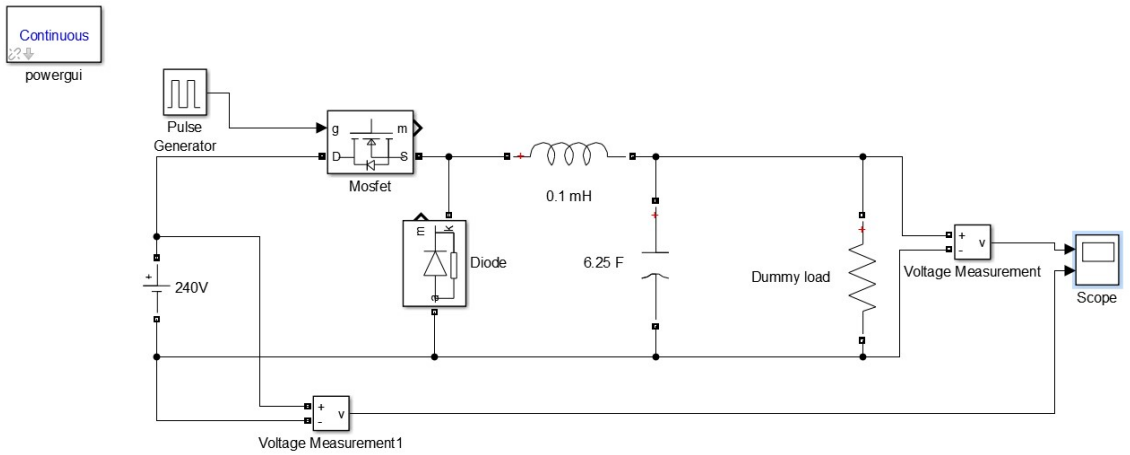

Figure 4.14.PV Array Buck Circuit Verification

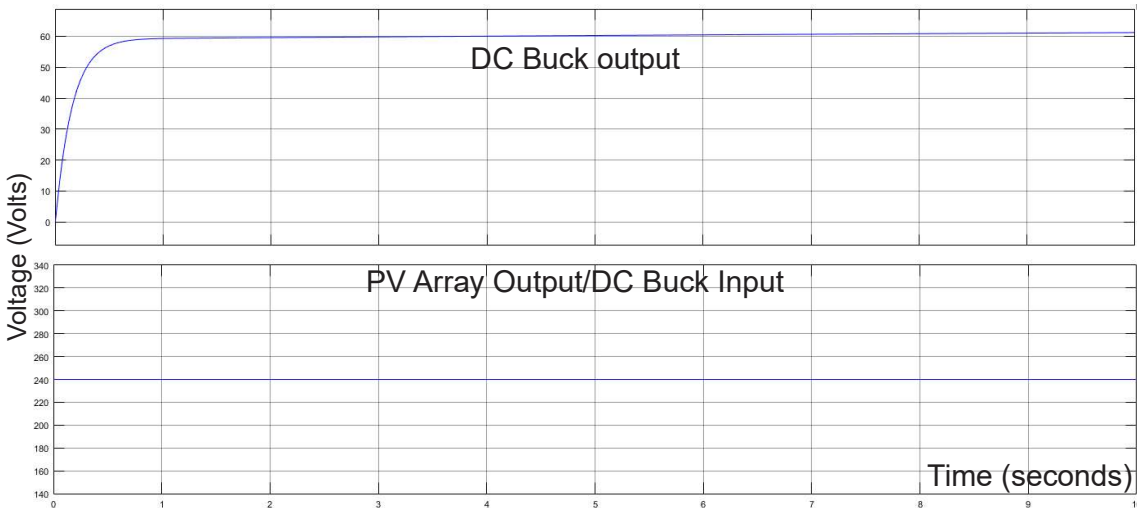

Figure 4.15.PV Array Buck Circuit Output Verification

Figure 4.15, illustrates that the circuit operates as designed.

Now that all the circuits have been proven to function as designed in the previous chapter, they can be tested using supercapacitors.

4.3 Main Discharge Circuit with Supercapacitors

The constant DC source from Figure 4.6 is replaced with a fully charged 51V 189F supercapacitor, resulting in the circuit diagram as shown in Figure 4.16. The simulation is first run without a load for a minute to determine the output behaviour and the output voltage for this condition is shown in Figure 4.17.

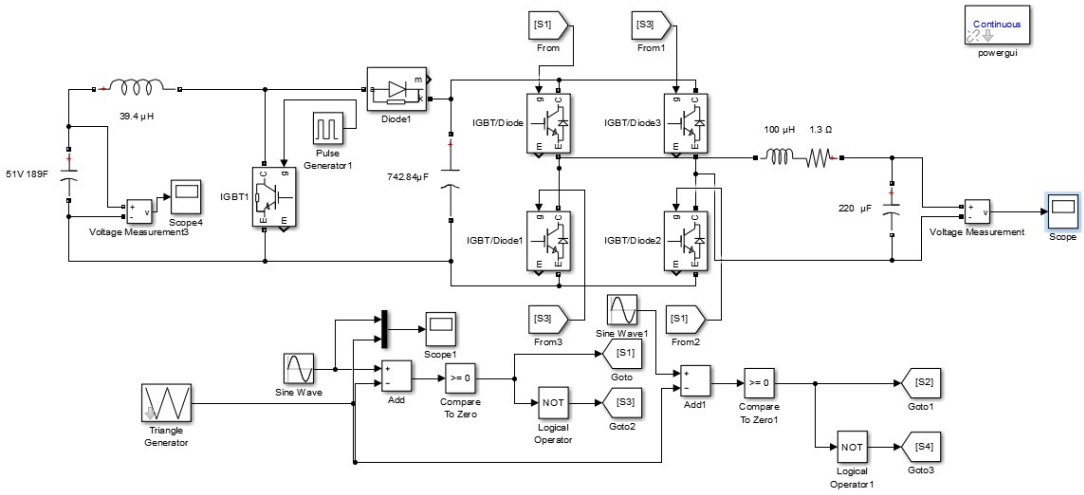

Figure 4.16. Main Discharge Circuit No Load

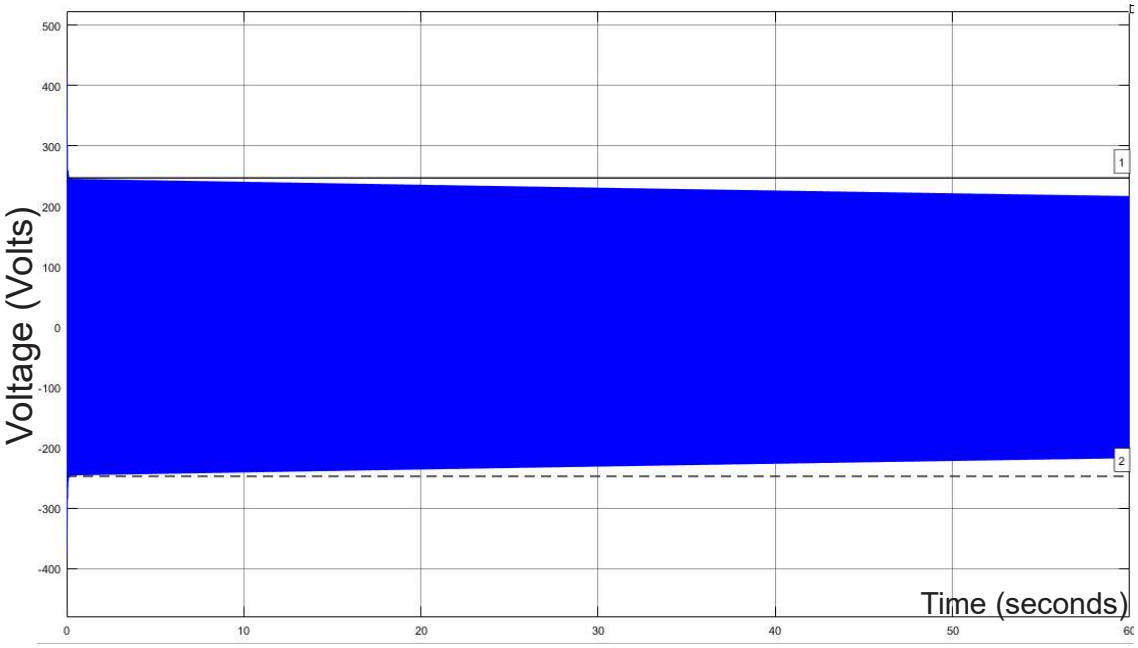

Figure 4.17. Main Discharge Circuit No Load Output

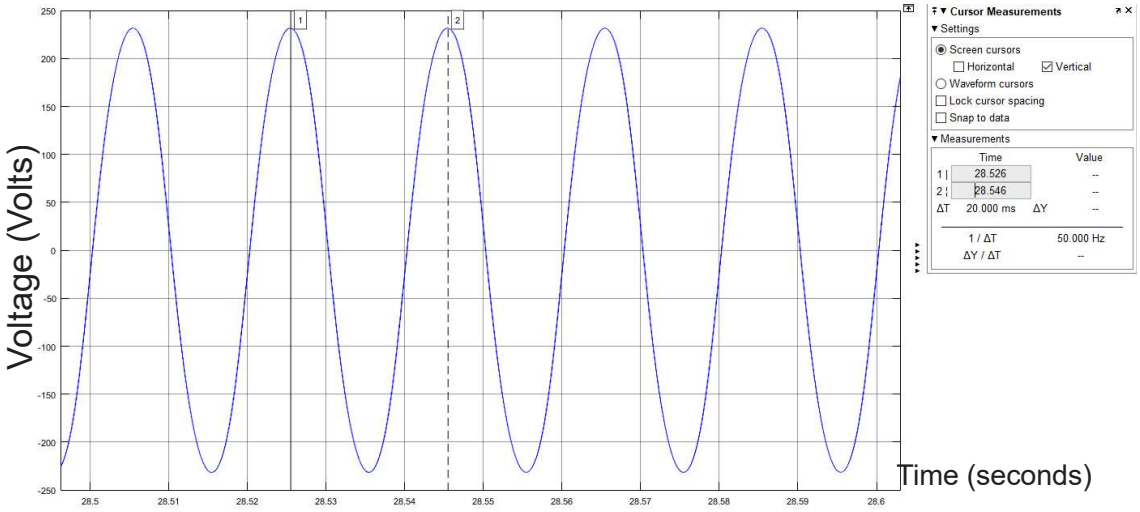

Figure 4.18.Main Discharge Circuit No Load Frequency Check

As can be seen in Figure 4.17, it shows a slight decline in the output voltage as the supercapacitor is slowly being discharged due to the circuit connected to the supercapacitor. Figure 4.18 zooms in on the output voltage as depicted in Figure 4.17. The diagram shows that the shape and frequency of the output voltage can be seen to be that of a sine wave with a frequency of 50 Hz. This verifies the design as covered in detail in section 3.3.2.

Table 4.1.Matlab/Simulink RL Series Load Block Inputs

Circuit 1	**Power**		
	Apparent kVA	**Active kW**	**Reactive kVAr**
Stove	5	4	3
Geyser	4.375	3.5	2.625
Lights	1.5	1.2	0.9
Fridge	0.625	0.5	0.375
Water Tank	0.4625	0.37	0.2775

Using Table 4.1 and the Series RLC Load block in Matlab/Simulink, the circuit in Figure 4.16 was modified to include domestic loads as labelled in Figure 4.19.

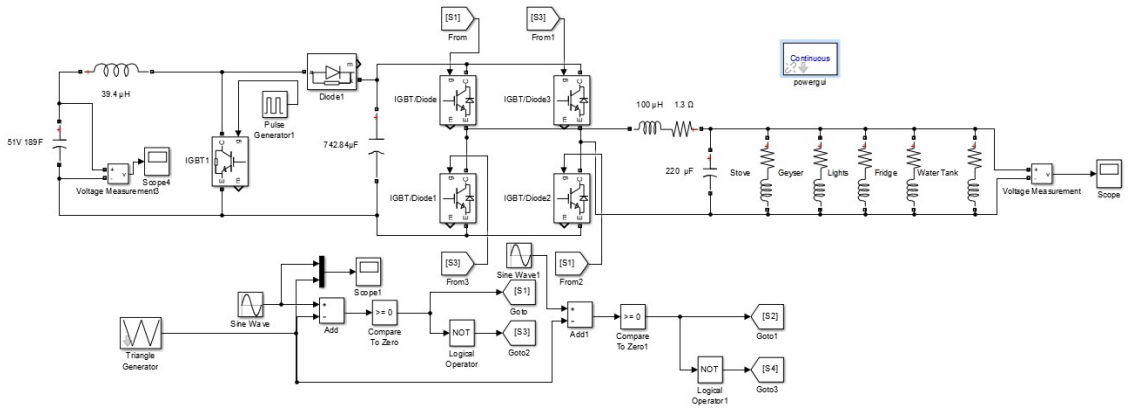

Figure 4.19. Main Discharge Circuit Full Load Circuit

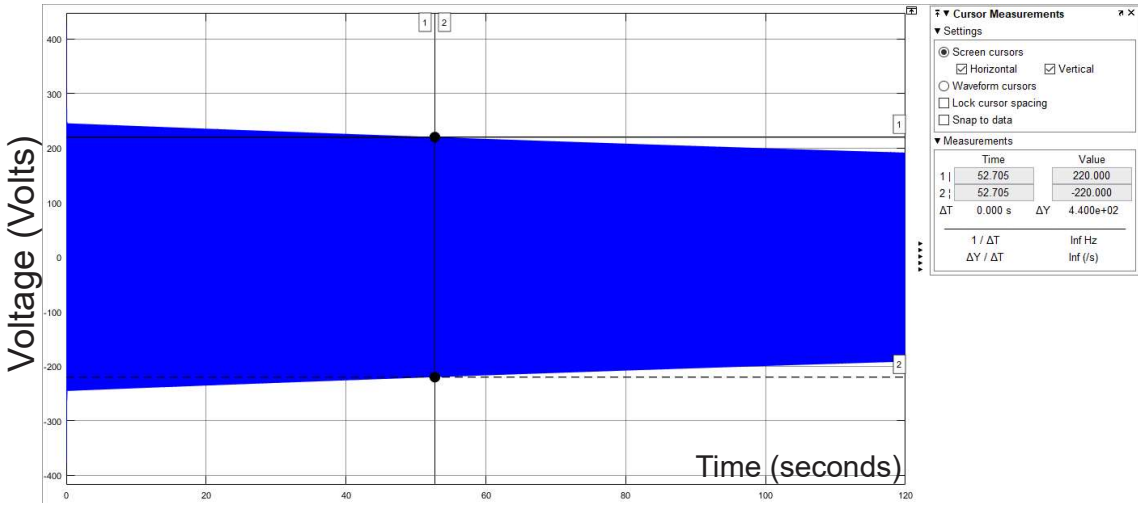

Figure 4.20. Main Discharge Circuit Full Load Output

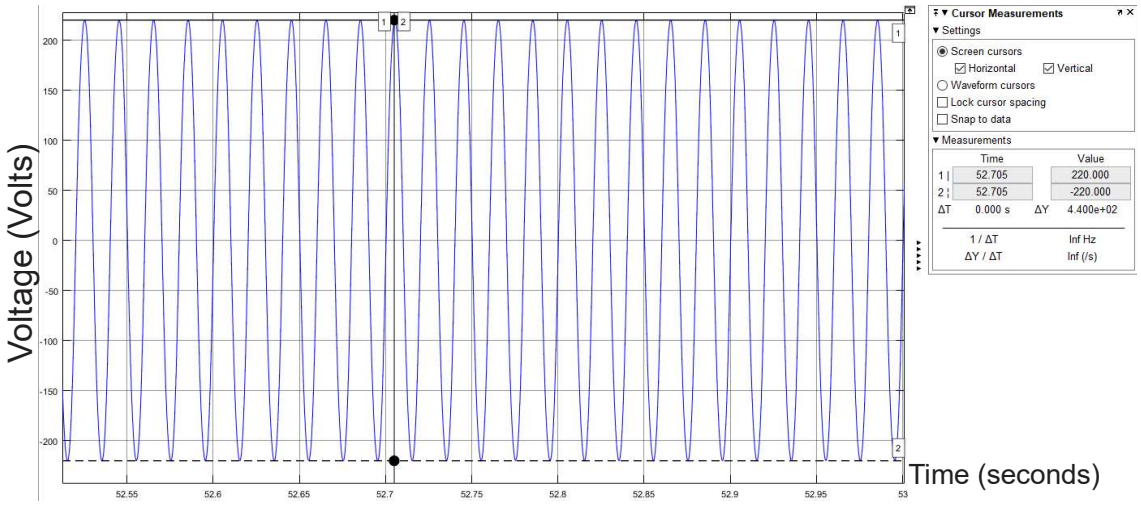

Figure 4.21. Main Discharge Circuit Voltage Below 220V

Based on the load condition diagram of Figure 4.19, the simulation results as depicted in Figure 4.20 shows the voltage applied to the loads as the supercapacitor is discharged. Since most appliances have an operating range of 220V-240V, a dotted line was placed at the lower limit of this range.

Figure 4.21 marks the time at which the voltage drops below 220V which is read off to be 52.705 seconds. This means that a single fully charged supercapacitor can adequately supply the loads listed in table 4.1 for 52.705s.

Using this data, the circuit shown in Figure 4.22 was constructed with two capacitors and a switching mechanism such that only a single supercapacitor is actively connected to the discharge circuit at a time. The switching time was selected to be 50s instead of 52.705s to incorporate a safety factor of 2.705s such that the load never experiences a voltage below that of 220V. In reality, the switching would not be time based but rather voltage based where a measuring voltage transformer would measure the output or input voltage and switch to a fully charged supercapacitor when the first has reached its lower limit. This principle can be applied to an "n" number of supercapacitors to continuously supply the load.

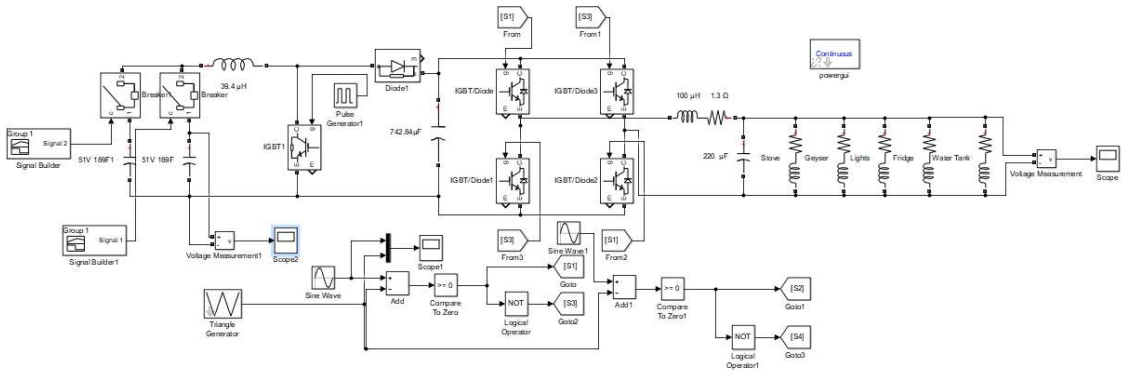

Figure 4.22.Main Discharge Circuit Full Load Circuit with 2 Supercapacitors

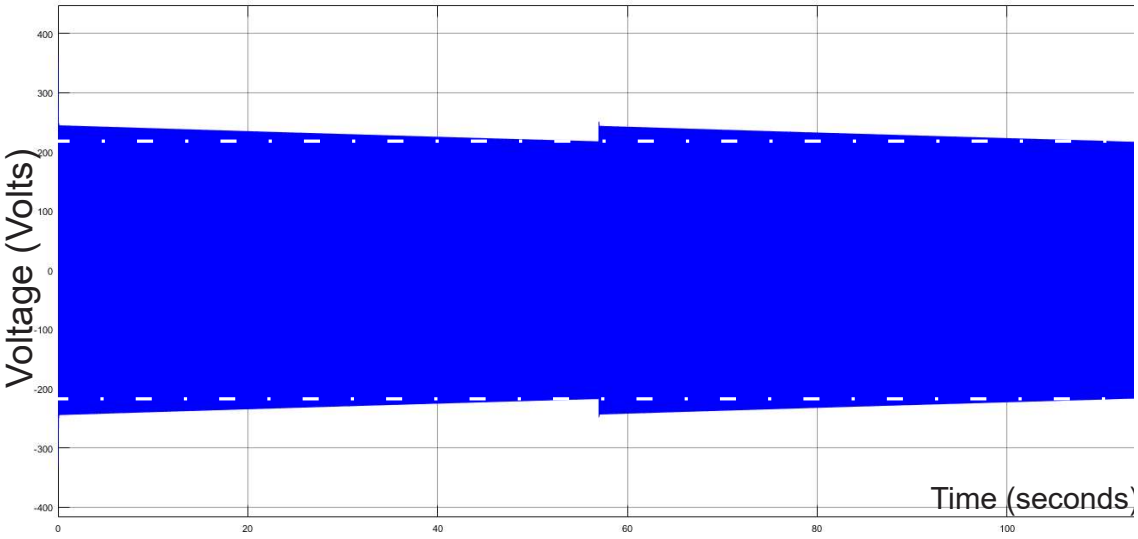

Figure 4.23.Output of Switching Between two Supercapacitors

The white dotted line in Figure 4.23 marks the 220V cut-off at which time the circuit switches over to a fully charged supercapacitor. For the loads listed in Table 4.1, using this it can be determined that the number of supercapacitors to supply this loads, simultaneously for a 24 hour period is:

$$\frac{(24 \times 60 \times 60)seconds}{50\ seconds} = 1\ 728\ supercapacitors \quad (4.1)$$

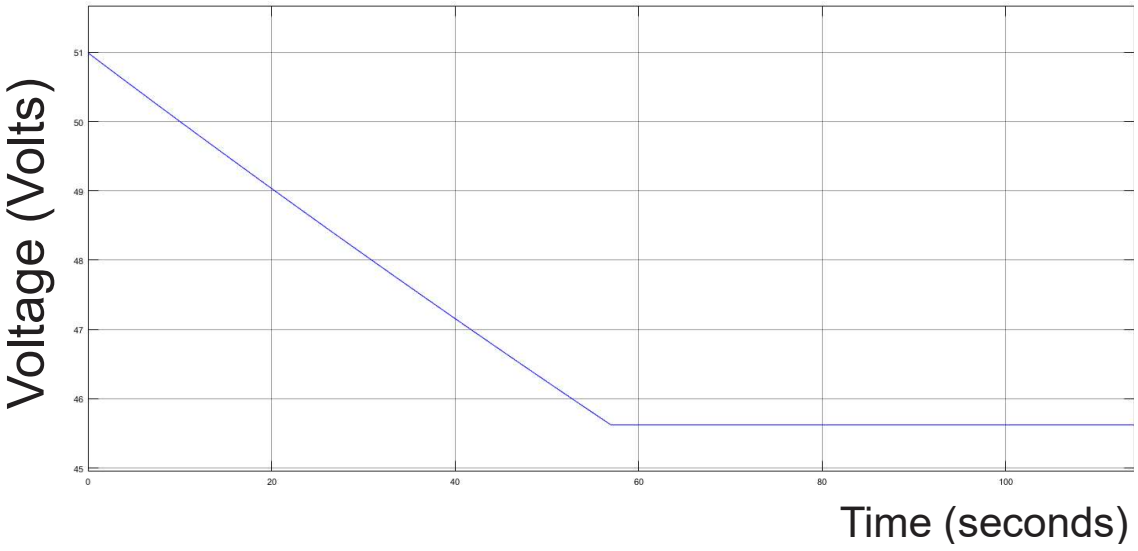

Figure 4.24. Supercapacitor Voltage at Time of Switching

Figure 4.24 shows at what voltage the supercapacitor is once it has been removed from the discharge circuit. The voltage at the time of switching is 45.75V. This data will be used in the next section.

4.4 Main Charge Circuit with Supercapacitors

Figure 4.25 is the designed circuit to charge the supercapacitor using the PV array. The PV array is represented by a constant 240V_{DC}source. The simulation is run in the following states or conditions:

- When the supercapacitor is completely discharged (0V)
- When the supercapacitor has been cut out from the discharge circuit. The voltage level at which the supercapacitor remains is determined to be 45.75V from Figure 4.24.

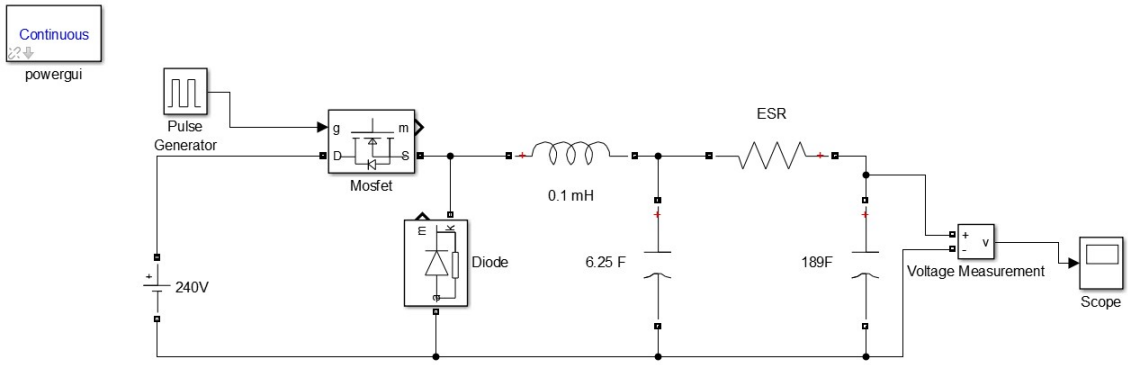

Figure 4.25. PV Array Buck Circuit Charging Supercapacitor

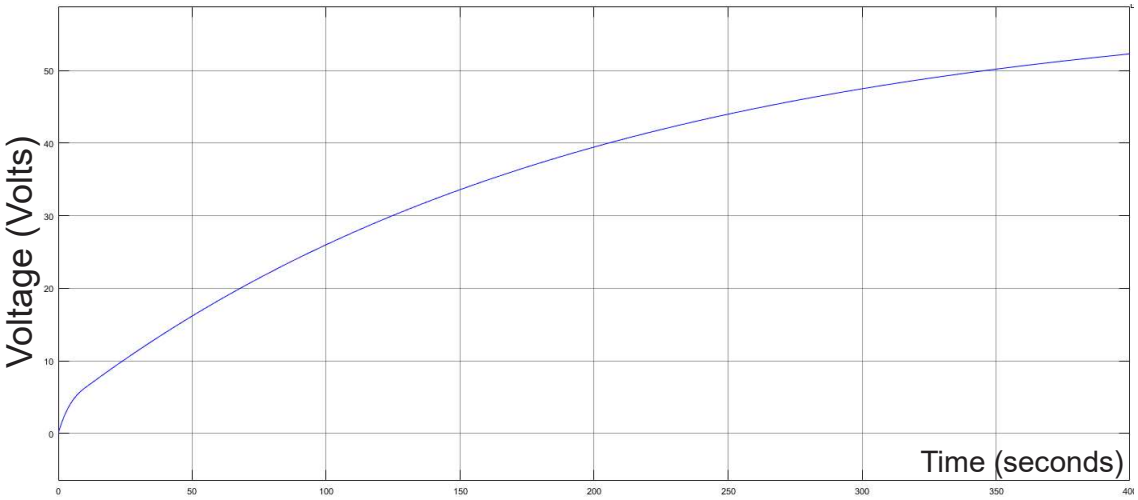

Figure 4.26. PV Array Charging: Supercapacitor Voltage from 0V

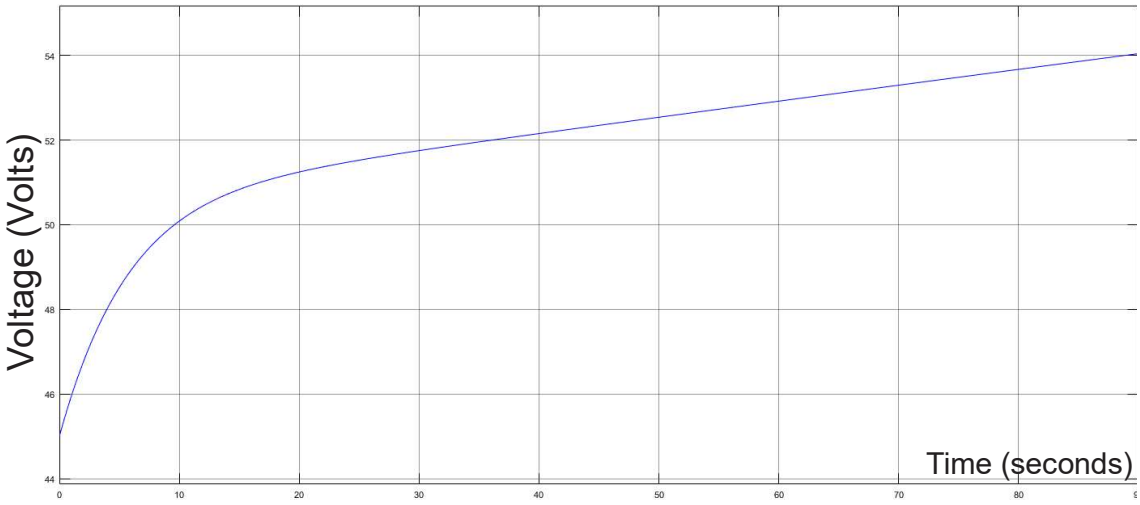

Figure 4.27. PV Array Charging: Supercapacitor Voltage from 45V

Charging the supercapacitor from 0V to an acceptable charge voltage above 51V takes over 400 seconds as indicated in Figure 4.26. However from Figure 4.27, charging from 45V, the full charge voltage is quickly achieved in 88 seconds.

A similar technique is applied for the wind turbine charging regiment, and the circuit diagram is as shown in Figure 4.28.

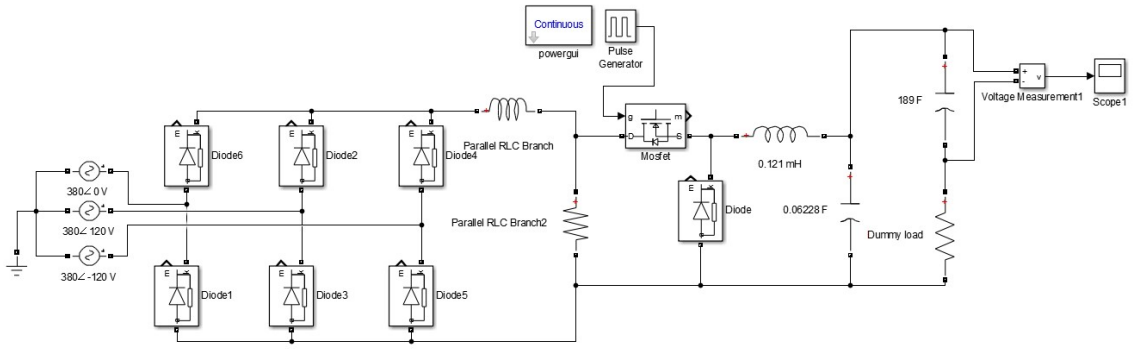

Figure 4.28. Wind Turbine Charging Supercapacitor Circuit

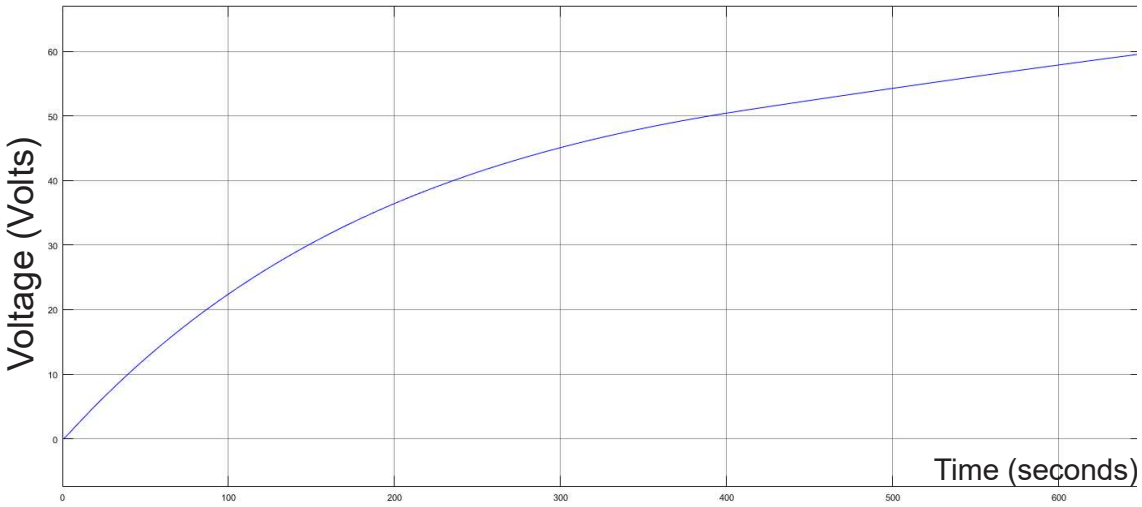

Figure 4.29. Wind Turbine Charging: Supercapacitor from 0V

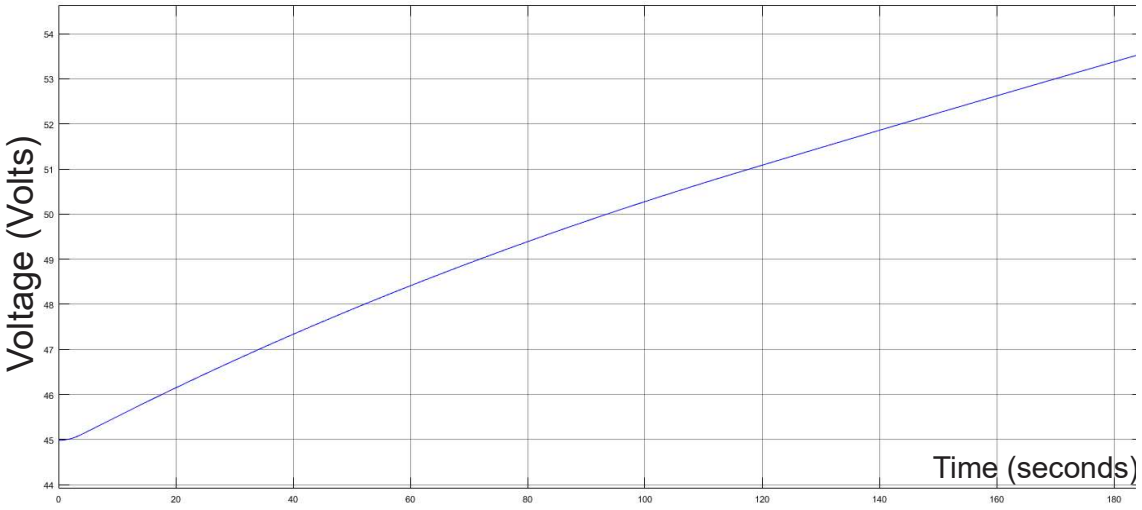

Figure 4.30. Wind Turbine Charging: Supercapacitor from 45V

As with the PV circuit, the wind turbine circuit was simulated with both starting supercapacitor voltages of 0V and 45V. As one would expect there is little to no difference between Figures 4.26 and 4.28, and Figures 4.27 and 4.29. This is due to the fact that the charging voltages of both circuits are the same.

Figure 4.31 shows how a charging circuit would continuously monitor the charge level on the supercapacitor and ensure that only one supercapacitor is charged at any time. At a potential difference of 53V, the supercapacitor is removed. The circuit in Figure 4.31 would require a microcontroller to ensure that only one supercapacitor is connected at a time. This requires a priority algorithm such that the voltage of each supercapacitor is continuously monitored and a queue of supercapacitors to be charged is created.

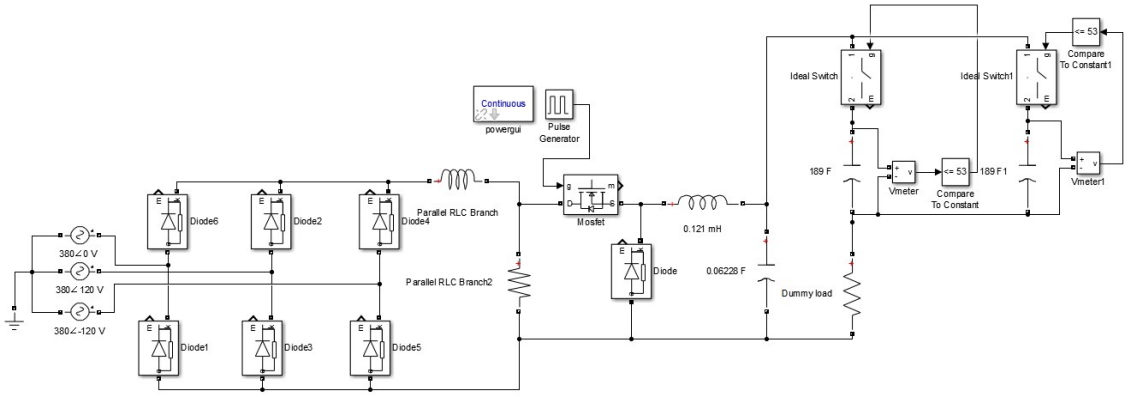

Figure 4.31. Wind Turbine Charging Circuit with 2 Supercapacitors

In order to obtain a possible feasibility for the future of supercapacitors, a fabricated supercapacitor capacitance of 1890 F was used in a discharge circuit simulation. This circuit is shown in Figure 4.32.

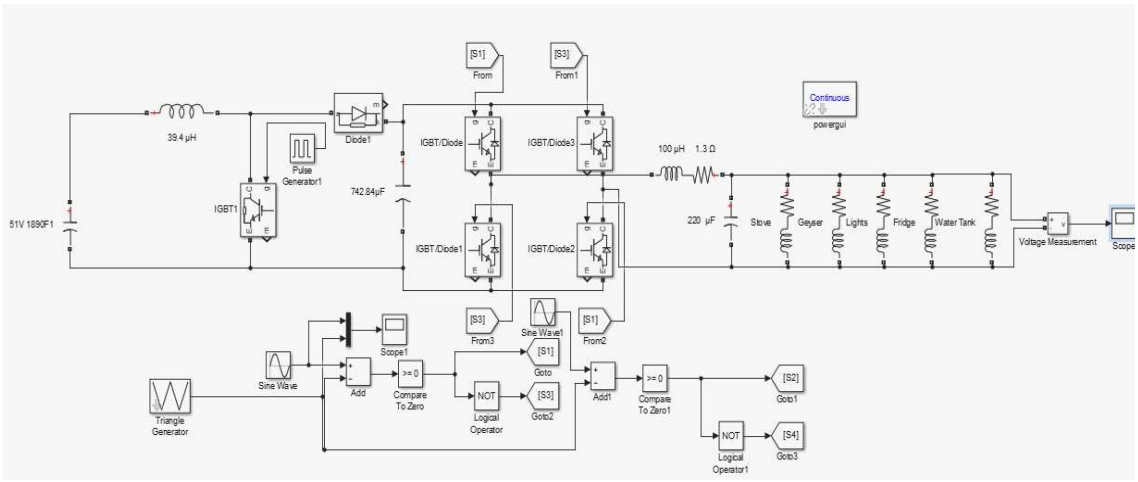

Figure 4.32. Discharge Circuit Using 1890F Supercapacitor

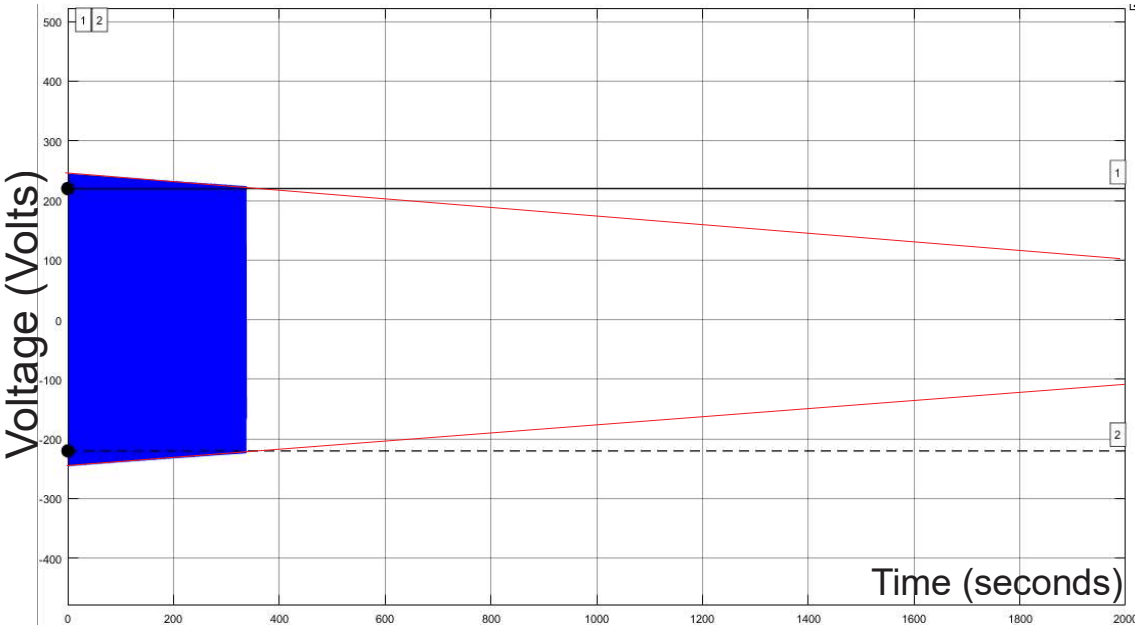

Figure 4.33. Output of Discharge Circuit Using 1890F Supercapacitor

Due to limited processing power, the output in Figure 4.33 could not be completed however the red lines are used as an extrapolation. The horizontal black dotted and solid lines mark the lower limit of domestic appliance operating voltages.

In order to determine the charging time for such a fabricated supercapacitor, Figure 4.28 was modified to charge a 1890F supercapacitor. In the beginning, the voltage of the supercapacitor was set to 45V due to limited processing power. The resulting charging time is depicted in Figure 4.34.

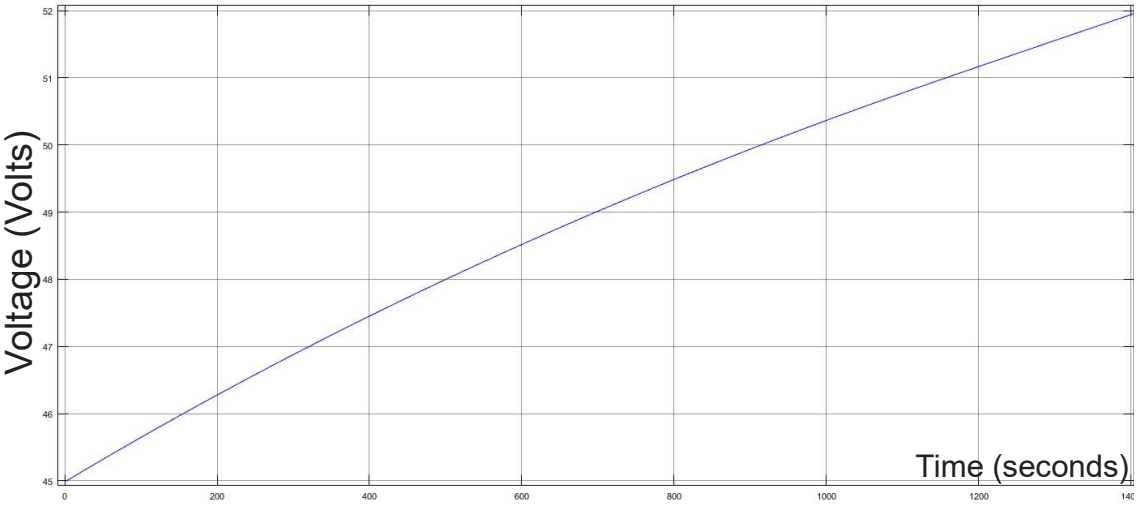

Figure 4.34. Charging Time for 1890F Supercapacitor

4.5 Analysis of Results

The supercapacitor was first tested as voltage source with no load conditions. Figure 4.16 illustrates the main discharge circuit with no load while the output wave form obtained from the operation of this circuit is shown in Figure 4.18. It in this circuit and its output that the output voltage and sine wave form can be verified. Figure 4.18 verifies that the supercapacitor can indeed operate as a voltage source since the output waveform is that of a sine wave with a frequency of 50 Hz. This means that the supercapacitor can supply AC loads.

Figure 4.19 is Figure 4.16 modified to include the domestic loads from Table 4.1. This simulation shows the behaviour of the supercapacitor when supplying a full load. Figure 4.20 illustrates how the voltage decreases as the charge with the supercapacitor is depleted. The dotted line in this figure marks the point where the output voltage drops below the lower limit of 220V. The moment that the voltage drops below the lower limit (52.705s from Figure 4.21), the supercapacitor must be ejected from the circuit and replaced by a fully charged supercapacitor. This technique can be seen in Figures 4.22 and 4.23. At this time of 52.705s, the supercapacitor itself is at 45.75V as seen in Figure 4.24. This infers that the supercapacitor can supply the circuit while it holds a voltage between 51V and 45.75V. However, the design can be modified to include additional circuitry such that the supercapacitor supplies the load continuously until it is at a much lower voltage. This modification could be in the form of additional DC boosters for different voltage levels which adds to the complexity of the circuit.

Equation (4.1) determines how many supercapacitors are required to supply the loads documented in Table 4.1 for a 24 hour period. The number of supercapacitors far exceeds that of battery cells required by a factor of approximately 29 (precisely 28.8).

In a more pragmatic environment, where the loads don't run continuously and simultaneously, the supercapacitor would be able to supply the load for longer periods. This would reduce the number of supercapacitors required.

When charging the supercapacitor there are two starting conditions must be considered, namely:

- charging from 0V
- charging from an initial supercapacitor voltage of 45.75V

The first charge of the supercapacitor should be from 0V since upon procuring the product the supercapacitor has no charge. Figure 4.26 and Figure 4.29 show that the time to charge the supercapacitor from 0V to a full charge of 51V is 400 seconds while Figure 4.27 and Figure 4.30 show that the supercapacitor achieves full charge in less than 90 seconds from 45V. The method of charging, either wind or solar, is irrelevant since the respective circuits lowers the charge voltage to

an acceptable level without exposing the supercapacitor to excessive voltages. With charging times such as 400 seconds and 90 seconds, the supercapacitor is perfectly coupled with renewable energy sources since due intermittency, available charge time is limited.

Chapter Five

Conclusion and Recommendations

Supercapacitors are already pragmatic in a number of applications. These applications range from electric vehicles to uninterrupted power supplies[84]. Much research is required before the technology can surpass and replace batteries.

Chapter 4, equation (4.1) calculated that to effectively supply the loads listed in Table 4.1 continuously for a 24 hour period, the total number of supercapacitors required is 1728. This is exorbitant when compared to the 60 cells that make up the battery bank calculated in chapter 3. The calculation in chapter 3 does not take into account that the loads listed are operating on a 24 hour period. Adjusting the calculation for all loads simultaneously operating, results in a battery consisting of 140 cells (ie. 140 X 12V 200Ah). Seven parallel strings each consisting of twenty cells. Even at this point the number of cells is far less than that of the number of supercapacitors required.

The supercapacitor is able to deliver the voltage and current required to supply the load with virtually no strain placed on the device itself. Should a battery be subjected to a similar load as presented in this study, it would suffer great physical damage and produce large amounts of hazardous gases including highly flammable hydrogen (to prevent this, a larger battery is required). The large load would irrevocably damage the cells and plates that make up the battery which would alter its ability to hold charge and greatly reduce its life span. The larger currents imposed on the supercapacitor by the load would make no difference to the life span of the supercapacitor since it still operates below the specified current requirement of each supercapacitor.

By using the maximum charge current of the battery, 40A, it is possible to quickly determine that the battery will reach full charge within 5 hours. Although it often undesirable to charge such batteries with larger currents since it may damage the chemical electrolytes and electrodes thereby affecting its overall performance. With regards to the supercapacitor, a single module is quickly charged from 0V to 51V in approximately 5 minutes. This result makes it extremely suitable for renewable energy sources. It must be stated though that the single battery would be able to supply a load for a much longer period.

In areas where sunlight is sparse, the supercapacitor arrangement can quickly absorb more energy without damage and later charge the battery bank.

Buses in China have appropriately taken advantage of supercapacitor characteristics. Namely, fast charging and low energy density or low specific energy. This is done by means of charging the

supercapacitors within the bus at each bus stop. The short trips around the city means that the low energy density is accounted for since the supercapacitors need only enough charge to take the bus to the next stop where it can be quickly charged once more [68]. This system may be seen as a hybrid. There is little literature on how these charging stations store energy and therefore an educated assumption leads to a battery bank since sunlight or other renewable energy sources are not always available. It is possible though that the charging stations do use supercapacitors. Nevertheless, this application is perfectly suited for supercapacitors.

Supercapacitors are much more expensive than batteries. One can expect to pay up to $820 for a single module of the supercapacitor used in this study. Whereas the battery used in this study (SDDirectPro AGM+ 12V 200Ah) can cost up to $340. That's 240% more for the supercapacitor. The supercapacitor ESS in this study requires a system to ensure that one supercapacitor is charged at a time and only one is discharged at a time. This places additional circuit requirements on the system such as voltage and current transformers to continuously monitor the charge level of the supercapacitor and more than one switching device. It was initially mentioned that the system would not require a control system, however it was later realized that it is indeed required to carry out the operations as mentioned. A micro-controller is required to determine when each supercapacitor must be charged and what order and which supercapacitor is to be discharged. All points discussed lead to a larger budget requirement whereas a battery ESS uses far less circuitry in the form of a rectifier and an inverter.

Figure 4.32 shows the voltage applied to the load with a supercapacitor of a theoretical capacitance of 1890 F, ten times the capacitance of that used in the study. From the output graph (Figure 4.33) it can be seen that the lower limit of 220V is reached in the region of 320 seconds, which is over 6 times slower than that of the system which uses the 189F supercapacitor. This means that 270 supercapacitors, each with a capacitance of 1890F would be required to supply the load for a 24 hour period. By increasing capacitance tenfold lowers the number of required supercapacitors by a factor of 6.4 and extends the usable charge by a similar factor of 6. It is worth noting though that a supercapacitor with such a capacitance would require a much longer charging time (1400 seconds or over 23 minutes to charge from 45V to 52V as seen in Figure 4.34).

While the supercapacitor technology does in fact have its advantages, the drawbacks are far too prominent to ignore. The number of supercapacitors required to supply the same load for the same period are far more than that of a battery system. This contributes to rising costs. These points lead to the conclusion that supercapacitors in their present form are not yet a viable form of energy storage. Increasing the capacitance to 1890F for a single supercapacitor module, made some improvement on the duration to supply a load but it still lags behind the battery.

The improvement of supercapacitor technology lies within the ionization or breakdown voltage. This limit must be increased by venturing into untested materials. This would allow for higher voltage supercapacitors and therefore larger energy densities. Using equation (2.7), it can be seen that the energy within the supercapacitor is directly proportional to the capacitance and the square of the voltage.

While a standalone supercapacitor ESS may not yet viable, one that includes batteries has been proven to be beneficial. A hybrid system[54] can offer advantages of both technologies. Supercapacitors can supply larger loads for short durations thereby placing less strain on the battery and extending its life. In conjunction with renewable energy sources, where short bursts of sunlight or wind are available, the supercapacitor can quickly store energy and later discharge it to the battery.

At present, supercapacitors may find its way into consumer electronics where the load is lighter and the voltage and current requirements are also lower. With regards to larger loads such as the domestic ones applied in this study, supercapacitor technology is not viable.

Further study into the chemical make up behind the construction of a supercapacitor may provide a method to solve the intermittency of renewable energy or at the very least a way to enhance existing energy storage techniques. Currently, PV arrays and wind farms use batteries as energy storage devices with supercapacitors beginning to enter the market on a small scale. The aim here will be to expand on this by using supercapacitors on a larger scale.

References

[1] J. Murray and D. King, "Climate policy: Oil's tipping point has passed," *Nature,* vol. 481, no. 7382, p. 433, 2012.

[2] S. Shafiee and E. Topal, "When will fossil fuel reserves be diminished?," *Energy policy,* vol. 37, no. 1, pp. 181-189, 2009.

[3] M. Sklar-Chik, A. Brent, and I. De Kock, "Critical review of the levelised cost of energy metric," *South African Journal of Industrial Engineering,* vol. 27, no. 4, pp. 124-133, 2016.

[4] C. W. Potter, A. Archambault, and K. Westrick, "Building a smarter smart grid through better renewable energy information," in *Power Systems Conference and Exposition, 2009. PSCE'09. IEEE/PES*, 2009, pp. 1-5: IEEE.

[5] D. Lindley, "Smart grids: The energy storage problem," *Nature News,* vol. 463, no. 7277, pp. 18-20, 2010.

[6] A. Evans, V. Strezov, and T. J. Evans, "Assessment of utility energy storage options for increased renewable energy penetration," *Renewable and Sustainable Energy Reviews,* vol. 16, no. 6, pp. 4141-4147, 2012.

[7] E. Martinot, "Renewables 2005: Global status report," *Washington, DC: Worldwatch Institute,* 2005.

[8] A. Muzaffar, M. B. Ahamed, K. Deshmukh, and J. Thirumalai, "A review on recent advances in hybrid supercapacitors: Design, fabrication and applications," *Renewable and Sustainable Energy Reviews,* vol. 101, pp. 123-145, 2019.

[9] S. Zeng, Y. Liu, C. Liu, and X. Nan, "A review of renewable energy investment in the BRICS countries: History, models, problems and solutions," *Renewable and Sustainable Energy Reviews,* vol. 74, pp. 860-872, 2017.

[10] W. F. Pickard, A. Q. Shen, and N. J. Hansing, "Parking the power: Strategies and physical limitations for bulk energy storage in supply–demand matching on a grid whose input power is provided by intermittent sources," *Renewable and Sustainable Energy Reviews,* vol. 13, no. 8, pp. 1934-1945, 2009.

[11] P. Jain, "Energy Storage in Grids with High Penetration of Variable Generation". *Asian Development Bank,* 2017.

[12] H. L. Ferreira, R. Garde, G. Fulli, W. Kling, and J. P. Lopes, "Characterisation of electrical energy storage technologies," *Energy,* vol. 53, pp. 288-298, 2013.

[13] B. Li *et al.*, "Activated Carbon from Biomass Transfer for High-Energy Density Lithium-Ion Supercapacitors," *Advanced Energy Materials,* vol. 6, no. 18, 2016.

[14] M. Winter and R. J. Brodd, "What are batteries, fuel cells, and supercapacitors?," ed: ACS Publications, 2004.

[15] R. E. Barlow and F. Proschan, "Statistical theory of reliability and life testing: probability models," Florida State Univ Tallahassee1975.

[16] H. Liu, C. Mao, J. Lu, and D. Wang, "Electronic power transformer with supercapacitors storage energy system," *Electric Power Systems Research,* vol. 79, no. 8, pp. 1200-1208, 2009.

[17] M. Kim and E. Hwang, "Monitoring the battery status for photovoltaic systems," *Journal of power sources,* vol. 64, no. 1-2, pp. 193-196, 1997.

[18] X. Zhou, X. Y. Chen, and J. X. Jin, "Development of SMES technology and its applications in power grid," in *Applied Superconductivity and Electromagnetic Devices (ASEMD), 2011 International Conference on*, 2011, pp. 260-269: IEEE.

[19] B. Bolund, H. Bernhoff, and M. Leijon, "Flywheel energy and power storage systems," *Renewable and Sustainable Energy Reviews,* vol. 11, no. 2, pp. 235-258, 2007.
[20] J. P. Deane, B. Ó. Gallachóir, and E. McKeogh, "Techno-economic review of existing and new pumped hydro energy storage plant," *Renewable and Sustainable Energy Reviews,* vol. 14, no. 4, pp. 1293-1302, 2010.
[21] M. Budt, D. Wolf, R. Span, and J. Yan, "A review on compressed air energy storage: Basic principles, past milestones and recent developments," *Applied Energy,* vol. 170, pp. 250-268, 2016.
[22] K. G. Vosburgh, "Compressed air energy storage," *Journal of Energy,* vol. 2, no. 2, pp. 106-112, 1978.
[23] B. Elmegaard and W. Brix, "Efficiency of compressed air energy storage," in *24th international conference on efficiency, cost, optimization, simulation and environmental impact of energy systems*, 2011.
[24] H. Chen, X. Zhang, J. Liu, and C. Tan, "Compressed air energy storage," in *Energy Storage-Technologies and Applications*: InTech, 2013.
[25] D. R. Brown and W. D. Chvala, "Flywheel energy storage: an alternative to batteries for UPS systems," *Energy engineering,* vol. 102, no. 5, pp. 7-26, 2005.
[26] H. Liu and J. Jiang, "Flywheel energy storage—An upswing technology for energy sustainability," *Energy and buildings,* vol. 39, no. 5, pp. 599-604, 2007.
[27] T. M. Mulcahy *et al.*, "Flywheel energy storage advances using HTS bearings," *IEEE Transactions on Applied superconductivity,* vol. 9, no. 2, pp. 297-300, 1999.
[28] N. Rampersadh, "Grid Energy Storage Devices (ESD)," University of KwaZulu-Natal, Howard College, 2016.
[29] Z. Kohari and I. Vajda, "Losses of flywheel energy storages and joint operation with solar cells," *Journal of materials processing technology,* vol. 161, no. 1-2, pp. 62-65, 2005.
[30] R. M. Dell and D. A. Rand, "Energy storage—a key technology for global energy sustainability," *Journal of power sources,* vol. 100, no. 1-2, pp. 2-17, 2001.
[31] R. Takahashi, L. Wu, T. Murata, and J. Tamura, "An application of flywheel energy storage system for wind energy conversion," in *Power Electronics and Drives Systems, 2005. PEDS 2005. International Conference on*, 2005, vol. 2, pp. 932-937: IEEE.
[32] H. Zhang, J. Baeyens, J. Degrève, and G. Cacères, "Concentrated solar power plants: Review and design methodology," *Renewable and Sustainable Energy Reviews,* vol. 22, pp. 466-481, 2013.
[33] H. Müller-Steinhagen and F. Trieb, "Concentrating solar power," *A review of the technology. Ingenia Inform QR Acad Eng,* vol. 18, pp. 43-50, 2004.
[34] D. Barlev, R. Vidu, and P. Stroeve, "Innovation in concentrated solar power," *Solar Energy Materials and Solar Cells,* vol. 95, no. 10, pp. 2703-2725, 2011.
[35] D. Fernandes, F. Pitié, G. Cáceres, and J. Baeyens, "Thermal energy storage:“How previous findings determine current research priorities”," *Energy,* vol. 39, no. 1, pp. 246-257, 2012.
[36] R. I. Dunn, P. J. Hearps, and M. N. Wright, "Molten-salt power towers: newly commercial concentrating solar storage," *Proceedings of the IEEE,* vol. 100, no. 2, pp. 504-515, 2012.
[37] T. Sarver, A. Al-Qaraghuli, and L. L. Kazmerski, "A comprehensive review of the impact of dust on the use of solar energy: History, investigations, results, literature, and mitigation approaches," *Renewable and sustainable energy Reviews,* vol. 22, pp. 698-733, 2013.
[38] J. Hoffmanna and K. Madalyb, "On Thermal Energy Storage Capacity for CSP Plant in South Africa." *R & D Journal of the South African Institution of Mechanical Engineering*, 31, pp. 46-51, 2015
[39] J. Kraus, "Electromagnetics, 318," ed: McGraw-Hill Book Co., Inc., New York, 1953.
[40] R. Kustom *et al.*, "Research on power conditioning systems for superconductive magnetic energy storage (SMES)," *IEEE Transactions on Magnetics,* vol. 27, no. 2, pp. 2320-2323, 1991.

[41] C. A. Luongo, "Superconducting storage systems: An overview," *IEEE Transactions on Magnetics,* vol. 32, no. 4, pp. 2214-2223, 1996.
[42] D. Linden and T. B. Reddy, "Handbook of Batteries. 3rd," *McGraw-Hill,* 2002.
[43] M. A. Laughton and M. G. Say, *Electrical engineer's reference book*. Elsevier, 2013.
[44] H. Keulenaer, "Spinnning reserve e balancing the net," *Minute lectures: Leonardo energy,* 2007.
[45] M. J. Sanger and T. J. Greenbowe, "Student misconceptions in electrochemistry regarding current flow in electrolyte solutions and the salt bridge,"*Journal of Chemical Education ,* 74 (7), pp. 819, 1997
[46] T. Motors, "Tesla powerwall," *URL https://www. teslamotors. com/no_ NO/powerwall,* 2016.
[47] J. Wen, Y. Yu, and C. Chen, "A review on lithium-ion batteries safety issues: existing problems and possible solutions," *Materials express,* vol. 2, no. 3, pp. 197-212, 2012.
[48] M. Holzapfel, A. Würsig, W. Scheifele, J. Vetter, and P. Novák, "Oxygen, hydrogen, ethylene and CO2 development in lithium-ion batteries," *Journal of Power Sources,* vol. 174, no. 2, pp. 1156-1160, 2007.
[49] S. J. Ericson and P. Statwick, "Opportunities for Battery Storage Technologies in Mexico," National Renewable Energy Lab.(NREL), Golden, CO (United States)2018.
[50] E. Muljadi, C. Butterfield, J. Chacon, and H. Romanowitz, "Power quality aspects in a wind power plant," in *Power Engineering Society General Meeting, 2006. IEEE*, 2006, p. 8 pp.: IEEE.
[51] L. Qu and W. Qiao, "Constant power control of DFIG wind turbines with supercapacitor energy storage," *IEEE Transactions on Industry Applications,* vol. 47, no. 1, pp. 359-367, 2011.
[52] P. K. Ray and S. R. Mohanty, "Nand Kishor," *Proportional-integral controller based small-signal analysis of hybrid distributed generation systems. Energy Conversion Management,* vol. 52, pp. 1943-54, 2011.
[53] F. Díaz-González, A. Sumper, O. Gomis-Bellmunt, and R. Villafáfila-Robles, "A review of energy storage technologies for wind power applications," *Renewable and sustainable energy reviews,* vol. 16, no. 4, pp. 2154-2171, 2012.
[54] A. M. van Voorden, L. M. R. Elizondo, G. C. Paap, J. Verboomen, and L. van der Sluis, "The application of super capacitors to relieve battery-storage systems in autonomous renewable energy systems," in *Power Tech*, 2007, vol. 1: Citeseer.
[55] H. I. Becker, "Low voltage electrolytic capacitor," ed: Google Patents, 1957.
[56] M. S. Halper and J. C. Ellenbogen, "Supercapacitors: A brief overview," *The MITRE Corporation, McLean, Virginia, USA,* pp. 1-34, 2006.
[57] S. Faraji and F. N. Ani, "The development supercapacitor from activated carbon by electroless plating—A review," *Renewable and Sustainable Energy Reviews,* vol. 42, pp. 823-834, 2015.
[58] A. Pandolfo and A. Hollenkamp, "Carbon properties and their role in supercapacitors," *Journal of power sources,* vol. 157, no. 1, pp. 11-27, 2006.
[59] A. Burke, "Ultracapacitors: why, how, and where is the technology," *Journal of power sources,* vol. 91, no. 1, pp. 37-50, 2000.
[60] H. Yang, S. Kannappan, A. S. Pandian, J.-H. Jang, Y. S. Lee, and W. Lu, "Achieving Both High Power and Energy Density in Electrochemical Supercapacitors with Nanoporous Graphene Materials," *arXiv preprint arXiv:1311.1413,* 2013.
[61] A. G. F. de Bobadilla and J. A. B. Bruna, "State-of-the-Art in EDLC," 2013.
[62] A. Manthiram, "An Outlook on Lithium Ion Battery Technology," *ACS central science,* vol. 3, no. 10, pp. 1063-1069, 2017.
[63] S. Miret, "Storage wars: Batteries vs. supercapacitors," *Berkeley Energy and Resources Collaborative, November,* vol. 10, 2013.
[64] P. Simon, Y. Gogotsi, and B. Dunn, "Where do batteries end and supercapacitors begin?," *Science,* vol. 343, no. 6176, pp. 1210-1211, 2014.

[65] J. Cao and A. Emadi, "A new battery/ultracapacitor hybrid energy storage system for electric, hybrid, and plug-in hybrid electric vehicles," *IEEE Transactions on power electronics,* vol. 27, no. 1, pp. 122-132, 2012.
[66] M. Glavin and W. Hurley, "Ultracapacitor/battery hybrid for solar energy storage," in *Universities Power Engineering Conference, 2007. UPEC 2007. 42nd International*, 2007, pp. 791-795: IEEE.
[67] L. Zhang, J. Zou, and J. Song, "RuO2. xH2O/AC Composite Electrode and Properties of Super-capacitors," *J. Inorganic Materials,* vol. 5, pp. 745-749, 2005.
[68] T. Hamilton, "Next stop: Ultracapacitor buses," *Technology Review, MIT Technology Review,* 2009.
[69] F. J. Baalbergen and P. Bauer, "Cost evaluation of generator-set with energy storage for 4q-load," in *Power Electronics and Motion Control Conference, 2008. EPE-PEMC 2008. 13th*, 2008, pp. 2170-2177: IEEE.
[70] Y. Yao, D. Zhang, and D. Xu, "A study of supercapacitor parameters and characteri stics," in *Power System Technology, 2006. PowerCon 2006. International Conference on*, 2006, pp. 1-4: IEEE.
[71] F. Belhachemi, S. Rael, and B. Davat, "A physical based model of power electric double-layer supercapacitors," in *Industry Applications Conference, 2000. Conference Record of the 2000 IEEE*, 2000, vol. 5, pp. 3069-3076: IEEE.
[72] M. Okamura, "A basic study on power storage capacitor systems," *Electrical engineering in Japan,* vol. 116, no. 3, pp. 40-51, 1996.
[73] A. Cultura II and Z. Salameh, "Modeling, evaluation and simulation of a supercapacitor module for energy storage application," *cell,* vol. 1, no. 1, p. 1, 2015.
[74] K. Sahay and B. Dwivedi, "Supercapacitors energy storage system for power quality improvement: An overview," *J. Energy Sources,* vol. 10, no. 10, pp. 1-8, 2009.
[75] M. Fahmi, R. K. Rajkumar, R. Arelhi, and D. Isa, "Study on the effect of supercapacitors in solar PV system for rural application in Malaysia," in *Power Engineering Conference (UPEC), 2015 50th International Universities*, 2015, pp. 1-5: IEEE.
[76] B. Panda, "Some studies on control aspects of grid connected photovoltaic system," 2017.
[77] A. M. Eid, M. Abdel-Salam, and M. T. Abdel-Rahman, "Vertical-axis wind turbine modeling and performance with axial-flux permanent magnet synchronous generator for battery charging applications," in *Power Systems Conference, 2006. MEPCON 2006. Eleventh International Middle East*, 2006, vol. 1, pp. 162-166: IEEE.
[78] P. Basu and A. Harichandan, "Power System Stability Studies Using Matlab," 2009.
[79] N. Huang, "Simulation of power control of a wind turbine permanent magnet synchronous generator system," 2013.
[80] M. Yin, G. Li, M. Zhou, and C. Zhao, "Modeling of the wind turbine with a permanent magnet synchronous generator for integration," in *Power Engineering Society General Meeting, 2007. IEEE*, 2007, pp. 1-6: IEEE.
[81] A. Rolan, A. Luna, G. Vazquez, D. Aguilar, and G. Azevedo, "Modeling of a variable speed wind turbine with a permanent magnet synchronous generator," in *Industrial Electronics, 2009. ISIE 2009. IEEE International Symposium on*, 2009, pp. 734-739: IEEE.
[82] S. Rahman and M. Pipattanasomporn, "Modeling and simulation of a DG-integrated intelligent microgrid," VIRGINIA POLYTECHNIC INST AND STATE UNIV BLACKSBURG2010.
[83] B. Omijeh, C. Nmom, and E. Nlewem, "Modeling of a vertical axis wind turbine with permanent magnet synchronous generator for Nigeria," *international Journal of Engineering and Technology,* vol. 3, no. 2, pp. 212-220, 2013.
[84] J. Libich, J. Máca, J. Vondrák, O. Čech, and M. Sedlaříková, "Supercapacitors: Properties and applications," *Journal of Energy Storage,* vol. 17, pp. 224-227, 2018.

DATASHEET 51V MODULE

DuraBlue™
Advanced Shock & Vibration Technology

FEATURES AND BENEFITS*

- Up to 1,000,000 duty cycles or 10 year DC life
- 51V DC working voltage
- Active cell balancing
- Temperature output
- Overvoltage outputs available
- High power density
- Extreme Vibration Environment Compatible

TYPICAL APPLICATIONS

- Hybrid vehicles
- Rail
- Heavy industrial equipment
- UPS systems

PRODUCT SPECIFICATIONS

ELECTRICAL	BMOD0189 P051 B2A
Rated Capacitance[1]	189 F
Minimum Capacitance, initial[1]	189 F
Maximum Capacitance, initial[1]	200 F
Maximum ESR $_{DC,}$ initial[1]	5.6 mΩ
Test Current for Capacitance and ESR $_{DC}$[1]	100 A
Rated Voltage	51 V
Stored Energy[3]	69 Wh
Absolute Maximum Voltage[2]	54 V
Over Voltage (OV) Alarm "ON" Range†	51.3 - 54.3 V
Nominal Module Balance "ON" Voltage	45.0 V
Absolute Maximum Current	1,900 A
Maximum Series Voltage	750 V
Capacitance of Individual Cells[7]	3,400 F
Stored Energy, Individual Cell[7]	3.8 Wh
Number of Cells	18
TEMPERATURE	
Operating Temperature (Cell Case Temperature)	
Minimum	-40°C
Maximum	65°C

* Results may vary. Additional terms and conditions, including the limited warranty, apply at the time of purchase. See the warranty details for applicable operating and use requirements.

† Module OV "OFF" signal is latched to low voltage power supply input. To reset the alarm signal the low voltage supply must be removed temporarily.

PRODUCT SPECIFICATIONS (Cont'd)

PHYSICAL	BMOD0189 P051 B2A
Mass, typical	16.8 kg (w/ fan)
Power Terminals	M8 Thru hole
Recommended Torque - Terminal	N/A
Vibration Specification	ISO 16750-3, Table 12
Shock Specification	IEC 60068-2-27, -29
Environmental Protection	IP65
Cooling	Forced Air
MONITORING / CELL VOLTAGE MANAGEMENT	
Internal Temperature Sensor	NTC Thermistor
Temperature Interface	OT Alarm
Cell Voltage Monitoring	Overvoltage Alarm
Connector (Mating)	Deutsch DTM06-4S, Amphenol ATM06-4S
Cell Management System	CMS 2.5
SAFETY	
Short Circuit Current, typical (Current possible with short circuit from rated voltage. Do not use as an operating current.)	9,200 A
Certifications	RoHS, REACH
High-Pot Test[8]	3,600 VDC

TYPICAL CHARACTERISTICS

THERMAL CHARACTERISTICS	BMOD0189 P051 B2A
Thermal Resistance ($R_{ca,}$ All Cell Cases to Ambient), typical[4]	0.12°C/W
Thermal Capacitance (C_{th}), typical	15,000 J/°C
Maximum Continuous Current (ΔT = 10 °C)[4] (BOL, Beginning of Life)	120 A, RMS
LIFE	
DC Life at High Temperature[1] (held continuously at Rated Voltage and Maximum Operating Temperature)	1,500 hours
Capacitance Change (% decrease from minimum initial value)	25%
ESR Change (% increase from maximum initial value)	110%
Projected DC Life at 25°C[1] (held continuously at Rated Voltage)	10 years
Capacitance Change (% decrease from minimum initial value)	20%
ESR Change (% increase from maximum initial value)	100%
Projected Cycle Life at 25°C[1,5,6]	1,000,000 cycles
Capacitance Change (% decrease from minimum initial value)	20%
ESR Change (% increase from maximum initial value)	100%
Test Current	100 A
Shelf Life (Stored uncharged at 25°C)	4 years

ESR AND CAPACITANCE VS TEMPERATURE

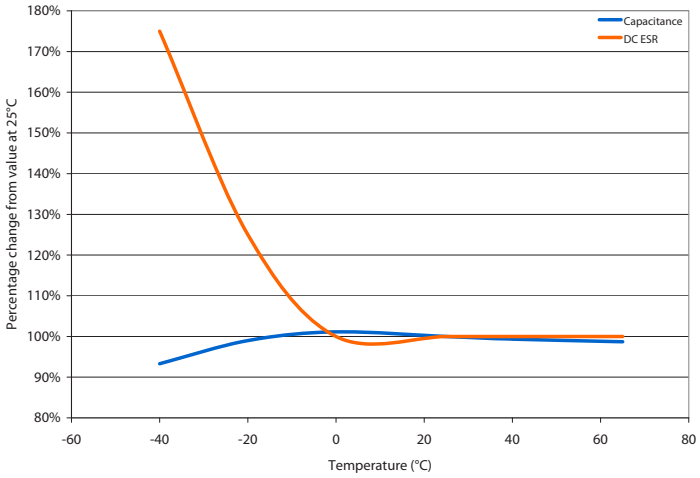

NOTES

1. Capacitance and ESR_{DC} measured at 25°C using specified test current per waveform below.
2. Absolute maximum voltage, non-repeated. Not to exceed 1 second.
3. $E_{stored} = \frac{½\ CV^2}{3{,}600}$
4. $\Delta T = I_{RMS}^{\ 2} \times ESR \times R_{ca}$
5. Cycle using specified test current per waveform below.
6. Cycle life varies depending upon application-specific characteristics. Actual results will vary.
7. Per United Nations material classification UN3499, all Maxwell ultracapacitors have less than 10 Wh capacity to meet the requirements of Special Provisions 361. Both individual ultracapacitors and modules composed of those ultracapacitors shipped by Maxwell can be transported without being treated as dangerous goods (hazardous materials) under transportation regulations.
8. Duration = 60 seconds. Not intended as an operating parameter.

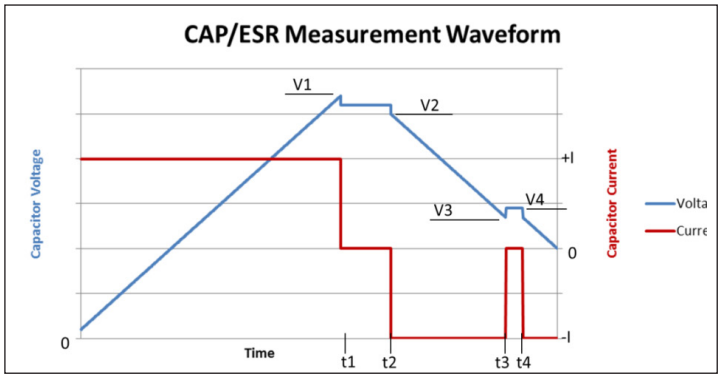

$V1 = V_{rated}$ t2 - t1 = 15 seconds Capacitance = I x (t3-t2)/(V2-V3)
$V3 = 0.5 \times V_{rated}$ t4 - t3 = 5 seconds ESR = (V4 - V3)/I

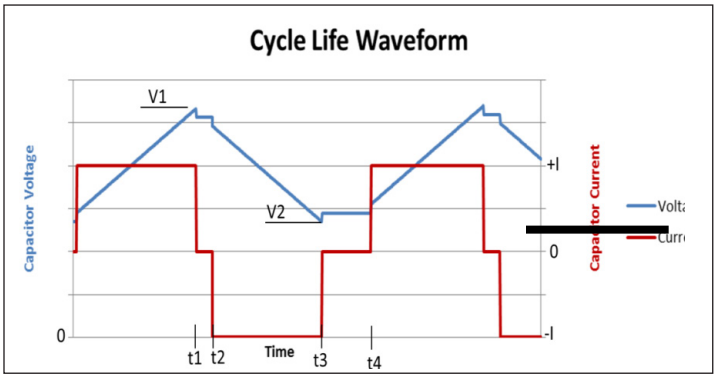

$V1 = V_{rated}$ t2 - t1 = 5 seconds (I=0)
$V2 = 0.5 \times V_{rated}$ t4 - t3 = 15 seconds (I=0)

BMOD0189 P051 B2A

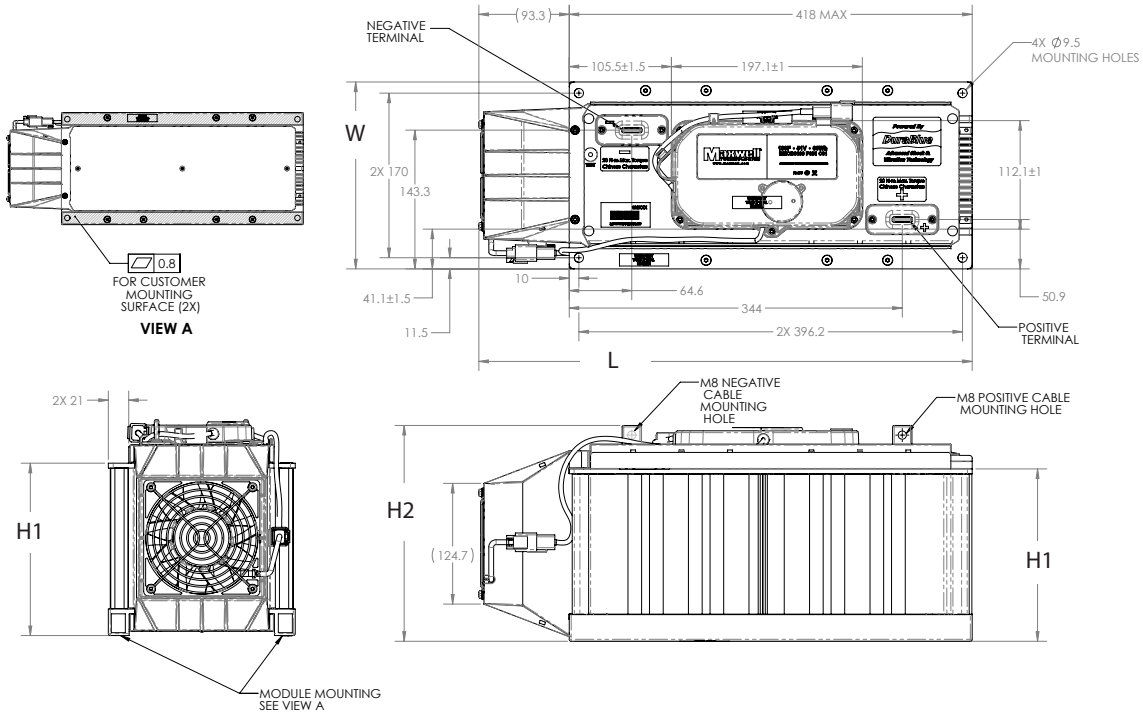

Part Description	Dimensions (mm) L (max)	W (max)	H1 (max)	H2 (max)	Package Quantity
BMOD0189 P051 B2A	515	197	181	228	1

Product dimensions are for reference only unless otherwise identified. Product dimensions and specifications may change without notice.
Please contact Maxwell Technologies directly for any technical specifications critical to application. All products featured on this datasheet are covered by the following U.S. patents and their respective foreign counterparts: 6643119, 7180726, 7295423, 7342770, 7352558, 7384433, 7440258, 7492571, 7508651, 7580243, 7791860, 7816891, 7859826, 7883553, 7935155, 8072734, 8098481, 8279580, and patents pending.

Maxwell Technologies, Inc.
Global Headquarters
3888 Calle Fortunada
San Diego, CA 92123
USA
Tel: +1 (858) 503 3300
Fax: +1 (858) 503 3301

Maxwell Technologies SA
Route de Montena 65
CH-1728 Rossens
Switzerland
Tel: +41 (0)26 411 85 00
Fax: +41 (0)26 411 85 05

Maxwell Technologies, GmbH
Leopoldstrasse 244
80807 Münich
Germany
Tel: +49 (0)89 / 4161403 0
Fax: +49 (0)89 / 4161403 99

Maxwell Technologies
Shanghai Trading Co. Ltd
Unit A2BC 12th Floor
Huarun Times Square
500 Zhangyang Road, Pudong
Shanghai 200122, P.R. China
Phone: +86 21 3852 4000
Fax: +86 21 3852 4099

Maxwell Technologies Korea Co., Ltd
Room 1524, D-Cube City
Office Tower, 15F #662
Gyeongin-Ro, Guro-Gu,
Seoul, 152-706, South Korea
Phone: +82 10 4518 9829

AGM G+ 12-200

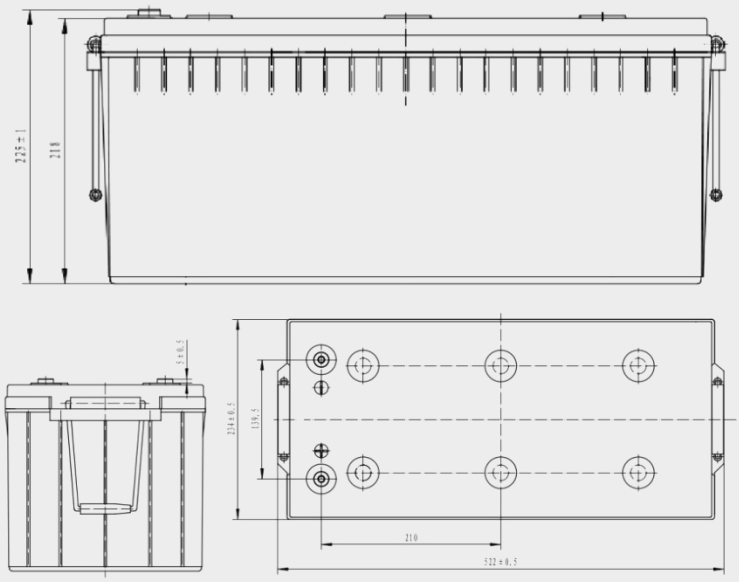

Product characteristics at 25˚C

Dimensions	522 x 234 x 223 mm
Weight	58 kg
Expected life	10 years*
Internal resistance	3.00 mΩ
Self discharge rate	≤ 1.5% per month
Max charge current	40A
Max discharge current	1400A/5 sec

Rated capacity at 25˚C and 1.8V per cell

C20	C10	C5
200 Ah	186 Ah	170 Ah

C20, C10, C5 = capacity at 20, 10, 5h discharge

Charge Voltage at 25˚C

Cycle use	14.4 V
*Standby use	13.5 V

Constant current discharge at 25˚C (A)

End voltage (V/cell)	1h	3h	5h	10h	20h	50h	100h	120h	240h
1.70	111.30	51.27	34.86	19.95	10.13	4.52	2.59	2.30	1.18
1.75	110.00	50.79	34.29	18.88	10.06	4.35	2.37	2.09	1.10
1.80	105.00	50.00	34.00	18.60	10.00	4.29	2.30	1.93	1.08
1.85	97.91	47.06	32.21	17.99	9.65	4.20	2.25	1.87	1.06
1.90	94.01	46.65	29.75	17.07	9.34	3.91	2.20	1.84	1.04

Constant power discharge at 25˚C (W/cell)

End voltage (V/cell)	1h	3h	5h	10h	20h	50h	100h	120h	240h
1.70	201.0	86.80	60.5	36.0	19.5	9.80	5.02	4.20	2.15
1.75	194.5	83.20	59.0	35.0	19.3	9.75	4.93	4.15	2.10
1.80	189.0	81.60	57.5	34.5	19.0	9.60	4.86	4.10	2.06
1.85	183.0	78.90	56.0	33.5	18.5	9.50	4.81	4.05	2.04
1.90	177.5	76.45	54.5	32.5	18.2	9.30	4.73	4.02	2.02

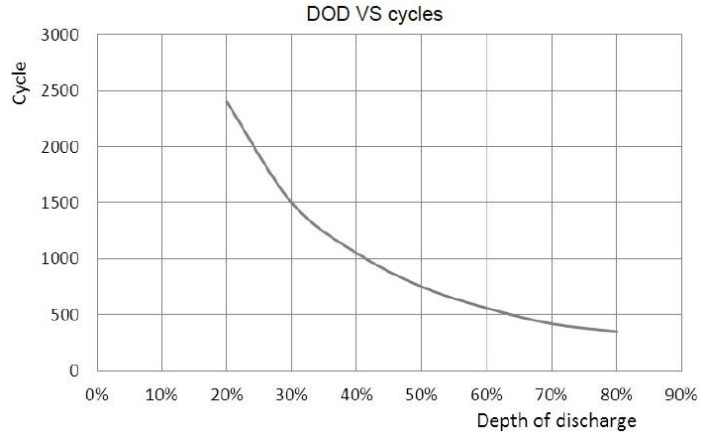

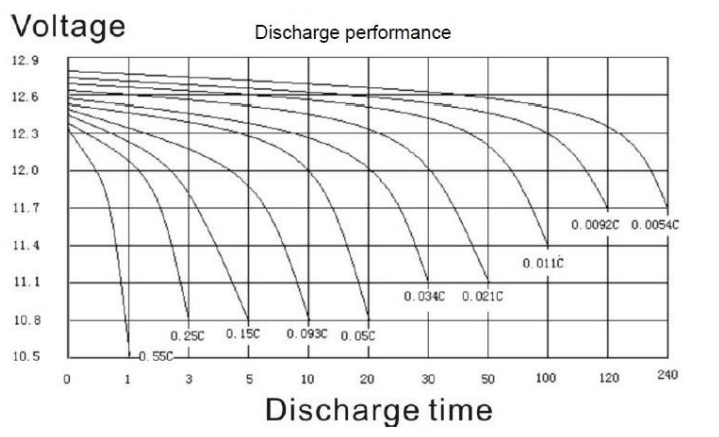

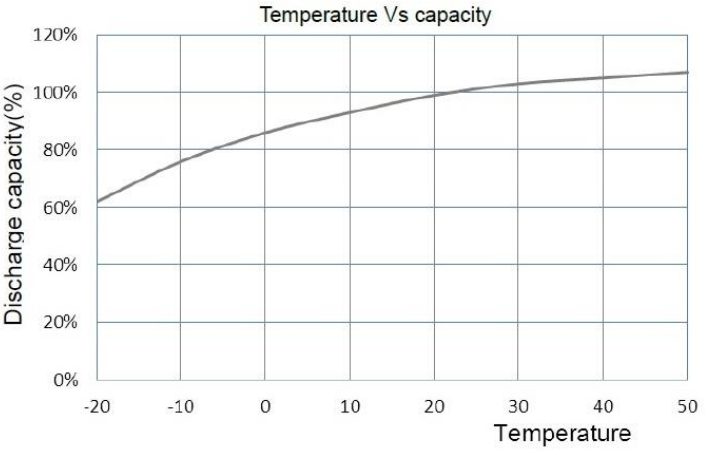

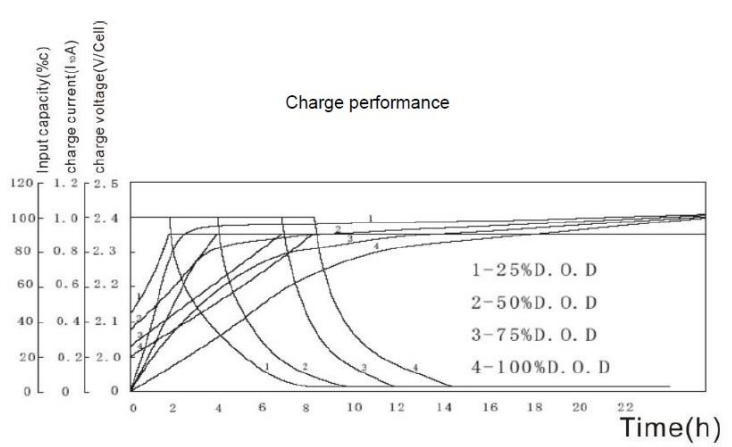

Appendix C Solar Panel Datasheet/Specification

PERFORMANCE UNDER STANDARD TEST CONDITIONS (1000W/M² AM 1.5, 25°C)

	DESERV C144-355	DESERV C144-380
Rated power (Pmax), Wp	355	380
Max power voltage (Vmp), V	38.75	39.40
Max power current (Imp), A	9.20	9.70
Open circuit voltage (Voc), V	45.85	46.70
Short circuit current (Isc), A	9.73	10.08
Module efficiency (%)	17.98	19.24

Operating Conditions

Ambient temperature, °C	-40 to + 85
Maximum system voltage,Vdc	1000
Hail impact velocity, m/sec	23
Maximum surface load capacity, Pascals	5400

Cell Temperature Coefficients

Open circuit voltage	- 0.323 % / °C	- 0.32 % / °C
Short circuit current	+ 0.047 % / °C	+ 0.05 % / °C
Nominal power	- 0.414 % / °C	- 0.37 % / °C

Physical Parameters

No. of cells	144
Module dimensions (mm)	1021X1934
Module thickness (mm)	40
Approximate weight (kg)	21.5

Mechanical Characteristics

Cable	NO. 12 AWG, 4mm2
PV connectors	MC4/MC4 (Compatible)/TYCO
Frame	Silver Anodized Aluminum Alloy
Junction box	IP67 Junction Box with 4 Rail/Split Junction Box with 3 bypass diodes
Glass	3.2mm Thick Low Iron Tempered

NOCT	DESERV C144-355	DESERV C144-380
Rated power (Pmax), Wp	264.20	282.81
Max power voltage (Vmp), V	35.44	36.03
Max power current (Imp), A	7.49	7.90
Open circuit voltage (Voc), V	42.63	43.42
Short circuit current (Isc), A	7.95	8.23

144 Cells PV Solar Module Dimensions

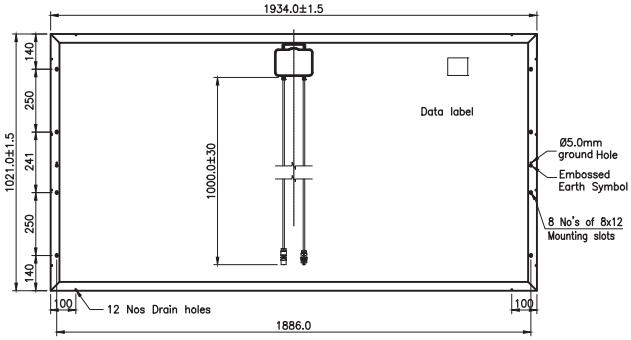

RenewSys DESERV C144 Galactic-3: PV Modules

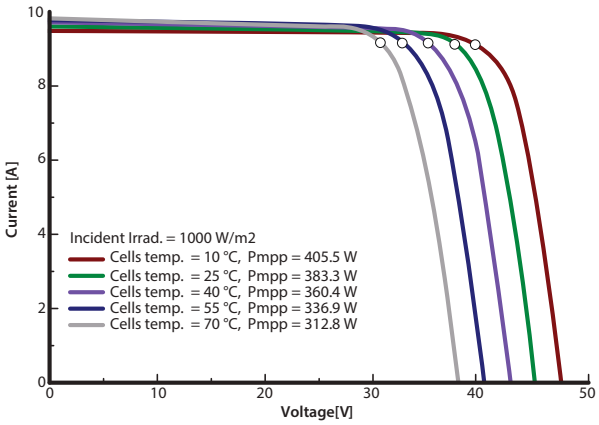

RenewSys DESERV C144 Galactic-3: PV Modules

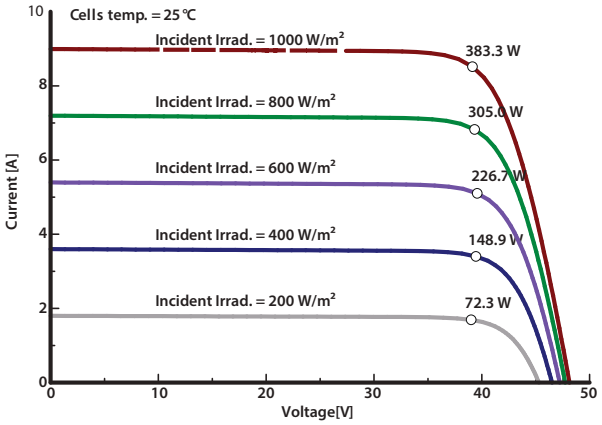

Registered Office
98, Jolly Maker Chambers No.2,
225 Nariman Point,
Mumbai - 400 021, Maharashtra, India
Tel.: + 91 22 30040500

Factory
Plot No.6, Survey # 114/P, Srinagar Village, Maheshwaram Mandal,
Dist-Rangareddy, Hyderabad - 501 359, Telangana, India
Tel.: + 91 40 67303000, Fax: + 91 40 67303003

renewsys@renewsysindia.com ❖ www.renewsysworld.com

Small Vertical axis wind turbine 700W Model DS700 for off-grid installations

PRODUCT SPECIFICATION

General Specification			
Rated Power	700w	Rated wind speed	12 m/s
Rated rpm	405 rpm	Cut-in wind speed	<3m/s
Cut-out	15m/s	Survivor wind speed	60m/s

Wind turbine specification	
Rotor Diameter(A)	1.930m
Total Height (B)	1.597m
Tower Height (Option)	3 meter height minimum recommended
Turbine Weight	60kg
External Darrieus	3 blades
Internal Savonius	2 layer
Blades material	Anodized Aluminum
Rotor Axis material	Anodized Aluminum

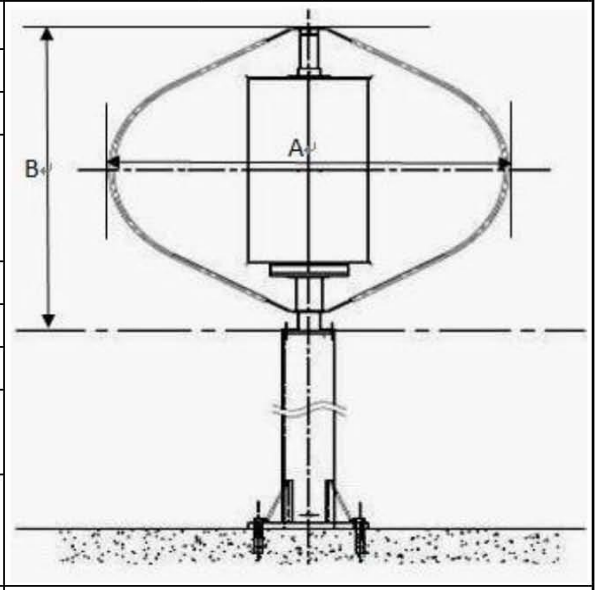

Generator Specification	
Type	AC, 3phase, Synchronism PMG
Rated power	1000W
Brake system	
Automatic	Over speed short circuit brake control
Manual	Electronic Switch Type
System Operation Conditions	
Ambient Temperature	-10~40℃
Ambient Humidity	95% max.

Power Curve